Physical Wave Propagation Modeling for Real-Time Synthesis of Natural Sounds

Georg Essl

A Dissertation

Presented to the Faculty

of Princeton University

in Candidacy for the Degree

of Doctor of Philosophy

Recommended for Acceptance

By the Department of

Computer Science

November 2002

Abstract

This thesis proposes banded waveguide synthesis as an approach to real-time sound synthesis based on the underlying physics. So far three main approaches have been widely used: digital waveguide synthesis, modal synthesis and finite element methods. Digital waveguide synthesis is efficient and realistic and captures the complete dynamics of the underlying physics but is restricted to instruments that are well-described by the one-dimensional string equation. Modal synthesis is efficient and realistic yet abandons complete dynamical description and hence cannot used for certain types of performance interactions like bowing. Finite element methods are realistic and capture the behavior of the constituent physical equations but on current commodity hardware does not perform in real-time.

Banded waveguides offer efficient simulations for cases for which modal synthesis is appropriate but traditional digital waveguide synthesis is not applicable. The key realization is that the dynamic behavior of traveling waves, which is being used in waveguide synthesis, can be applied to individual modes and that the efficient computational structure can be utilized to achieve an approximate dynamical description in the neighborhood of modes. Secondly this realization is connected to related work on the theory of asymptotics and periodic orbits and hence shown to apply to higher dimensions also.

This theoretical approach is studied in applications to bowed bar percussion instruments, complex stroke patterns on Indian Tabla drums as well as rubbed wine glasses and Tibetan singing bowls. None of these instruments and performance types has been synthesized efficiently before. The simulations are compared to experiments.

Acknowledgments

Since this was written and needs must be —

My whole heart rises up to bless

Your name in pride and thankfulness! – **Robert Browning**[1]

There is much to be thankful for and I will definitely not do everyone and everything justice that helped me work on and complete this thesis.

Piles of gratitude are due to my advisor Prof. Perry R. Cook. I had not anticipated how good a match Perry would be for me. Not only is he at the very frontier of physical modeling of sound, but also did he provide the interactions, freedoms, supports and atmosphere I needed, academically and beyond. He handled my doubts and uncertainties with grace that is rare to be found.

Also Prof. Ken Steiglitz was a great man to be around (and he is a giant for his size). I had uncountable enjoyable conversations, whether it was scientific or humoristic, political or casual. A source of ideas, experience and knowledge and a role-model for open-mindedness, curiosity and versatility. Profs. Tom Funkhouser — who also dug through all these pages as a reader — and Adam Finkelstein sat through many a talks of mine gave me advice on publishing or on questions concerning graphics. Also Prof. Paul Lansky for the kindness of being on my committee and hence agreeing to put up with tons of "engineer's speak". All of them were great sources of feedback during the formation process of this thesis.

Lots of thanks to George Tzanetakis, as collaborator, lab fellow, dog owner and more.

I greatly enjoyed the collaboration with Prof. James. F. O'Brien and a visit at Berkeley. Professors J. P. Singh, Kai Li, Jonathan Cohen, Joan Girgus and John Hop-

[1] "The Last Ride Together," lines 5-7, (1855) in Arthur Quiller-Couch, ed. "The Oxford Book of English Verse" (1919) available online at `www.bartleby.com/101/727.html` also [147, p. 150, q. 19].

field were a great resource during me exploration for the right direction of research at Princeton. Needless to say I had countless great exchanges, help, support and fun with many people in the department including Melissa, Ginny, Trish, Mitra, Tina, also Profs. Bernhard “Santana” Chazelle (thanks for the jam sessions), Szymon Rusinkiewicz, Ben Shedd, Brian Kernighan, Mona Singh, Andrew “Expresso” Appel (thanks for keeping the caffeine coming!), David August, Randy Wang and Doug Clark. Many thanks to Department Chair David Dobkins for lots of guidance.

Best thanks also to Gary Scarvone for insightful feedback on banded waveguide implementations in STK, in particular with regards to bandwidth questions. To Professor Julius Smith for the kind permission to use the Friedlander-Keller diagram (see Figure 2.8) from him book-in-progress. Ed Gaida for the kind permission to use his beautiful photograph of Franklin’s glass harmonica (see Figure 4.23), James F. O’Brien for rendered bowl mode shapes (see Figure 4.26) and Ajay Kapur for his tabla picture (see Figure 4.18).

Davide Rocchesso, Ingolf Bork, Antoine Chaigne, Bob Schumacher, Chris Chafe, Anindya Ghoshal and Rolf Runborg kindly provided reprints, advice and feedback of various sorts.

Also thanks to Jim Johnston and Schuyler Quakenbush of AT&T Research.

Tons of thanks to Lujo Bauer, the first friend I made in Princeton and the best I had throughout the years.

Also best thanks to all my office mates, Ben Dressner, Wagner Correa, late Cheng Liao, Eun-Young Lee, Dongming Jiang, Yilei Shao, Bo Brinkman, Chris Richards, Sumeet Sobti, Tony Wirth, Fengzhou Zheng and John Hainsworth for providing both a friendly environment and necessary diversions. And all the people I enjoyed outside my office, including but by no means limited to Iannis “Rager” Tourlakis, Amal Ahmed, Jie Chen,

Mattias Jacob, Allison Klein, Ketan Dalal, Neophytos Michael, Patrick Min, Emil Praun, Ricki Smith, Yefim Shuf, John Forsyth, Kedar Swadi, Gary Wang, Dan Wang, Brent Waters, Matt Webb, Jiannan Chen, Wenjia Fang, Dirk Balfanz, Rudro Samanta, Tammo Spalink, Lena Petrovic, Limin Wang, Limin Jia, Jessica Wang, Lisa Worthington and Kevin Wayne.

Undergrads I worked with Ajay Kapur, Neal Shah, Anoop Gupta, Gakushi Nakamura, Fei-Fei Li, Cory Elder and Hagos Mehreteab.

And to all the friends in all the other colleagues in the departments and all the interesting people I got to meet. Kai Chen for his friendship and hour-long discussions of ethics. Sharon Bingham, Troy Smith, Matt Hindman, Andy Burlingame, Jo Hertel, Steven Miller, Kyoko Sato, Johannes Chudoba, Debbie Abrams, Yesim Tozan, Mikalis Dafermos, Matt Devos, Adrian Banner, Konstantinos Drakakis, Tessy Papavasiliou, Yannis Papadoyannakis, Lyndon Dominique, Ilana Moreno-Shields, Emily Doolittle, Mary Wright, Azul Wright, Colby Leider, Tae-Hong Park, Laurie Hollander, Dan Trueman, Monica Mugan, Jennifer Burkowski, Kim Weaver, Jeff, Vera Koffman, Tim Hall, Tre Green, Herdes Teich, Mike Buchanan, Sarah Thomas, Cliona Golden, Steve Tibbets, Traci, Ade, Sinda, Natasha, Joe, the FireHazards, especially Chinook, Anina, Chuck, Greg, Maria, Liz, Betsy, Christina, Katherine, and Sarah Rod plus all the newbies Laure, “Ardvark”, Tudor, Chinny, Sarahs (both), Holly, Janine and Paris. Family and friends back home (Peter, Andy) or scattered around the globe (Jörg, Robert) are last but never least. Love you guys, thanks for all.

Of course I’m grateful for financial support throughout the years. My first two years of work has been supported by a post-graduate stipend of the Austrian Federal Ministry of Science and Education. In later years I enjoyed industrial support through Intel, Arial

and Microsoft and academic support through NSF Grant Number 9984087 and the State of New Jersey Commission on Science and Technology Grant Number 01-2042-007-22.

Dedicated to my parents.

To my mom who gave me the love of music,

and my dad who gave me the love of science.

Contents

List of Figures

Chapter 1

Introduction

> There are two things which I am confident I can do very well: One is an introduction to any literary work, stating what it is to contain, and how it should be executed in the most perfect manner; [..][1] – **Samuel Johnson**[2]

> Let me introduce to you three of my friends: the red herring called insight, the blue trout called hindsight, and the translucent amoeba called blindsight.

1.1 The Thesis Stated

The core of the thesis is to propose the usefulness of a certain algorithm, a certain filter structure or a certain numerical method for the real-time synthesis of sounds on the computer. This method is depicted using a block-diagram style typical for digital filters in Figure 1.1

[1] Quote continued in the concluding chapter.

[2] James Boswell, "Life of Samuel Johnson," (1755) available at `http://newark.rutgers.edu/~jlynch/Texts/BLJ/blj55.html` or according to [147, p. 371, q. 17] in vol. 1, p. 292 (1755)

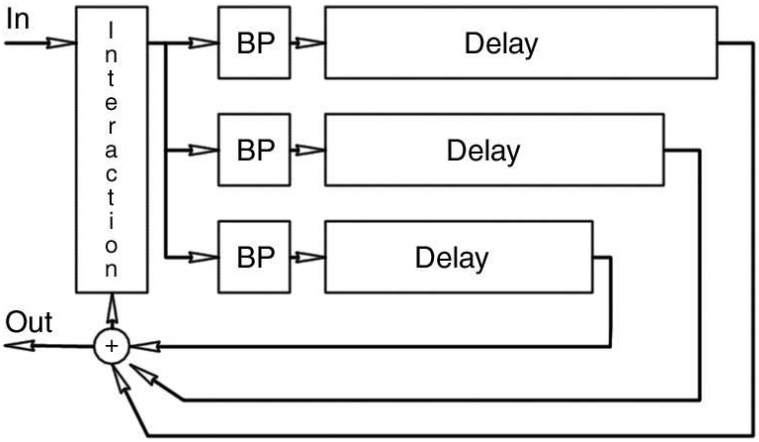

Figure 1.1: The object of the thesis.

Throughout this thesis, I will discuss properties of this structure, various forms of conceptual interpretation and connection to physically systems as well as the relation of this structure to prior work and knowledge. I will argue that this structure is a generalization of prior methods and by this generalization allows for an extended domain of application. I will also argue that this structure is useful for thinking about notions of efficiency and stability for numerical simulation. Finally I'll compare the usefulness of the method in application and with respect to alternative methods.

The statement of my thesis is that the method, which I like to call "banded digital waveguides," is a significant advance in the field of physical sound simulation, by offering a number of theoretical and practical contributions.

1.2 Contributions of this Thesis

In thesis, I propose a physical modeling method for musical instruments and other sounding objects. The method itself is a generalization of previous methods and broadens their

realm of application. In particular, this method extends the class of possible interactions. It also broadens the types of materials that can be modeled. In addition it allows for simulation of some two and three-dimensional geometries in real-time.

I have illustrated the practical application of the method for bowed bar percussion, Indian Tabla drums, the glass harmonica, and the Tibetan prayer bowl. All of these examples share complex performance patterns and are examples of objects of different geometries. In all cases, the simulation is validated by experiments on real instruments.

In addition, the relation to alternative simulation methods are investigated. This highlights the differences, advantages, disadvantages, and limitations of the respective methods. In the case of modal and waveguide synthesis, it is shown that the proposed method generalizes both and extends the applicability to dynamic modeling of solid objects in higher dimensions. In the case of frequency warping, the proposed method shows a significant performance advantage. Finite difference and finite element methods are more general in application than the proposed method, though they are significantly slower in comparable applications.

1.2.1 Publications and their Place in this Thesis

The bowed bar research (section 4.1) was first presented at a conference [60] and in its final version in an archival journal [61]. Finite element methods (section 6) as an alternative solution was investigated in collaboration with James F. O'Brien of UC Berkeley [135]. The generalization of the simulation method to higher dimensions and examples of Tabla and glass harmonica (sections 4.2 and 4.3) is in preparation for publication, though an unpublished manuscript has been circulated [62]. The work on the glass harmonica and Tibetan prayer bowls (section 4.4) as well as theoretical considerations (parts of chapters 3 and 5) have been submitted for review for a conference [63, 64]. Real-time interaction

work with Ajay Kapur, Philip Davidson and Perry Cook for the Tabla drums [98] will not be discussed here beyond the Tabla simulation.

1.3 Thesis Outline

I will first discuss the background, prior art and related literature chapter 2. Then the theory of propagation modeling using banded waveguides will be discussed in chapter 3. Then, in chapter 4, four examples will be discussed: bar percussion instruments (section 4.1), Indian Tabla drums (section 4.2), glass harmonicas (section 4.3), and Tibetan singing bowls (section 4.4) with relevant experimental work. Then the simulation method is compared with alternative methods in chapter 5 and the case of finite element methods is described and discussed in detail in chapter 6. Finally possible future directions and applications of the method are proposed in chapter 7.

Chapter 2

Background, Previous Art and Related Literature

Only the more rugged mortals should attempt to keep up with current literature. – **George Ade**[1]

The combined collections total more than six million printed works, five million manuscripts and two million nonprint items, and increase at the rate of about 10,000 volumes a month. – **History of the Princeton University Library Online**[2]

Six months in the lab can save you a day in the library. – **old reference librarian proverb (according to Sally Jo Cunningham**[3]**) or by Albert Migliori (according to Julian D. Maynard**[4]**)**

Information come and stay, sink in and if you don't — go away.

[1] As attributed at `http://www.geocities.com/~spanoudi/topic-I5.html`

[2] `http://libweb.princeton.edu/about/history.php` as retrieved on April 14, 2002.

[3] `http://www.cs.waikato.ac.nz/GradConf/talks/sallyjo/`

[4] Julian D. Maynard, "Resonant Ultrasound Spectroscopy," Physics Today 48(1) 26-31, January 1996.

This work is interdisciplinary in nature. The background of this work is not solely placed in firmly established fields within Computer Science, but rather draws on a wide range of different disciplines, knowledge and ideas. Traditionally work along these lines has been connected with an emerging discipline called "Computer Music" [202]. More specifically within the sound synthesis community, this line of work falls into the category of "physical modeling" [165, chapter 7].

The work to be presented draws from a wide range of different fields. Yet I first want to present only the background and prior art as understood in the Computer Music community and I would like to introduce relevant texts that are not commonly known in the community as part of the theoretical discussion or, if applicable, in other sections throughout this thesis. The purpose of this approach is mostly to motivate the relevance of these works with the development of the ideas, so it can be appreciated by the community[5].

Wave phenomena are so ubiquitous that a review of knowledge pertaining to this phenomena can be a daunting and overwhelming task and in the end it seems to me that claims to completeness would imply proof of insanity. Still, I made an attempt to be as broad as I possibly could be in finding material and the search for literature was confined mostly by basic ideas presented in this thesis. Literature deemed worthy of investigation have some connection to a number of questions:

- Who has studied wave propagation analytically and numerically and how?
- What is known about stick-slip interactions and perceptible noise generated from it?

[5]This is also connected with problems of presentation of interdisciplinary work, as for example noted by Margrit Eichler [59, p. 59] of translation, language and reception. I hope of a benefit in reception if unfamiliar literature is presented along familiar lines of arguments rather than in isolation.

- What is known about certain sounding objects, like bars, membranes, tuned bars, tuned membranes, Tabla drums and wine glasses?
- What is known about measurement, parameter estimation of responses of the above objects?

Also before the background search took on its full depth I knew already that in my immediate community, people who study physical modeling of musical instruments — a fairly small community of mostly electrical engineers, acousticians, musicians and computer scientists — the ideas proposed in this thesis were novel. There was hence also the question:

- Which of these ideas are known in what form outside my core community?

And finally the literature search is also a foundation of the research presented in this thesis:

- How can literature answer questions that arise in my way of framing and investigating the problem?

Investigating these last two questions leads to an assimulation of various strands of research that are apparently (sometimes only partly) unaware of each other. For example, the mode-ray duality is known in as diverse fields as structural engineering, seismology, electromagnetism, theoretical physics, and applied and pure mathematics. All these fields have, however only a partial overlapping in awareness of the connection of their work and progression of insight in other fields. While traveling wave methods are widely used in structural engineering [126] there seems to be little awareness of the correspondence of their approach to asymptotic theory [139] or periodic orbits in chaos theory [48]. Even

within mathematical physics the interaction between U.S. [103], Western Europe [58], and Russia [110] is evidently not always present (see for example remarks in [58]). This contributes to the fact that very similar concepts in literature have very different nomenclatures and attributions (for example, an asymptotic traveling wave Ansatz can go by any of the following names or acronyms: LG, WKB, JWKB, EBK, periodic orbits, traveling wave method, wave method, ray method, ray tracing method, billiard, phase integral method, asymptotic method.) A brief glossary trying to unravel some of this confusion can be found in Appendix A[6]. One contribution of this thesis is a shy attempt to unearth these connections and find a synthesis that is approachable by the researcher in physical modeling for sound synthesis.

All these questions will be addressed throughout the thesis. Next I would like to review the prior art of sound synthesis as a precursor to this work.

2.1 Sound Synthesis Methods

Sound synthesis methods can be classified into various groups. The previously used methods with direct relation to this work are generally classified as *physical modeling synthesis* [165][7]. Though Roads [165] classifies many separate categories of methods within the field, many are conceptually very closely related. For instance McIntyre, Schumacher, and Woodhouse synthesis [122], Karplus-Strong synthesis [100, 94, 99, 195] and Waveguide synthesis [185, 187, 188] are very closely related. In the case of Karplus-Strong and Waveguide synthesis, the difference can be seen as mere physical interpretation of the structure.

[6]The confusion that is part of the process of unifying various lines of research is nicely described by Daubechies in the case of the evolution of wavelets [51].

[7]A related taxonomy can also be found in [198].

McIntyre, Schumacher, and Woodhouse realized that separation of non-linear excitation and linear resonant instrument response with a persistence on a time-domain view allows for quite efficient and qualitatively good simulation that captures the rich behavior of the overall dynamics very well. The work of Karplus and Strong then highlighted that, in fact, the traveling wave that gives rise to the resonant behavior of strings under tension and air-filled pipes can be very efficiently modeled using delay-lines. This efficient implementation of a delay line uses a circular buffer [55, p. 227][194, p. 258-260], something that had been realized by Schroeder and others while studying synthetic reverberation and room-acoustic simulation [105, 75, 76, 12, 175, 90, 28].

In the remainder of the thesis I will refer to all of these categories simply as *waveguide synthesis*[8].

Another line of physical modeling are methods which are concerned with direct discrete simulation of the local dynamics responsible for sound generation. These include methods using finite differencing [174, 33, 20, 113, 35, 146], mass-spring-damper networks [30, 71, 31], finite element methods [27, 21] and transmission-line methods for solving differential equations [214, 18] (which includes highly scattering digital waveguide simulations and digital waveguide meshes)[9]. Again, all these methods are in close relationship to each other. For instance there is a direct correspondence between finite differencing and scattering networks [18]. Though not necessarily known in the Computer Music community, the matrices arising in solid mechanics finite element methods have a direct mass-spring-damper interpretation [222] and finite elements can be seen as generalization of finite difference methods [222, 5, 201].

[8]Julius Smith often uses the term *waveguide digital synthesis* to indicate that this is a digital synthesis method, throughout this thesis all methods are digital in the sense that are all numerical discretization on digital computers.

[9]This is an important note to make. Digital waveguide meshes are, for the purpose of these thesis, not classified with waveguide simulations but rather with finite element methods.

For the purpose of this thesis I will refer to all of these methods as instances of *finite element methods*.

The final class of physical synthesis methods models the spectral response of the physical system. This can be achieved through additive sinusoidal modeling [182, 210], resonant filter modeling [219, 42], model decomposition modeling [1].

These methods will be referred to as *modal synthesis methods* throughout this thesis[10].

Other methods of sound synthesis, as found in [165, 55, 198], are not reviewed as they are not relevant to this thesis. They are either not physically informed or stochastic in nature.

2.1.1 Waveguide Synthesis

There are many references which comprehensively review waveguide modeling at it current state [188, 45, 187, 99, 8]. Here I will only mention the key ideas and ideas in previous work that are relevant to this thesis.

The derivation of the basic idea of waveguide synthesis is usually presented starting with the ideal wave-equation which describes the perfectly elastic string under tension and oscillations in an air-tube or related wave-guiding structure for small displacements [132, 194, 188]:

$$\frac{\partial^2 y}{\partial t^2} = c^2 \frac{\partial^2 y}{\partial x^2} \tag{2.1}$$

[10]Note that modal means different things to different communities. The word *modal* was chosen over *spectral* because the later usually is used in the Computer Music community in a context that is not physically motivated, for instance in spectral shaping methods, whereas *modal* implies an underlying physical system. This means however that *modal* may only correspond to eigenfrequencies and does not necessarily imply eigenfunctions. I will make sure when appropriate if the latter is included in the discussion.

where c is a material constant. The "generalized solution" [111, p. 636] — also known as d'Alembert solution — has the form:

$$y(x,t) = f^{-}(x-ct) + f^{+}(x+ct) \tag{2.2}$$

where f^{-} and f^{+} are any twice-differentiable functions that satisfy imposed boundary conditions. As can be seen, with increasing time t, the solution has two functionally described waveforms traveling in the positive and negative spatial dimension x at speed c.

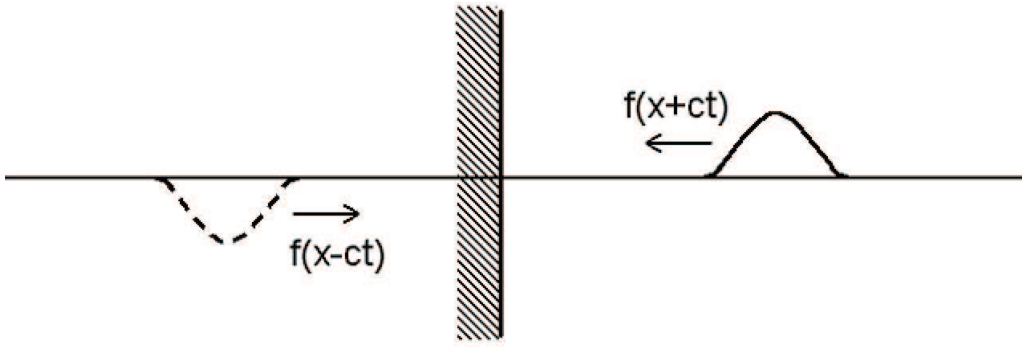

Figure 2.1: Reflection of a traveling wave on a boundary.

The fixed string (or reflective wall of air tube) (or open air tube) are important cases of boundary conditions[11] and it can easily be shown [194] that:

$$f^{+}(x_B,t) = -f^{-}(x_B,t) \qquad \text{for a fixed end reflection at position } x_B \tag{2.3}$$

$$f^{+}(x_B,t) = f^{-}(x_B,t) \qquad \text{for a lose end reflections at position } x_B \tag{2.4}$$

[11]These boundary conditions are also referred to as Dirichlet and von Neumann boundary conditions [111, p.651]

that is, the traveling waveform reflects with a sign-change at fixed ends and without one at open ends. This can also be interpreted as a virtual wave traveling in from behind a rigid boundary has to match an incoming wave with a sign-change. This is depicted in Figure 2.1.

Discretizing time of this solution with boundary conditions imposed on both ends immediately yields a waveguide simulation for the ideal, lossless case (Figure 2.2).

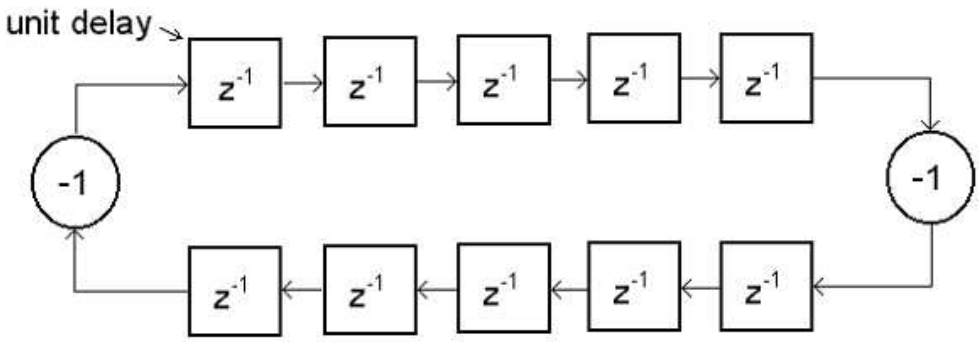

Figure 2.2: Waveguide synthesis of ideal lossless string

Arbitrary bounded function shapes discretized over time are then represented as sampled data points of that function at distance $c\Delta t$ where Δt is the chosen discrete time step. Advancing per time step corresponds to shifting by one memory cell per propagation direction. Data-points reflect by copying and possibly inverting sign.

Of course in a more physically realistic situation, certain assumptions made when deriving the wave-equation do not exactly hold. Physical strings dissipate energy and are not perfectly elastic or perfectly thin. While intuitively all these effects happen at each local point on the string, if exact local representation at every point is not necessary, all losses can be accumulated (“lumped”) and modeled at one position in the model. If the

structure is seen as a filter, one can interpret that the lumped losses, bending stiffness [6, for a review] as filters.

The classical Karplus-Strong synthesis method (Figure 2.3) can then be seen as a waveguide synthesis method including losses. Note that the boundary reflections have been lumped too, which, in the case of two fixed ends, correspond to a double sign inversion which overall cancels.

Figure 2.3: The Karplus-Strong algorithm as waveguide synthesis.

The delay lines used in this model are of integer length. Hence, at a fixed time step of $1/44100$ corresponding to CD quality audio [155] with shorten string length, the frequency resolution suffers. A filter modeling the fractional delay between the integer and actual length is necessary to accommodate for accurate tuning. This is achieved by using various filter design methods [114].

A number of modifications to the ideal waveguide have been studied to achieve more realism. These extensions are usually instrument-specific, for instance the bending stiffness of piano-strings [6] has little relevance for most plucked string instruments [99] (for physical as well as perceptual reasons [96]) whereas tension modulation (the change of tension with displacement) is more important for the latter where the strings are under less overall tension than piano strings [199].

2.1.2 Finite Element Methods

Finite element methods are a vast field with general applications. For a very recent and exhaustive reference see the three-volume work by Zienkiewicz and Taylor [222, 223, 224]. A review specific to finite difference methods can be found in [5].

In the computer music community, finite element style methods are used in two settings. One is the study of musical acoustics, in the evaluation and theory-forming of the dynamical behavior of musical instruments. Finite differencing has been used by to study piano-strings [33, 34], bar percussion instruments [20, 35, 56], and square plates [36, 115]. Finite element methods have been used to study tuning of bar percussion instruments [27, 21] and the kettledrum [162]. These studies focus on accuracy and validity and not on performance parameters relevant for synthesis.

The other setting is simulation. Ruiz studied the finite differencing of the string equation [174]. Interest in this approach re-emerged, usually in the context of the one-dimensional wave-equation [112, 113, 146]. Cadoz and co-workers don't explicitly start with model differential equations, but rather build ad-hoc networks of masses, springs, dampers and other coupling mechanisms [30, 71, 31]. Finally, waveguide meshes were proposed to model higher-dimensional structures [214]

The core to all of these methods is that the object to be simulated is discretized spatially and the local interactions between discretization points are modeled. In the case of finite differencing, the mesh is usually uniform [5]. An example can be seen in Figure 2.4. Non-uniform meshes are usually simulated by the more general finite element method [222]. For a typical mesh structure see for example Figure 2.5.

The dynamics of the system that is set up is problem-dependent. However finite element methods are usually set up as a three-stage process [222, chapter 20], a preprocessing stage which takes mesh connectivity, element specification, constraints, and force

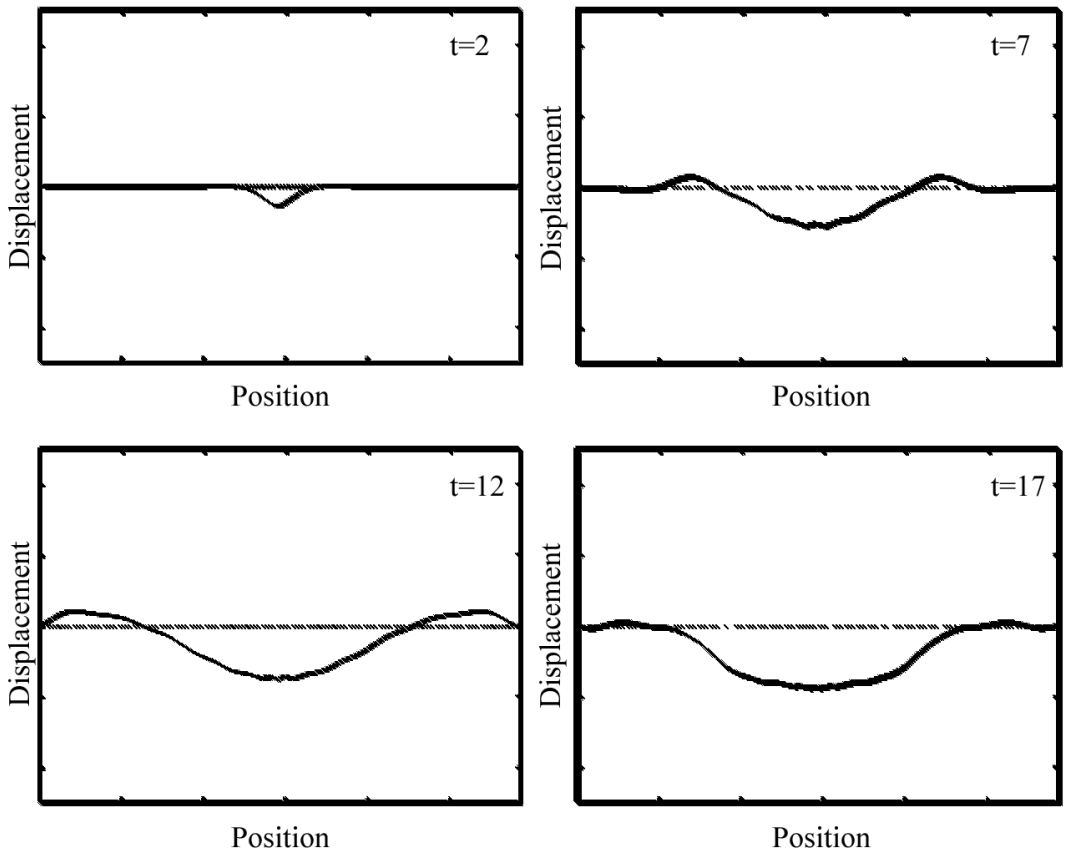

Figure 2.4: A finite difference simulation of a tuned bar (using the method of Chaigne and Doutaut [35])

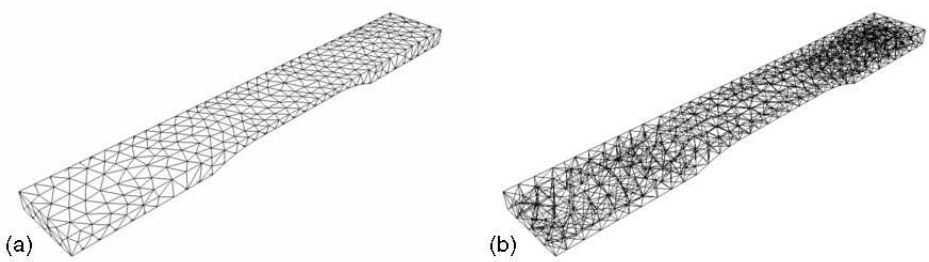

Figure 2.5: Tetrahedral mesh for an $F\sharp 3$ vibraphone bar. In (a), only the external faces of the tetrahedra are drawn; in (b) the internal structure is shown. Mesh resolution is approximately 1*cm*.

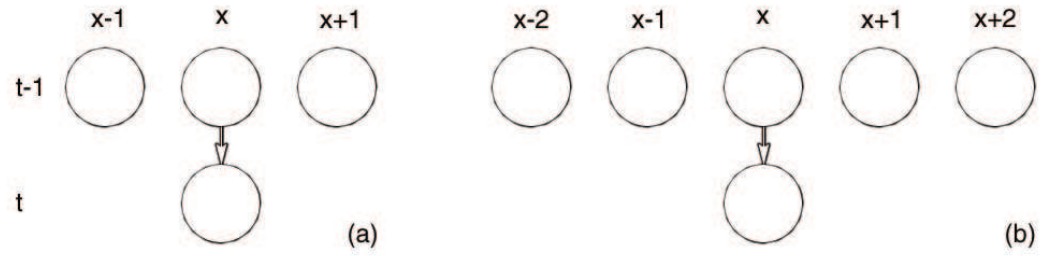

Figure 2.6: Computational molecules of (a) second order and (b) fourth order discretizations leading to banded entry in the model matrix of a finite element solver.

inputs and assembles them into a global matrix formulation. The second step is solution of the system for each time-step in case of time-dependent problems or until convergence in relaxation problems. The third stage is postprocessing which consists of extracting the solution from the global vectors and reinterpreting as element data.

The core computational step is hence the solution of a matrix equation where the size of the matrix is (at least in the basic case) at least as large as the number of elements. In special cases, like one-dimensional string and bar equations on a uniform grid [35], the formulation leads to a banded matrix (in the case of strings the band is 3 and in case of bars the band is 5 as depicted in Figure 2.6), in which case the solution of the system is $O(NM)$ with N being the number of spatial mesh points and M being the width of the band [156, pp. 50-55].

Higher dimensional and more complex domains and meshes generally don't form well-structured matrices, which increases the complexity. Multigrid methods [220, 22, 190, 217, 204] address this problem by solving on a coarse scale and adding refinement steps. Other possibilities are matrix preconditioning techniques [77, pp. 532ff] and manipulation (sparsing) [177]. In any case, usually the optimal performance is assumed

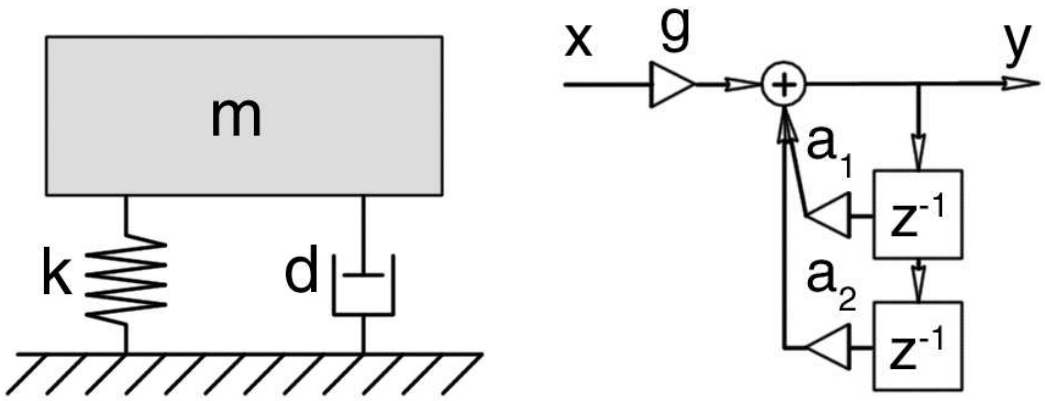

Figure 2.7: A mass-spring damper system and connected digital filter simulation

to be $O(N)$ (for diagonal or band-diagonal matrices [156, 37]) or $O(N \log N)$ for dense matrices [37].

2.1.3 Modal Synthesis

Modal sound synthesis refers to modeling the sound of an object as a sum of exponentially decaying sinusoids. Physically this corresponds to simple damped harmonic oscillators, like mass-spring-damper systems (see Figure 2.7). These second-order resonant structures have a simple representation in the form of two-pole filters, which are very efficient to model, and hence a large number of modes can be modeled with ease.

The digital filter equation corresponding to Figure 2.7 for each time step n is:

$$y(n) = a_1 \cdot y(n-1) + a_2 \cdot y(n-2) + g \cdot x(n) \tag{2.5}$$

The mass m, spring constant k and damping d can be used to derive the digital filter coefficients a_1, a_2 and g. In fact this digital filter is a discrete physical model of the mass-spring-damper system.

As can be seen each filter only requires a small and constant number of multiplications and additions and memory operations and hence the complexity of this method is $O(M)$ where M is the number of modes modeled.

Models of this type have been proposed and used on a wide array of objects and instruments [1, 219, 182, 210, 211, 208, 212].

Modal shapes can be reconstructed by sampling the surface and hence reconstructing the modal shapes through an amplitude envelope as function of discrete space k. Then equation 2.5 becomes:

$$y(n,k) = a_1(k) \cdot y(n-1) + a_2(k) \cdot y(n-2) + g(k) \cdot x(n) \tag{2.6}$$

This approach has recently been used by Pai and co-workers (see for example [208], and note that their equation (1) is a sum of sinusoid form of equation 2.6, and a derivation showing the connection can be found in [212]).

There are approaches which analytically derive the modal shapes for the dynamics using transfer function methods [157, 200]. This method was also proposed to arrive at the full solution over the whole spatial domain. By doing so, oscillation related to spatial sampling is reintroduced and the computational complexity becomes $O(NM)$, where N is the number of spatial sampling points. Hence the transfer function method is assumed to belong to the class of finite element methods for the purpose of this discussion.

2.2 Excitations

The vast majority of sound-producing physical events as used in musical instruments can be well-separated into excitations and a responding sounding object [165]. In a performance sense, this relates to control of the instrument (because the excitation drives the sound production it provides control over the production) and in a physical sense, it relates to energy input or transfer.

This energy transfer can be classified in two ways. One is that it happens independent of the state of the driven system (i.e. excitation and production are "decoupled" [165, p. 269]) or they are not. Then the energy transfer depends on the state of the system and excitation and production are "coupled" (Wawrzynek classifies a similar distinction as "driven" versus "nondriven" [219].)

While Roads emphasizes the performance aspect of this separation [165, p.269] there is a good physical reason for this distinction affecting sound production, control and performance.

The distinction has to do with interactions which classify as linear as opposed to those that don't.

2.2.1 Linear or Impulsive Excitation

The definition of a linear excitation is that the variables driving an interaction are not affected by the state of the system that is being interacted with.

Note, that this explicitly refers to the interaction rather than the system being interacted with. The system could be non-linear, meaning that it does not respond to twice the input with twice the output, but the interaction remains unaffected. For the following discussion I will, however, assume that the system is linear and time-invariant too. This

means that the the interactions can be divided into separate linear contributions[12] and that the system is invariant under a time-delay operation [142, p. 19].

It is easy to show that any discrete linear time invariant system can be completely described by the system's impulse response [142, p. 21].

In this light, a linear interaction refers to an interaction where the driving physical quantity (for example the impact force of a strike) is, to a good approximation, unaffected by interaction itself and hence directly relates to a digital impulse in the simulation.

In a finite element formulation this corresponds to a force function F which is independent of any state variables of the system.

A wide class of instruments have been modeled with their typical types of interactions. The interactions which are well approximated as linear interactions are plucking, striking with hard beaters, and certain rough-surface frictions (those where the rough surface action is well-captured by periodic impulses) [210, 209, 211, 163, 54, 208, 212, 42, 44].

2.2.2 Nonlinear or Friction Excitation: Stick-Slip

For non-linear excitations, the independence of excitation from the state of the system does not hold. Hence, the force function of a finite element approximation is a function of the state of the system and weighted impulse input to discrete-time linear time-invariant systems are dependent on the filter state.

The discussion will be limited to a class of non-linear friction phenomena called "stick-slip" friction [3]. A particular instance of stick-slip friction is the action of a violin bow on a bowed object (typically a string). Early work has been performed by Helmholtz

[12] This condition is usually divided into linearity within one input, called homogeneity or scaling property and linearity between multiple different inputs, called additivity or superposition property [142, p. 18].

[86], Rayleigh [159] and Raman [158], though early mentionings can be traced back to Galileo Galilei [69, p. 331] and Chladni [40, 218]. Keller and Friedlander [101, 72] independly developed the theoretical foundation of bowed string action that is still widely used today in computer models [186, 133]. The friction characteristic used by them is depicted in Figure 2.8. This basic model was subject to a number of refinements taking into account the width of the bow [150] and more detailed knowledge of the action of rosin on the bow [183, 184] and has been used in waveguide synthesis [180].

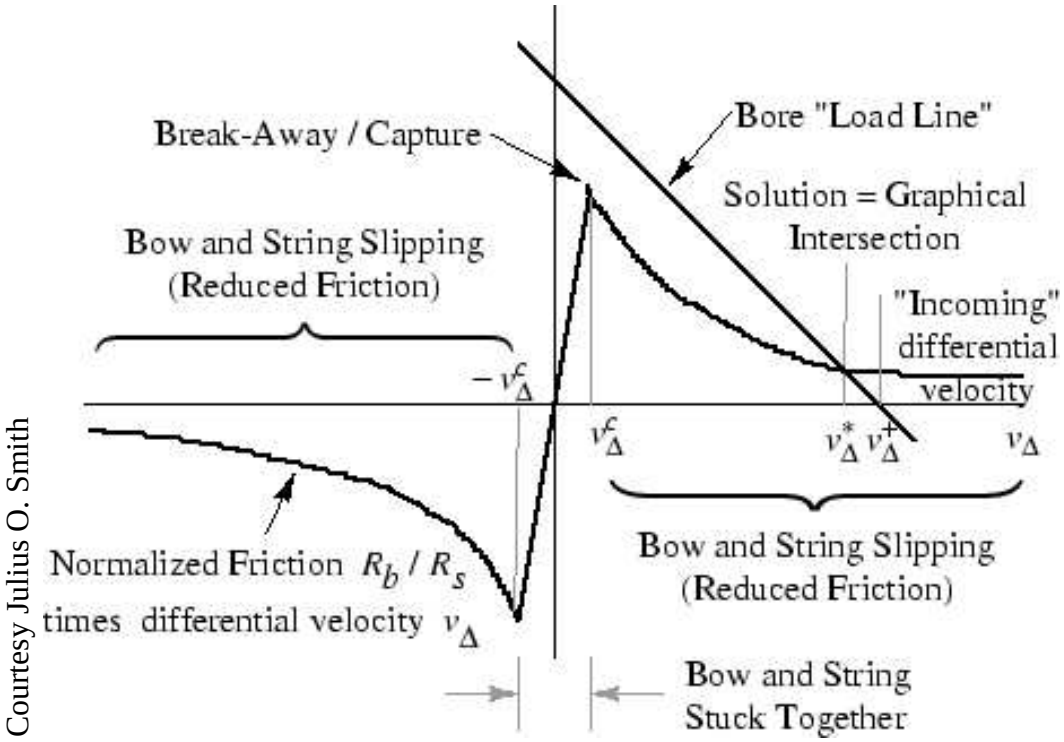

Figure 2.8: Friedlander-Keller friction diagram (from [188]).

It has been known since Chladni [40, 218] that other objects (in particular bars and plates) can be bowed using a rosined bow. In particular this has been recently used to study the glass harmonica [172]. Nonetheless the specifics of the musical application of the violin bow to other systems remains largely unexplored. A notable and fascinating

example is the Chinese Dragon Wash which includes not only the friction-induced sound production but also water waves [53, 52].

Stick-slip friction as excitation of sound is in other contexts considered undesirable. Examples are brake noises [3, 87], propeller shaft noises of submarines [69], squeals from train wheels [84, 82], friction noises of insects [3] and more. This lead to a large corpus of research on friction-based oscillations [3, 69, 92, 93, 203, 123, 87] is concerned with the damping (i.e. control) of such sounds [83, 197, 85].

Chapter 3

Theory of Propagation Modeling Using Banded Digital Waveguides

Anybody else could have told me this in advance, but I was blinded by theory. – **Bertrand Russell**[1]

I hear that you write poetry as well as working in physics. How on earth can you do two such things at once? In science one tries to tell people, in such a way as to be understood by everyone, something that no one ever knew before. But in poetry, it's the exact opposite. – **Paul Dirac to Robert Oppenheimer**[2]

Junta ist totz (*sic*) der langen Regeln einfach zu erlernen[3] – **From the German instructions to the board game Junta**[4]

[1] In "The Autobiography of Bertrand Russell," vol. 2, chap. 5, p. 288 (1967).

[2] Attributed by Leo Moser in H. Eves, "Mathematical Circles Adieu," Prindle, Weber and Schmidt, p. 70 (1977).

[3] *Junta is easy to learn, despite the long rules.*

[4] By ASS/Schmidt, 1986.

3.1 Overview and Motivation of Propagation Modeling for Sound Synthesis

In the real world, sound is generated through a wide variety of interactions between objects. Some interactions can be modeled easily, using simple and efficient methods, whereas others cannot. In a virtual world it is desirable that all interactions are captured by real-time simulation methods. In this chapter I study and generalize propagation models to explore possible intermediate solutions between simple resonant modal methods and slow but general finite-element methods.

3.1.1 Local Displacement to Moving Disturbance

Traditionally, when thinking of numerical simulation of elastic vibration, we are used to describing the change of displacement in the form of partial differential equations, which are derived from the constituent equations of general elasticity. Then these differential equations are approximated by discretization, which creates a finite sampling of the displacements in and on the physical objects. The finite difference operators describe how one sampling point moves depending on its neighbors. In this approach, the perspective of oscillation is a stationary one — the focus of observation is on the displacement of the local data points. There is, however, a different perspective possible: How do disturbances propagate in a medium? This question suggests keeping the focus on the position or the behavior of the disturbance itself, rather than focusing on the local displacements of the medium. This is the approach that is being taken in this thesis and will be described in the following sections.

3.1.2 Propagation of Sound in Air

Wave propagation as a way of thinking is by no means new to sound modeling. Some acoustical phenomena strongly suggest looking at propagation directly. Imagine you want to model an echo effect: A person calls into a valley and the call returns at various delays of time, having traveled down and up the valley and reflected at the side and bottom rocks. Propagation modeling of this kind is well known and widely used in simulating room acoustics [74]. As this propagation has a finite speed, air as a medium delays the arrival of sound . The listener does not really know or need to know the peculiarities or details of the sound traveling down the valley and returning but only how long it takes and how the sound changes. It does not matter when exactly a change in temperature affects the traveling speed, but that the delay was decreased or increased. It does not matter so much that there was a strong cross-wind in the valley as much as its effect on the heard sound. To abstract this picture, one can see the calling as input into a propagation system (the air confined in the valley) and the sound returning to the listener is the output (Figure 3.1).

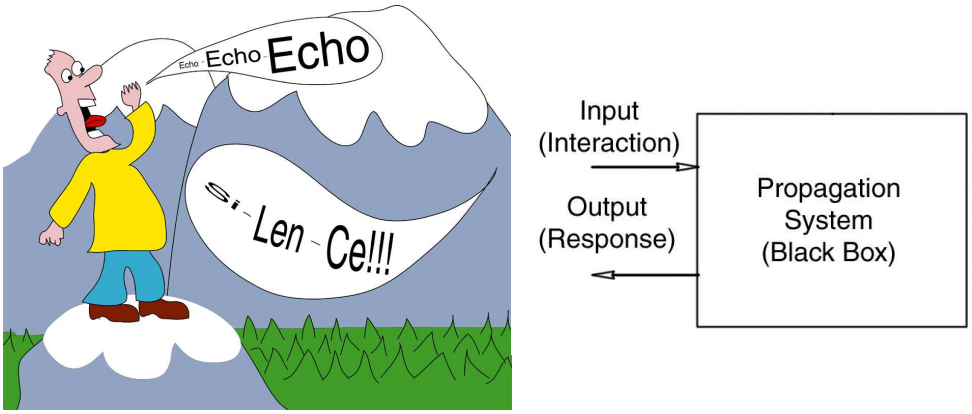

Figure 3.1: Input, propagation system, output.

3.1.3 Guided Waves

Air waves in tubes also propagate at a finite speed and get attenuated over time due to losses, but because of the constraints of the tube walls, the propagation direction is confined and or "guided." So-called *waveguide* models of musical instruments use this knowledge. It turns out that disturbances traveling on elastic strings have the same property and that string instruments can also be modeled using the same method.

Waveguide models assume that all frequencies travel at the same speed. This is not true for many media, in particular it is not true for solid objects of almost any material. However, the waveguide model can be modified and extended to accommodate slight variations in propagation speeds. Low piano strings, for instance, are thick enough so that the bending stiffness becomes important and does introduce noticeable effects on the sound. High frequencies travel slightly faster than low frequencies and the resulting effect on wave shapes is called dispersion. This effect is relatively weak and can either be modeled by spreading the reflection function [122] or by adding an all-pass filter which introduces the appropriate propagation response [187]. If the dispersion becomes a dominant behavior, as in the transverse oscillation of solid bars, both these approaches becomes expensive.

3.1.4 Limits and Alternatives to Propagation Modeling so Far

So it might seem like the propagation idea is in trouble when it comes to modeling vibration of solid objects. This is a large class of real-world objects of interest for musical and non-musical sound simulation. In this case, we have two approaches that don't explicitly use the propagation idea. A very general approach is to discretize the object in space and simulate the constituent equation that describes the interactions in

the object using finite or boundary-element methods [135]. At present, these methods are computationally expensive and not suitable for real-time application. A second approach uses just the modal frequencies of objects to simulate their sound. These modal frequencies are typically derived from measurements [208] but could also be derived from the general equations used for finite element methods. This method is efficient and works well for all types of linear interactions. This means that the interaction can be well described by impulsively adding energy to the system. For many complex interactions, however, this assumption is not true. Rather the interaction does depend on the physical state (i.e. force, velocity, displacement) of the object, like multiple bounces of interacting objects or strongly non-linear interactions like stick-slip friction. The following section discusses how this limitation can be overcome using propagation modeling.

3.2 A Sketch: Generalizing the Propagation Idea

We have previously proposed for one-dimensional objects that, in fact, the propagation idea can be preserved and leads to efficient simulation [61]. Here we would like to extend the idea to sounding objects of two and three dimensions. In later sections, we will explain the application of this idea to bars, Indian Tabla drums, and glass harmonicas, each being an example of one, two and three-dimensional structures, respectively.

The key point of our method is to maintain the sound propagation interpretation in objects and use an understanding how this propagation gives rise to the sound response of the object.

In essence there are two possible sound responses of an object to interaction:

- *Resonant mode:* After the wave has traveled through the object and come back, the wave closes onto itself in its original phase. In the absence of damping, the

energy of that frequency will be maintained while traveling on the object because this situation constitutes "constructive self-interference." This principle is called the principle of closed wavetrains [47] or simply *wavetrain closure*.

- *Anti-modal response:* The traveling wave does not close onto itself in phase. The energy will dissipate quickly at that frequency due to destructive self-interference.

Hence, there is an intimate connection between the modal response of an object to excitation and the propagation of frequencies in the object.

To be valid, propagation modeling has to observe these two points. Sound waves at resonant frequencies have to close on themselves in phase after traveling through the objects and returning, or an anti-modal response occurs otherwise.

Generalized propagation modeling takes these constraints literally. The propagation of frequency bands is modeled in such a fashion that at the wavetrain closure exactly matches the modal response of the system and that at other frequencies the waves are damped out quickly. A digital structure which has exactly this property is a frequency-band-limited delay line, which closes onto itself. As described before, a delay line which closes onto itself is a basic building block of waveguide models. We have named this structure the "banded waveguide" [61]. However, this physical analog is valid only for structures where waves are strictly guided: essentially one-dimensional structures like solid bars. For higher-dimensional structures it would be more appropriate to refer to wave-paths than wave-guides. Banded waveguides can be implemented efficiently : delay lines have constant execution time per time step. The band-limiting can be achieved by using a simple band-pass filter, as most applications do not require modeling the anti-modal response precisely[5]. Finally, fine tuning of the length of the delay is necessary,

[5]A higher order filter design could be used if precision is desirable.

especially for high frequencies. This can be achieved by adding a simple fractional delay filter [187]. The computation time for these filters is negligible.

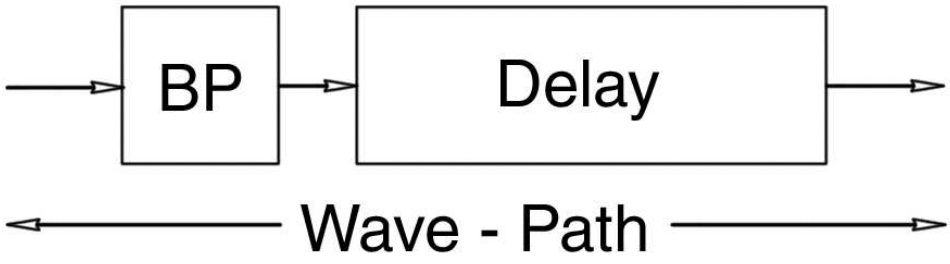

Figure 3.2: A single banded wave-path. BP is a band-pass filter.

The relationship between frequency and traveling speed is not unique, because it depends both on the traveling distance and the traveling time, so knowledge of both is necessary to maintain the proper relationship between propagation and frequency. The additional information to remove this ambiguity can either be measured or derived from constituent equations. When the traveling speed and the traveling length is known, the traveling time can uniquely be calculated. If this information is not known, we can take a good guess and use that guess in the simulation. The system spectrum will be modeled correctly, but the response time may differ. This affects only the transient response of the system, as the modes come in either too fast or too slow, but once the mode is established, it physically looks no different. For non-linear interactions this means that an object may lock to a mode more quickly or not as quickly as expected, but it won't affect that it locks to the mode. Hence, the result sounds and behaves qualitatively correct.

The minimal structure of a complete model consists of one "banded wavepath" per mode of the structure. The sought physical quantity is the sum of the output of all paths. Simplifications can easily be achieved by ignoring less significant modes, which

is analogous to only considering the most prominent eigen-frequencies of a system in principle component analysis. The total computational complexity depends only on the number of significant modes of the objects, which for many real-life objects is very small, as we will see in the examples described in the following sections.

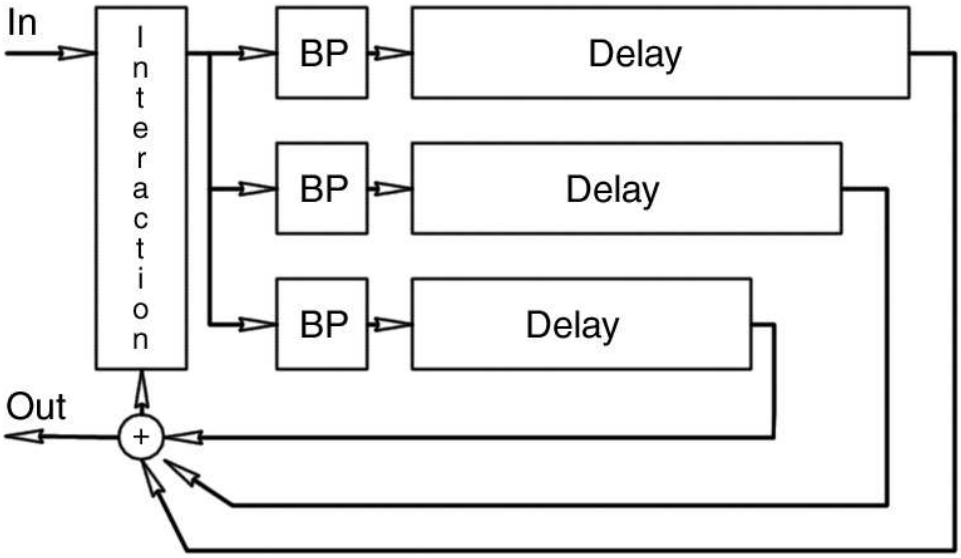

Figure 3.3: A simple banded waveguide system.

More complex structures are possible, if details of propagation are known and deemed necessary for improved simulation. Figure 3.4 shows two concatenated banded waveguide structures to show the propagation of waves to a reflection point, the reflection interaction being explicitly modeled and the propagation back to the start. Also note, that by splitting traveling paths, interaction and observation points can be made different as can also be seen in the location of the output in Figure 3.4.

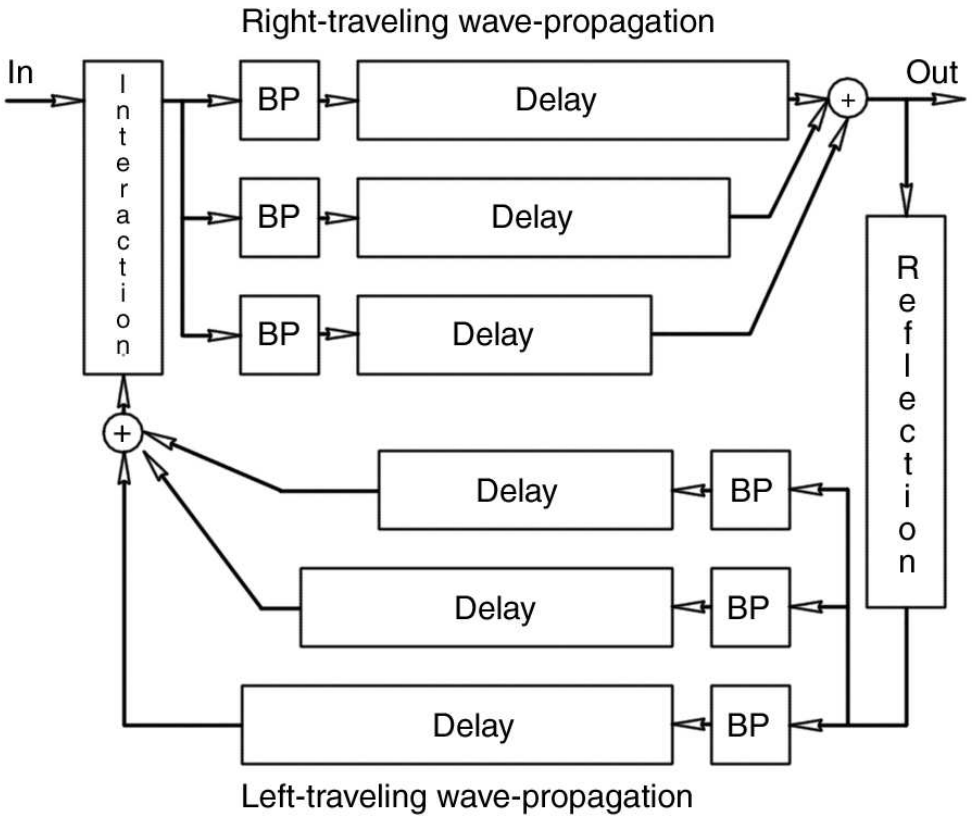

Figure 3.4: A banded waveguide system including explicit modeling of the reflection.

3.3 Description of Abstract Banded Waveguides

Banded waveguides can be viewed in various different ways. In this section, I will present them in their most abstract form, without additional interpretation. In the following sections, I will then go on discussing them in various interpretations.

In the most abstract sense, banded waveguides are frequency-domain decompositions of propagation phenomena. The complete behavior is separated into sub-domains and the overall behavior is assumed to be the sum of contributions of each sub-domain. More formally, banded waveguides start with the assumption that the closed frequency domain

Ω of a propagation phenomenon can be decomposed into $N = 1 \ldots n$ sub-domains Ω_n such that:

$$\Omega = \sum_{n=1}^{N} \Omega_n \tag{3.1}$$

The operator F when acting on Ω has the property of returning Ω_n for all n and hence will be called the domain sub-division operator. This operator may or may not be separable into operations F_n such that:

$$F_n \Omega = \Omega_n \quad \forall n \tag{3.2}$$

Secondly, it assumes that within each sub-domain Ω_n the modeled behavior can be separated into one or more components D_n^i with $i \in I$ of wave-propagation of constant speed within Ω_n and zero or more components H_n^j with $j \in J$ which don't observe that property.

Thirdly, each sub-domain component structure (the set of all D_n^i, H_n^j, which may or may not include F_n, for a particular n) or the sum of all substructures (including F for separation and the summation for combination Σ[6]) is cyclic, in general. That is, the domain Ω and also the domains Ω_n each have their boundaries connected.

The cyclic domains, with or without the equation 3.1, can be seen in Figure 3.5.

[6]May also be denoted by F^{-1}. The Σ is preferred as it corresponds to the definition of recombination in equation 3.1

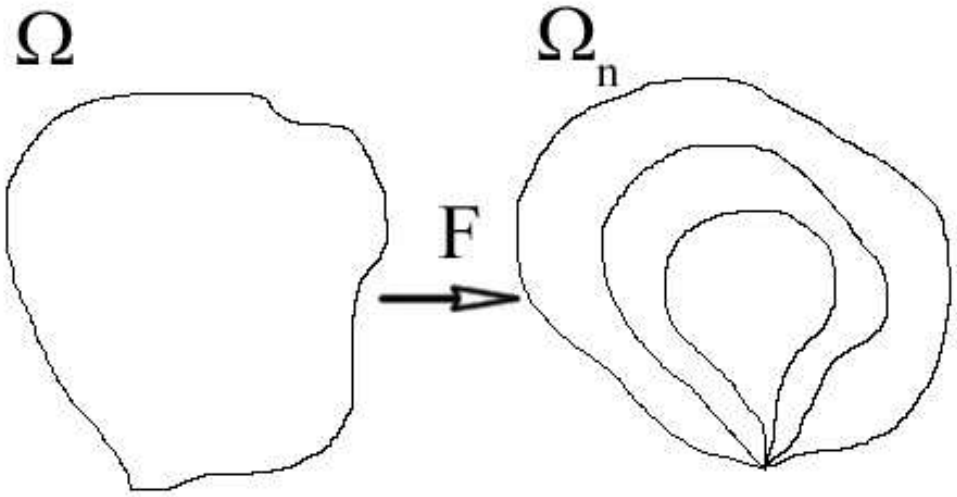

Figure 3.5: Abstract depiction of the cyclic property of domains and their decompositions

According to the above definition, the minimum banded waveguide consists of domain-decomposition F, and a set of constant-speed wave-propagators D_n, one per sub-domain Ω_n.

3.3.1 Notation

As a notational convention[7], D_n^i and H_n^j refer to abstract components (one could also think of them as continuously defined within the domain Ω_n). An index ω in parenthesis following the components denotes the frequency response of the component, i.e. $H(\omega)_n^j$ usually with $\omega \in \Omega_n$[8]. The z-transform [194, 142] will be denoted caligraphic script letter followed by z in parenthesis by $\mathcal{H}(z)_n^j$. In all instances, indices and parenthesis may be omitted if properties are discussed which are true for all instances of a component, that is

[7] See also [48, section 10.2] for a related symbolic notation. I chose a different notation to relate more closely to filter theory and also because I would like to capture more than just the transition dynamics with this notation.

[8] Note that in cases of non-exact decomposition into sub-domains this may be loosened to Ω, that is the frequency over the whole domain may be considered.

$\mathcal{H}$ describes properties of all $\mathcal{H}(z)_n^j$ with $n = 1 \ldots N$ and $j = 1 \ldots J$. Also an index may be dropped if the size of the index set is one. For example, if $N = 1$ then we write $\mathcal{H}(z)^j$.

Operator Σ should usually be read as summation over index n corresponding to equation 3.1.

3.4 Banded Digital Waveguides as Filters

The abstract model described in the previous section can readily be turned into a digital filter model by assuming that the domains Ω and Ω_n are discretized and that all operators are discrete linear operators. In fact, we'll assume uniform discretization of the domain or a mapping to a uniform discretization. Hence all structures involved are indeed linear time-invariant digital filters [142].

From the definition of the properties of the operator in the previous section, a number of properties of the digital filters can be inferred. This connection will be discussed in the following sections for all operators.

3.4.1 Domain Decomposition Filtering

Though the filter structure for achieving domain decomposition is quite general, I will, in this thesis restrict the considerations to single-rate systems. Hence time-domain decimation as in decimation filterbanks and wavelets [204] are not considered. While in the abstract notion of banded waveguides there is little motivation to this restriction, I will justify this decision when discussing physical interpretation of the structure (section 3.6) and computational performance (section 3.11).

While, per se, in the abstract definition, the functional form of the propagating wave of the decomposition is not prescribed, we will assume that a sum of sinusoids (that is

a Fourier basis) is a good basis. Hence any frequency band decomposition observes this assumption and the definition of section 3.3.

$\mathcal{F}(z)$ then could be any type of bandpass filterbank or a discrete Fourier transform, and $\mathcal{F}(z)_n$ would correspond to individual bandpass filters or bins in a discrete transform. Which particular structure should be chosen depends on the desired decomposition, which in turn will depend on the application and interpretation of the structure. This choice will be discussed in sections 3.5–3.10.2

3.4.2 Constant-Speed Wave Propagation Filter: Delay line

The decomposition chosen in the previous section separates into Fourier subdomains, so Ω_n can be read as a discrete band-limited frequency domain. As by definition, the propagation operators D_n propagate waves at constant speed independent of frequency content, the corresponding filter has to delay all frequencies by the same amount within the frequency band defined by the respective subdomain Ω_n. One operator which satisfies this condition can be written by the z-transform [194, compare p. 69]:

$$\mathcal{D}(z)_n = z^{-d} \quad \text{with } d \in \mathbb{R} \tag{3.3}$$

where d is the delay in samples per time-step. I will limit myself to this operator in the following discussion. In particular the delay operator can be split into two parts, a delay part of integer length (we will choose the largest integer less than or equal to d) d_i and a non-integer or fractional delay part d_f:

$$\mathcal{D}(z)_n = z^{-(d_i+d_f)} \quad \text{with } d_i \in \mathbb{N} \text{ and } d_f \in [0,1) \in \mathbb{R} \tag{3.4}$$

$$\mathcal{D}(z)_n = z^{-d_i} z^{-d_f} \tag{3.5}$$

The integer time delay is simply a queue[9] of length d_i. The fractional delay is a sub-sample delay operator whose practical realization is reviewed in [114].

3.4.3 The Perturbation Filter

By definition in section 3.3, the operators H_n are not restricted, except that they contain behavior that cannot be modeled by the propagation operators D_n with the sub-domain Ω_n. The only real restriction of H_n is that it operates within the sub-domain and hence can be any filter structure with this condition. Here we will add another restriction, namely, that of $\mathcal{H}(z)_n$ being a linear time-invariant filter. The meaning of this restriction and its possible loosening will be discussed in the context of the interpretation of the concrete interpretation of $\mathcal{H}(z)_n$ in application. The same is true for the actual form of the filter which again is highly dependent on the application and interpretation and hence will be revisited in sections 3.5-3.10.2.

3.4.4 Domain Reconstruction Filtering

Domain reconstruction can either be derived from the abstract combination equation 3.1, where the reconstruction is simply the sum of the sub-domains, or one could also see the reconstruction as the inverse to the decomposition operator $\mathcal{F}(z)$, that is a reconstruction filterbank or an inverse Fourier transform.

[9] More precicely a queue with first-in, first-out property.

3.5 Banded Digital Waveguides as Phase-Corrected Modal Synthesis

As discussed in the background chapter in section 2.1.3, modal synthesis simulates the decaying modal frequencies of sounding objects using either additive sinusoidal synthesis or resonant filterbanks. The advantage of the latter is that it has a direct physical interpretation as equivalent mass-spring-damper oscillators and hence force inputs can be converted conveniently into appropriate digital units.

Modal synthesis is a degenerate form of the banded waveguide structure, lacking closed loop delays D_n or perturbation filters H_n. Hence, the domain Ω of this structure is simply a point. The total model equation is:

$$F \cdot F^{-1} \tag{3.6}$$

In particular F is a resonant filter bank and F^{-1} is the sum over all the output of the filter bank.

Compare this structure with the structure of the decomposed domains of an abstract banded waveguide (Figure 3.5), which can be symbolically written as:

$$F \cdot [D_1 \cdots D_n] \cdot F^{-1} \tag{3.7}$$

where $[\,]$ implies that the operators D_n are applied to the sub-domains created by operator F.

The operators D_n are all-pass filters and hence only modify the phase of the signal within each frequency band and as the F^{-1} is only a linear combination of the separate bands, the difference between modal synthesis and banded waveguides of the form of equation 3.7.

$$F \cdot D \cdot H \cdot F^{-1} = D \cdot H \tag{3.8}$$

That is, there is only one subdomain which is equal to the original domain (hence both the decomposition and reconstruction operators are unity) and there is only one chain of propagation.

3.6 Banded Digital Waveguides as Generalized Digital Waveguides

Digital waveguides as introduced in section 2.1.1 have the following abstract notation:

$$D^1 \cdot H^1 \cdot D^2 \cdot H^2 \cdots D^j \cdot H^j \tag{3.9}$$

or, if all H^j can be commuted it has the abstract “Karplus-Strong” equation:

$$D \cdot H \tag{3.10}$$

As can be seen the digital waveguide structure simply is a banded waveguide structure without domain-decomposition (which is equivalent to saying over one sub-domain, $N = 1$).

3.7 Banded Digital Waveguides as Multi-scale Numerical Method

The abstract definition of the banded waveguide structure as introduced in section 3.3 does not directly specify a physical interpretation of the structure. It does contain a notion of delay which in a physical sense does link to a notion of time. Assuming that D_n^* is the total accumulated delay operation of the subdomains Ω_n then the original definition leaves undefined the relationship between these delays. The case of equal delay of all sub-bands has been treated in the previous section and simply corresponds to the standard digital waveguide structure. In this case, digital waveguide filters also carry a physical interpretation of space. The d'Alembert solution describes the propagation of waves along the spatial extension of a string. Correspondingly a unit time delay Δt represents a unit of spatial length Δs, which can be calculated from the time-delay via the wave-velocity c (compare to equation 2.1):

$$\Delta s = c \cdot \Delta t \tag{3.11}$$

In the more interesting case of sub-domain having distinctive delays, if a subset is interpreted to follow the same spatial trajectory of length l then, given a defined temporal unit Δt, the speed c_n within each sub-domain is:

$$c_n = \frac{l}{d_n^* \cdot \Delta t} \tag{3.12}$$

where d_n^* is the accumulated delay of D_n^* from equation 3.3. Then the spatial unit Δs_n of each sub-domain, using these two equations, can be calculated as:

$$\Delta s_n = \frac{l}{d_n^*} \tag{3.13}$$

which by definition of d_n^* being different between sub-domains and l being constant implies that Δs_n is different between sub-domains. This means that different sub-domains describe different spatial scales within such a spatial interpretation. This property is depicted in Figure 3.6 using two delay lines of length n and m. As can be seen the second delay line has a coarser spatial resolution than the first one.

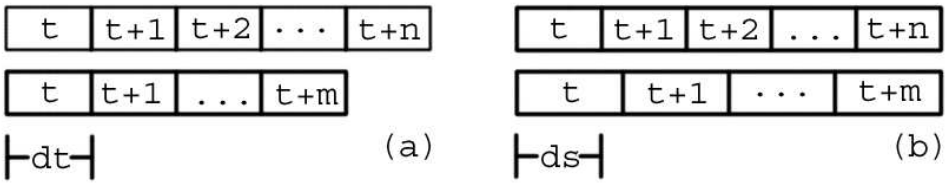

Figure 3.6: (a) Constant time representation and (b) constant space representation of a banded wave-path.

3.8 Banded Digital Waveguides as Discrete Asymptotics Simulation

The principle of wavetrain closure states that a mode will occur when a traveling wave after following some path closes onto itself and the wave is in phase with itself at the closing point of the path. Otherwise no mode occurs. In essence, the mode comes about as constructive interference of a traveling wave with itself.

3.8.1 Previous Work: Traveling Wave Solutions

The idea of constructive and destructive interference of linearly independent traveling waves is a long known phenomenon, that has explained many observations involving waves, like diffraction patterns.

The d'Alembert solution of the ideal finite string is maybe the first specific example of a description of a dynamical system that follows the wavetrain closure principle.

Extension of this type of description to other dynamical systems happened in the middle of the last century independently in the acoustics community and the mathematical physics community. Among the acousticians who developed the idea were Mead [124, 125, 126, 127], Cremer and Heckl [47]. The focus was primarily on bar structures but attempts were made to extend to square plates.

Another line of research again comes from the eminent scientist Joseph Keller who is in the community mostly known for his work on theoretical non-linear friction behavior of the bowing violins [101] and the friction characteristic is generally known as Friedlander-Keller diagram [188] (it has been simultaneously and independently studied by Friedlander [72]).

Keller studied asymptotic approximations to dynamical systems, in particular optics and quantum mechanics. In joint work with Rubinow, he proposed that the method could also be used to find eigenvalues of dynamic structures [104]. The idea is that the dynamics of structures can be well approximated by studying the behavior of traveling wave rays. This is similar to using principles of geometric optics to describe general optical wave phenomena asymptotically, as Keller did in his geometric theory of diffraction [102]. Keller and Rubinow showed how, using their approach, circular membranes and elliptical domains can be solved. They also showed how whispering gallery modes and bouncing ball modes can be derived on more arbitrary two-dimensional domains. Though the theory of asymptotics has found a lot of interest and applications in many fields [103], the study of structural dynamics as relevant for many musical instruments has been quite limited, the exception seems to be work by Chen, Coleman and co-workers who study the effect of bending stiffness using Keller's approach [39]. In less direct form, this approach has seen extensive interest in the mathematics and physics community. Finding a closed path on a closed domain of some shape can be seen as a billiard ball rolling on a surface and bouncing off the walls and returning to its starting position. In this setting, billiard balls are said to be on periodic orbits, and the task is to find them. On the convex domain this has been extensively studied by Birkhoff and others [109].

Traveling wave methods are studied and used in a vast number of different fields. Connected theories have been developed in pure and applied mathematics with various motivations. Among them is approximate and exact solutions of ordinary and partial differential equations, even when they may not be integrable [139, 215, 68] often motivated by equations that arise in classical mechanics [205, 108] or quantum mechanics (the asymptotic approach is usually referred to as "semiclassical mechanics" for the limit of the asymptotics establishes the correspondence between classical results and quantum

mechanical formalism) [103, 25] and has been instrumental in both areas (and others) in the study of chaos [48][10]. Even in simple integrable dynamical systems, a traveling wave Ansatz usually has points where a unique solution cannot be derived (referred to as caustics, see also Appendix A). Solutions at and in the neighborhood of these points are sought via connection formulas [13] and special functions [139, 14], as topological projection [129, 110][11] and via hyperasymptotic expansions [78, 24, 89] [38, for a detailed review including the connection to rays in two-dimensional elasticity dynamics]. Asymptotic methods find applications in electromagnetics [23] and seismology [50].

3.8.2 Previous Work: Numerical Traveling Waves

Numerical simulation based on discretized traveling waves for the wave-equation was accidentally discovered by Karplus and Strong and was quickly recognized to be a very efficient method of simulating the dynamics of strings and air-tubes. This method is called "digital waveguide filter method" [187]. It is an accurate simulation for ideal strings and other idealized waveguide systems that are basically one-dimensional. It can be seen as discrete implementation of the d'Alembert solution of the governing equation. However, it is probably much more intuitive to consider the d'Alembert solution a proper dynamical description rather than a solution. Deviations from the ideal are then introduced while maintaining the traveling wave picture. Local damping and dissipation are described as damping and dissipation of a traveling wave along its path and at boundary reflections. Stiffness is introduced as a change in propagation characteristic, and so on. If the perturbations from the ideal case are small, this works quite well:

[10] The usefulness of asymptotics in studying phenomena has also been the focus of interest within the philosophy of science [10] especially as a way of reasoning between different levels of details with quantitatively different behavior. For a short and popular account see [15, 73].

[11] A very brief but lucid review of the the connection between "Lagrange manifolds" and caustics through projection can be found in [58].

the digital waveguide filter method is widely successful for many musical instruments. Digital waveguide filters have a number of additional advantages over finite differencing. Stability considerations are much more simple and intuitive, as in the case of waveguides, the deciding factor is simply whether the loop gain is below or above unity. The transportation within the waveguide is "numerically safe" as disturbances are transported multiplication-free, i.e. they are simply copied and hence even a gain of unity yields a perfectly sustained oscillator which is difficult to achieve with "algebraic propagation" involving multiplications and additions, as in the case of finite differencing. The key benefit though is that, in addition, or rather because of this condition, waveguides can be implemented with constant numbers of operations (read, write and pointer updates) independent of the length and hence the spatial sampling, whereas finite differencing schemes depend on the spatial sampling resolution.

Figure 3.7: A digital waveguide filter.

An interesting note to make is that we are, in fact, using an asymptotic method that is valid for the short wave-length limit and ceases to be strictly valid for long wavelengths. One might hence be tempted to conclude, that all this should not work. Surprisingly though it has repeatedly noted, that even for the long wavelength solutions (that is the low eigenmodes), the asymptotic method performs well [104, 178]. In specific cases, like the d'Alembert solution for the wave equation, the "asymptotic" traveling wave Ansatz is in deed exact.

3.8.3 Discrete Asymptotic Simulation

The relationship between banded waveguides and traveling-wave, ray or Wenzel-Kramers-Brillouin (short WKB) methods[12] can be seen using the following line of reasoning. Starting with the minimal banded waveguide equation 3.7 and letting the number of sub-domains go towards infinity, one arrives at a function defined in $\omega \in \mathbb{R}_0^+$ over the initial domain Ω:

$$d(\omega) = \lim_{n\to\infty} F \cdot [D_1 \cdots D_n] \cdot F^{-1} \tag{3.14}$$

$$\tag{3.15}$$

$d(\omega)$ can then be interpreted as a continuously (though not necessarily smoothly) defined function of delays over the domain. Writing the delay using an exponential propagator and interpreting ω as frequency one gets:

$$e^{-i \cdot d(\omega)\omega} \tag{3.16}$$

This form corresponds to the Keller-Rubinow-form of the WKB-asymptotics found in their seminal treatment of oscillatory problems in two dimensions [104, eq. (3)] describing the sum of all paths:

$$u = \sum_{j=1}^{N} e^{i \cdot kS_j} \left[A_j + O(1/k) \right] \tag{3.17}$$

[12] For a glossary of terms used in the asymptotics literature also refer to Appendix A of this thesis.

If the the loop described by the domain Ω is interpreted as two parts, a forward propagating half and a backward propagating half, then this becomes:

$$e^{+i\frac{d(\omega)}{2}\omega} + e^{-i\frac{d(\omega)}{2}\omega} \tag{3.18}$$

This form corresponds to the oscillatory (that is imaginary part) of the Olver-form [139, p. 190, eq. (1.02)] of the WKB-asymptotics[13]:

$$w \sim A \cdot e^{x\sqrt{\{f(x)\}}} + B \cdot e^{-x\sqrt{\{f(x)\}}} \tag{3.19}$$

Hence, in the limit of infinite sub-domains, banded waveguides can be considered equivalent to WKB-asymptotics, and, in the finite case, it is a finite approximation of it. It should be noted though that this does not imply that the method is necessarily just approximative to any dynamics. In the case of the wave equation the d'Alembert solution of the exact dynamics, the traveling-wave Ansatz are exactly equivalent (derivation of the d'Alembert solution can be found in many standard textbooks, for example [111, chapters 11.3 and 11.4]).

The correspondence between WKB-asymptotics and banded waveguides is of immediate relevance because the known results of properties of asymptotics, ray and traveling-wave methods become immediately relevant to the mathematical and physical understanding of banded waveguides. This correspondence will become relevant in the follow-

[13] Which Olver calls LG approximation, see Appendix A.

ing section discussing banded waveguides in dimensions higher than the one-dimensional line-model[14]

3.9 Banded Digital Waveguides in Higher Dimensions

In previous sections, I have introduced a spatial interpretation (section 3.6), and the domain composition has been given a spectral interpretation (section 3.4) of the abstract banded waveguide model of section 3.3. However, the domain separation of operator F can also be interpreted geometrically. Then operator F can be interpreted as:

$$F_m \Omega = \Omega_m \tag{3.20}$$

with Ω_m being geometric sub-domains, which in turn each can be decomposed into spectral domains:

$$F_n \Omega_m = \Omega_{mn} \quad \forall m \tag{3.21}$$

For the remaining discussion, the geometric sub-domains will be assumed to be ray or line domains, and hence the discussion that has previously been carried out in one dimension can be interpreted as applying to the one-dimensional trajectory of that domain.

[14]Dimension here refers to the number of spatial dimensions of the dynamical system under consideration or, equivalently, the number of independent spatial dimensions in the constituent differential equations describing the dynamics. The time and possibly orthogonal deflection dimensions are excluded.

3.9.1 Previous Work: Single-band Multi-path or Multi-dimensional Models

Waveguides have been used in higher dimensions under a ray-casting paradigm. This work mostly relates to work in room reverberation algorithms as already mentioned in section 2.1, where delay-lines were introduced. Not all works in the field that use delay-lines use them beyond a listener-receiver path description [90, p. 38, for example]. The use of multiple connected feedback delays has been introduced by Stautner and Puckette [191] and is now generally referred to as feedback delay networks (FDN) [170, and references therein]. In the early work of Stautner and Puckette, the delay-paths were associated with channels and only loosely associated with the geometry of the room, though the association of geometry to room response has been introduced by Allen and Berkeley [12, see p. 183-185 for a brief review]. The "room of mirrors" idea behind their "image" or "image-source" method describes how a reflected source is equivalent to a mirror image acting as a source through the reflected wall. This topological mapping of a reflected path to an unreflected path corresponds to the construction of a resonant torus as introduced by Keller and others [104, 25][15] (see section 3.9.2). The connection between resonant response of a geometric enclosure and its shape has been realized in this context by Rocchesso and studied in the case of a rectangular box[166, 170] and sphere [167].

An alternate approach to multi-path feedback delay models can be found in the literature of physical models for string instruments. Until recently, the focus has been on studying physically separate but coupled structures like coupled piano strings [8, 9, 6] or sympathetic strings in plucked string instruments [99]. Here two separate paths couple at some point. These paths are geometrically independent otherwise. A more interesting

[15] I'm unaware that this connection has previously been pointed out.

recent example is the detailed modeling of the action of a bow on a string as presented by Serafin and Smith [180]. This work showed that strings are not ideally thin but have in fact finite thickness. Torsion in direction of the bow is introduced though torsional waves in a linear string traveling independedly from transverse waves. Hence Serafin and Smith arrive at a two-path waveguide model with one path for each wave type. In fact, a four waveguide model has been suggested by Smith to implement waves in two orthogonal planes for transverse oscillation, longitudinal waves and torsional waves [187].

3.9.2 Topology of Resonant Paths

In general, the problem presents itself in the form of a given geometric shape that is responsible for the sound-generating dynamic (e.g., the shape of the membrane of a drum) and by ray-casting on that shape, finding closed paths which then correspond to eigenfrequencies. This is a very general problem that is still under intensive investigation (for detailed pointers into review literature I refer to Appendix A). Here I will confine myself to 2-dimensional discussion of square and circular domains. There two are fully treated domains in Keller and Rubinow's seminal paper on the subject [104][16]. A more contemporary and generalized treatment of the subject not confined to these particular domains and dimensions can be found in [25, p. 78 ff.].

For simplicity we will assume just the finding of a closed path and will ignore the propagation dynamics in this treatments.

Taking a rectangular domain, we assume that the behavior of the boundary of the domain is complete geometric reflection. Starting of with a family of parallel rays shooting of at some angle, geometric reflection just means an inversion of the travel direction normal to the boundary.

[16]The derivation has been repeated in many places, for instance [103, 39].

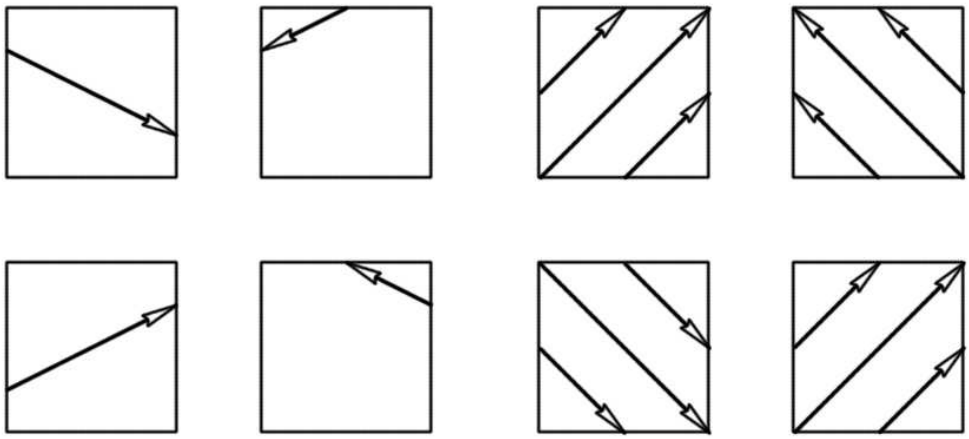

(a) Reflections of a single ray (b) Type of Reflections for ray family

Figure 3.8: Reflection of a ray at the boundary

This behavior is depicted in Figure 3.8. Figure 3.8 (a) shows the first for reflections of a ray starting with the configuration in the lower right corner and going around counter-clockwise. Figure 3.8 (b) shows the same general behavior for a whole family of rays. This picture should be interpreted as states rather than as actual ray paths, meaning that there are four possible propagation configurations that change depending on reflections at the boundary. Any family of rays with an angle different than 90° will eventually reflect and change directions. As a ray propagates through the domain it can reflect many times until it closes onto itself but it still can only be in one of these configurations. Up-down reflections are cyclically repeated as well as left-right reflections[17]. As is widely known in signal processing, an open infinite domain with regular repeating substructure (e.g. periodic sampling) can be mapped onto a closed circular domain (e.g. the z-transform of a periodically sampled signal) [194, chapter 11]. The same holds here, though there is

[17]This resembles the familiar picture of alternating configurations of image-sources for increasing orders of reflections in the image-source method. For a related depiction see [12, Figure 4.55, p. 185].

repetition in two dimensions, hence the circular folding has to happen along both axis. The first folding turns the two-dimensional sheet into the surface of a cylinder by gluing the top and the bottom edge together and the second folding merges the ends of the cylinder to form a torus (see Figure 3.9).

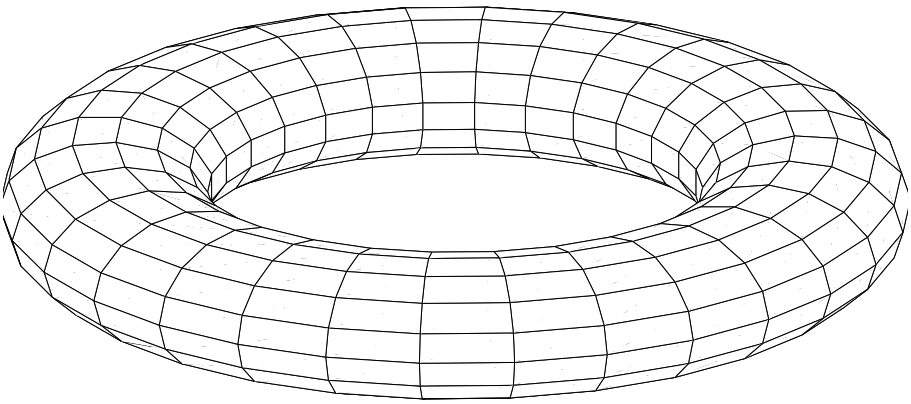

Figure 3.9: Resonant torus of EBK quantization of two-dimensional closed paths.

More generally any integrable system can be brought into the form of an N-torus embedded in a $2N$-space by canonical transformation [25, p. 79 ff].

The torus structure has an intuitive appeal as it highlights that there are two topologically independent dimensions that lead to closed curves. In the 2-torus case the first follows along the outer rim to close onto itself and the second follows the radius of the thickness to close onto itself[18]. A general path will wind around both dimensions (and hence the related numbers are sometimes called “winding numbers” [48]) to close back onto the same position on the torus. It also illustrates that the actual starting position

[18]Hence authors describing two-dimensional domains often use two-number labelings to identify closed paths. For an example in the square case see [154], for one on circles and circle-segments see [161].

does not matter due to the symmetry of the structure which justifies the initial treatment of families of rays rather than rays with specific positions. Finally, as the surface area on the torus is the same as the area traveled on the original domain, short and long closed path configurations can be intuitively observed. For instance if the angle is very flat with regards to one topological dimension, then the path will have to wind around this dimension many times before having traveled around the other dimension once. Finally it can be immediately seen that closure can only occur if and only if the ray has traveled through an integer number of windings in all topological dimensions (because if a winding number in a dimension is not integer the winding is incomplete).

This yields the closure condition, which by requiring integer solution, and by attribution to early contributions to this technique by Einstein, Brillouin and Keller is usually called EBK quantization.

We are interested in total ray length and its relationship to the frequency of standing waves, but we have so far ignored the effect of the boundary.

Classical Dirichlet boundary conditions correspond to a sign inversion in the amplitude, which in turn can be written as a phase-contribution of π because:

$$e^{i\cdot\pi} = -1 \tag{3.22}$$

The principle of equal phase closure demands that the phase is single-valued after one round-trip on a closed path. If ΔS denotes the change in phase, then it can be written as:

$$\Delta S - \mu \cdot \frac{\pi}{2} - b \cdot \pi = 2\pi \cdot n \tag{3.23}$$

for all n in $\mathbb{N}_0^+$, which leads to the common form of the quantization rule:

$$\Delta S = \left(n + \frac{\mu}{4} + \frac{b}{2} \right) \cdot 2\pi \tag{3.24}$$

where μ is called the Maslov index, which counts the number of touched turning points inside the domain (also called caustics, see Appendix A), and b is the number of Dirichlet boundaries reached.[19] In the case of the rectangular domain, there is no caustics, and hence $\mu = 0$, and there are multiple of two reflections b. The caustic will be revisited in the case of the circular domain.

Returning to the two-dimensional case described by the torus, this quantization rule must hold for both dimensions. Rescaling the quantization condition by the path-length $2 \cdot l_n$ (the domain is transitioned twice for each winding) and using the relation:

$$f = \frac{c}{l} \tag{3.25}$$

and using the triangle inequality to calculate combined path contributions we get:

$$f = \frac{c}{2} \cdot \left(\frac{{m_1}^2}{{l_1}^2} + \frac{{m_2}^2}{{l_2}^2} \right) \tag{3.26}$$

where c is the speed of the traveling wave and l_1 and l_2 are the dimensions of the rectangular domain. m_1 and m_2 are positive integer quantization numbers. This corresponds to the classical solution of the square plate [132, p. 205].

[19] Note that some authors include the contribution of b in μ.

3.10 Theory to Application: Use of Banded Waveguides

With all this theoretical description, the question remains, how practical synthesis methods can be achieved using it. In other words, how are the components of the theory described in previous sections practically combined. First, I will talk about practical aspects of reaching implementations of simulations from actual physical instruments through the theory so far discussed. Then I will mention that the application does not necessarily require the physical interpretation of the previous section.

3.10.1 Physical Simulation

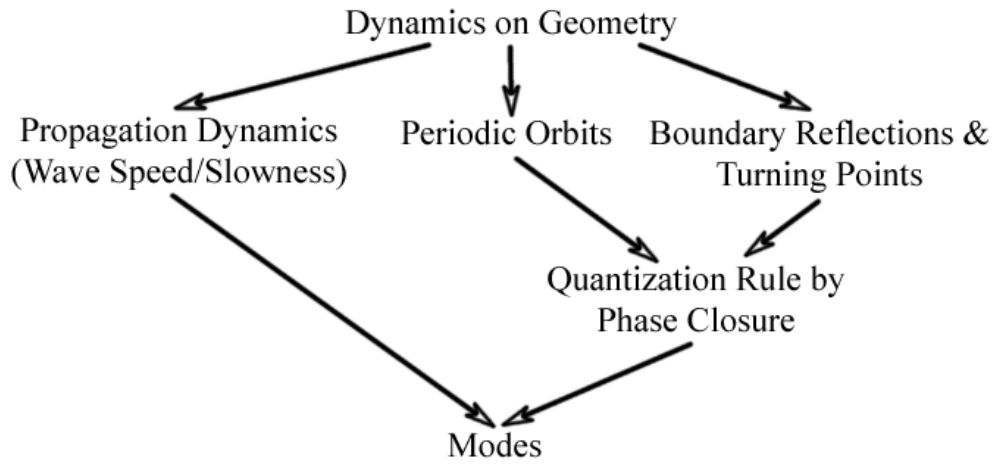

Figure 3.10: Relationship of geometry and dynamics to modes.

If the goal is to arrive at the simulation of actual musical instruments or physical but non-musical sound production mechanisms, then the question remains, how one arrives at specific implementable structures (section 3.4) from the theoretical approach to describing the dynamic (sections 3.8 and 3.9).

The connection between geometry and dynamics and modes as primary components of sound production is summarized in Figure 3.10.

In fact, the connection between components in Figure 3.10 can follow two directions. First, if following the direction of the arrows, this corresponds to a construction of a simulation from complete dynamical and geometrical description. Then the tasks are:

- Find periodic orbits.
- Identify boundary conditions and turning points and their phase contribution to periodic orbits.
- Find wave propagation speed characteristics.

However, this is not necessarily the most practical approach. Finding periodic orbits can be difficult, and the theoretical dynamics of a complex instrument may not be known. Hence it may be difficult to find the wave propagation speed characteristics. Finally this construction is not precise.

More realistically, if the physical instrument is available, certain parameters can be measured. Other parameters may be known only approximately. Thirdly, not a complete construction may be desirable.

In this context, the relationship between measured modes and theoretically constructed modes is of interest. As said, the theoretically constructed modes are approximate. The measured modes are, however, precise within measurement accuracy. The proposal is, to tune closed wave-paths to the precise frequencies. Then, the deviation between approximate theoretical, exact theoretical, and actual behavior is bridged by introducing the theoretical deviation from the measurement in form of a path-length correction to the theoretical path.

3.10.2 Application as Non-physical Entities

The abstract structure, and even the filter interpretation thereof, does not necessarily need a physical interpretation. In this case, banded waveguides can be seen as a purely abstract synthesis methods with certain properties. The choice of parameters then becomes aesthetically motivated rather than physically.

Here I only want to mention one example of non-physical application of this structure that was discovered by accident. If the output of the reconstruction operator is numerically integrated (accumulated sum), and the appropriate "physical" interpretation of the result of reconstruction would have been displacement, one arrives at a quantity that is not properly physically informed. If this integrated displacement is then fed into a standard bowing interaction model, rich, chaotic sounds can be produced in a stable manner using this method.

3.11 Performance and Critical Sampling

The performance of banded waveguide synthesis is defined by the behavior of the various building blocks. In general, the delay operator for integer sample delay can be cheaply implemented using circular buffers (as mentioned already in section 2.1). In fact, the performance is independent of the length of the delay and hence $O(1)$. The remaining parameters defining the computational complexity of the algorithm is the number of subdomains n, the number of separate delay and perturbation blocks i and j.

Hence a driving parameter for the performance is the number of non-delay blocks that are incorporated in the model.

In fact, the asymptotic WKB ansatz is equivalent to neglecting coupling of in- and outgoing waves [32]. The interplay between precise differential equations, couplings

(also referred to as scatterings) and discrete traveling wave approximations has been extensively studied by Bilbao [18], though the treatment of scattering in digital waveguides has long been known [188]. Hence one critical area for performance gain is the process of deciding when neglecting local scattering in a dynamical system is a good approximation or not (physically and perceptually).

Finally, the implementation of the domain decomposition, perturbation filters and fractional delays also affect performance.

In this thesis I do not consider decimation in time for sub-bands. This is justified by the realization that the critical performance improvement from $O(M)$ to $O(1)$ (where M is the spatial sampling) has already been achieved and that the computational load (i.e. the constant in $O(1)$ of time-stepping a delay line is very small). In the same vein, inexpensive second-order bandpass filters can be used for domain-decomposition making this method overall $O(N)$, where N is the number of modeled subdomains with a small multiplicative constant only. Whether a trade-off with decimation and interpolation operators versus sub-domain time-stepping yields significant gains remains to be explored (see section 7.6.3).

3.12 Interaction Models

Physical interactions usually take place on the whole domain Ω. Hence either at interaction points the whole domain has to be reconstructed or the interaction needs to be translated into contributions to each sub-domain. If the latter is a choice depends whether or not the interaction implies local scattering. In general, scattering should be assumed for non-linear interactions and may be absent for linear ones (see section 2.2). The implications will be discussed by example in chapter 4. Here it should only be

mentioned that in case of modeling the contribution separately to the various spectral sub-domains implies contributions to spatial samplings of different scales (as described in section 3.7), and hence the contribution has to follow the same scaling.

3.13 Conclusions

We introduced propagation modeling using banded waveguides to the spectrum of methods to simulate sounds of objects. The guiding question with regards to this and other methods is: What is the least amount of information we have to consider to get the desired result? The propagation idea allows for significant reduction of complexity and dimensionality while allowing for retaining essential features. It allows for complex, non-linear, yet natural interactions which cannot be modeled by other comparably efficient models. It does this at the price of making a direct geometric interpretation specific and potentially difficult.

Chapter 4

Applications of the Banded Digital Waveguides

> Grau, teurer Freund, ist alle Theorie,
>
> Und grün des Lebens goldner Baum[1]. – **Johann Wolfgang von Goethe**[2]

> Few things are harder to put up with than the annoyance of a good example.
>
> – **Mark Twain**[3]

> Trust me, it sounded good before I improved the model. Now it sounds more realistic.

In this chapter I will discuss application of the theory of banded waveguides to particular musical instruments. In general the progression will be an increase in spatial dimensionality. In addition, experimental data will be presented to evaluate simulations.

[1] *All theory, dear friend, is gray, but the golden tree of actual life springs ever green.*

[2] In "Faust" pt. 1 (1808) according to [147, p. 309, q. 5]

[3] "Pudd'nhead Wilson," chap. 19 (1894) available online at `http://www.cs.cofc.edu/~manaris/books/Mark-Twain-The-Tragedy-of-Puddnhead-Wilson.txt` and according to [147, p. 706, q. 23]

4.1 1-D Case: Rigid Bars

Bowed bar percussion instruments have found increasing interest and application in musical composition and performance in recent years. However, the excitation of a sustained oscillation of a bar by means of a rosined bow for musical purposes has not yet been studied systematically.

So far research on bar percussion instruments has focused on the issue of tuning by removing material at various locations along the bar [143, 20, 149, 27], the influence of the resonators on the vibrating bar and the radiated sound [20, 56], and the effect of striking excitation using mallets [35]. Material properties have also been studied [29, 88]. Numerical simulations use either finite difference [20, 35, 56][4] or finite element methods [143, 27, 21]. Summaries and reviews of the research on bar percussion instruments are available [131, 171, 70]. When the sound of bar percussion instruments is synthesized for real-time performance using electronic sound generation, the above mentioned finite difference and element methods lack the necessary efficiency on current hardware to be appropriate. Hence, current techniques only model the modes of the system, using modal filters [219, 42] or additive sinusoidal synthesis [182, 210] ignoring the modal shapes. Hence, the notion of physical shape and interaction is lost, and a direct way to use these approaches for bow interactions is not possible. In essence, the spatial dynamics is removed by replacing the actual physical system by an equivalent mass-spring system which models the same modal response. However, the dynamics (in particular the propagation of disturbances) of the original system is lost. Hence it cannot, in general, be expected that non-linear interactions are captured by the simplified mass-spring model. If the modal shapes are known, the spatial information can be maintained

[4]Since the writing of this passage for archival journal publication [61] finite differencing through corresponding wave digital filters as been proposed by Bilbao [18] and others [2].

and bowing interactions remain meaningful. This approach has not yet been tried for bars of musical instruments, but was used to study the stick-slip interaction [183, 184]. To use this method, the modal shapes have to be known a priori. These are difficult to get analytically because the undercutting of tuned bars make the equations non-linear, and experimental measurement is much more costly than simple frequency analysis.

This section describes how banded waveguides can be used for simulation for the purpose of preserving a notion of spatial shape while achieving real-time performance. An a priori knowledge of modal shapes is not necessary. These results have also been presented in [60, 61, 62] and will be discussed in section 4.1.1.

The action of the bow has only been studied extensively when exciting strings [46, 91]. Numerical simulations typically use an efficient time-domain approach which follows from the constant phase delay characteristic of the ideal string equation [122] and this approach has been refined for synthesis purposes [186, 181]. The string has also been studied using a finite difference approach [33, 34, 146]. The action of the bow on solids is known to be able to excite a sustained oscillation and is especially famous in the creation of Chladni figures [218]. However, a study of the dynamics and kinematics of this system is lacking as is a study of parameters which are relevant for musical performance. The violin bow has also been used to study the excitation of glass harmonicas [172]. Experimental work on the action of a bow in rigid bars will be presented in section 4.1.2.

4.1.1 Simulations

Propagation Model Implementation

As noted in section 3.10.1, for the implementation of banded waveguides for a physical system, three tasks have to be performed. Periodic orbits have to be found. Boundary

conditions and turning points with their phase contribution have to be identified. Finally the wave propagation speed characteristics has to be found. Starting with the uniform bar, the first two tasks are trivial. The latter can, in this case, be derived from the known constituent equation of the system. Transverse vibration of bars is well described by the 1-D Euler-Bernoulli-model [47], given that the bar is thin compared to its length and the exact frequencies of very high order partials is not important:

$$\frac{\partial^2}{\partial x^2}\left(EI\frac{\partial^2 y}{\partial x^2}\right)+\rho A\frac{\partial^2 y}{\partial t^2}=f(x,t) \tag{4.1}$$

EI is the flexural rigidity (E being Young's modulus and I being the cross-sectional moment of inertia) and ρA is the mass term (ρ being mass density per unit length and A being the cross-sectional area). In general these quantities are not constants but may depend on x. $f(x,t)$ is an externally applied transverse force on the bar. In order to model friction additional terms have to be added (see [35]). If cross section and elasticity properties are uniform, (4.1) becomes a linear 4th order partial differential equation which lends itself easily to analytical solution. In particular, when inserting the solution of a single frequency $y=Y(x)e^{j\omega t}$ the wave velocity (that is the propagation characteristic) can be calculated from (4.1) with $f(x,t)=0$ letting $a=\sqrt{EI/\rho A}$:

$$v=\sqrt{a\omega} \tag{4.2}$$

The wave velocity depends on the frequency of the traveling wave and hence arbitrary wave shapes disperse as higher frequencies propagate faster than lower ones. An illustration of the idea of the approximation in the banded waveguide method is depicted in figure 4.1 using the propagation delay of equation (4.2). The depicted constancy of the phase delay within a frequency band is only for illustration purposes, as the actual delay

depends on the band-pass filters $\mathcal{F}(z)_n$ and possible perturbation filters $\mathcal{H}(z)_n^j$ used. It is depicted because it shows the effect of using the constant delay $\mathcal{D}(z)_n$ per subdomain.

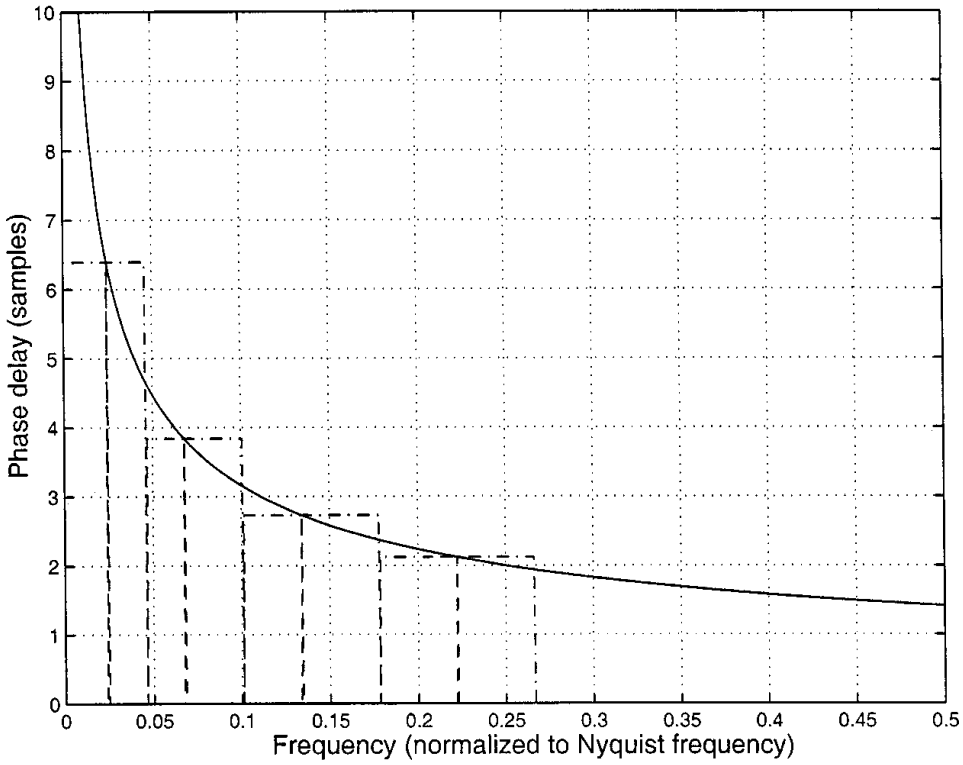

Figure 4.1: Discretization of the phase delay in a banded waveguide simulation.

This flat quantization over a region in the phase response (see figure 4.1) makes the phase delay constant in that region which can be cheaply modeled using a standard waveguide filter. If the loop delay is tuned to a mode of the system, this corresponds to an exact simulation of the wave train closure and approximation in the neighborhood of that mode. To avoid large errors in this neighborhood approximation, the higher harmonic resonances of the waveguide should not be within the modeled frequency band. This criterion guides the choice of the bandwidth of the bandpass filter $\mathcal{F}(z)_n$.

Figure 4.2 shows the structure of a single banded waveguide and the frequency characteristic. The dashed curve is an ideal bandpass filter response which windows the

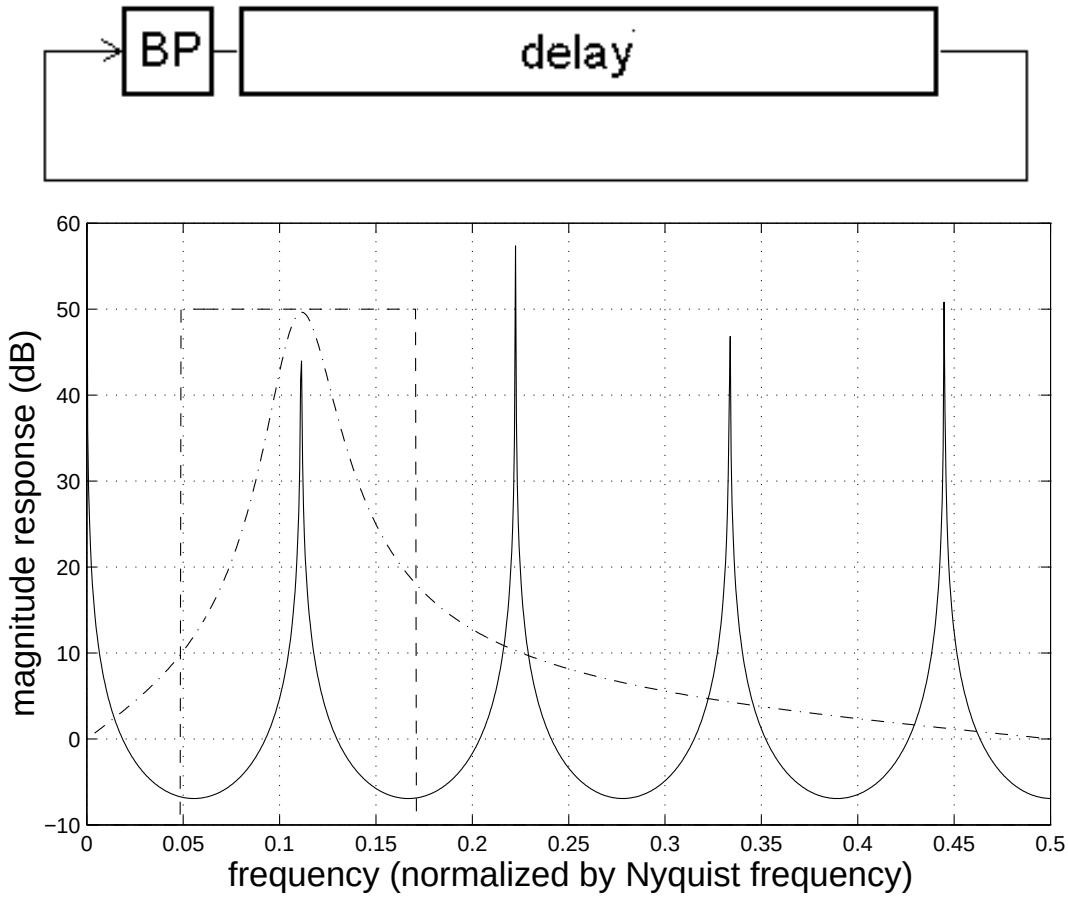

Figure 4.2: One banded waveguide (top) and its spectrum.

desired frequency band. The dash-dotted curve depicts the filter response of the second order resonant filter used as a bandpass filter approximation (for implementation details see Appendix B).

As can be seen, the propagation characteristic is, by construction, modeled exactly at modal frequencies. This is helpful as it allows precise simulation of modal responses even if one or more of the implementation tasks cannot be exactly performed. For example, exact phase effects at the boundaries may be unknown or the actual instrument may differ from the ideal. This explains the usefulness of the method for undercut bars. If the undercutting is not too deep, the physics of the bar can be expected to be close to

the behavior of the uniform bar and this method is appropriate. The wavetrain closures change with the undercutting and the banded waveguides have to be tuned to the changed frequencies. However, it is important to observe that for severe undercutting, reflections at the points of changing impedance have to be expected that are not captured in a straightforward way in an unmodified banded waveguide. In this case local scatterings and modifying effects would have to be modeled.

The nature of this correcting property of frequency tuning to the approximate nature of the starting assumption can be seen in the case of the uniform bar. The general solution of (4.1) for constant coefficients and in the absence of an external force can be derived to be [47]:

$$y = e^{j\omega t}(Ae^{kx} + Be^{-kx} + Ce^{jkx} + De^{-jkx}) \tag{4.3}$$

The first two terms are stationary oscillations (the so-called “near-field” terms) and the second two terms are left- and right-going propagation terms. The constants A, B, C and D depend on the particular boundary conditions.

As only propagation is modeled, the near-field oscillations are not modeled directly. If the wavetrain-closure frequencies containing the are modeled, then the contribution of the near-field terms to the frequency is modeled as propagating waves (that is, as phase contributions) and not as standing waves. Hence, it can be seen that this approach models the spatial shape only approximately. The near-field contribution, which should spread over the whole domain is localized into phase points. The propagation delay, modeled frequency and overall loop dynamics remain, however, exact. The same reasoning holds for other deviations and one can say that modifications to the uniform propagation are not exactly localized in this method.

In implementation the frequencies can either be measured, theoretically tuned or derived. In case of the uniform bar, using the "free-free" boundary condition, as is typical for bars in musical instruments, yields the well-known stretched and inharmonic partials of a uniform bar ($1 : 2.756 : 5.404 : 8.933 : \ldots$) as heard from glockenspiels. Marimba, xylophone and vibraphone bars are undercut, stretching the partials into harmonic ratios of either $1 : 4 : 10$ or $1 : 3 : 6$ [131].

Interaction Model Implementation

In the case of bowing on the narrow side of the bar, disturbances leave only in one direction and only this propagation has to be modeled.

In the implementation used for simulations used here, Smith's method of applying the bow-nonlinearity to a waveguide simulation [186] was used. This simplified approach simulates the behavior of sticking and sliding friction. During sticking, the friction coefficient is independent of the input velocity but once the differental velocity exceeds a certain value, the friction characteristics drops rapidly to a weak sliding friction. Figure 4.3 depicts the actual functional shape used. This model does not contain the hysteresis effect which arises in a slightly more detailed model [122]. Yet the model used seemed to capture the measured phenomena and an extension to incorporate the hysteresis rule has not been found to be necessary. Only the wavetrain closures of the lowest four modes were modeled by banded waveguides. This is reasonable considering the stretching of the partials in a bar. Hence, higher modes quickly fall outside the audible range. In addition, higher frequency modes are severely damped. For higher accuracy additional modes could easily be added for low computational cost.

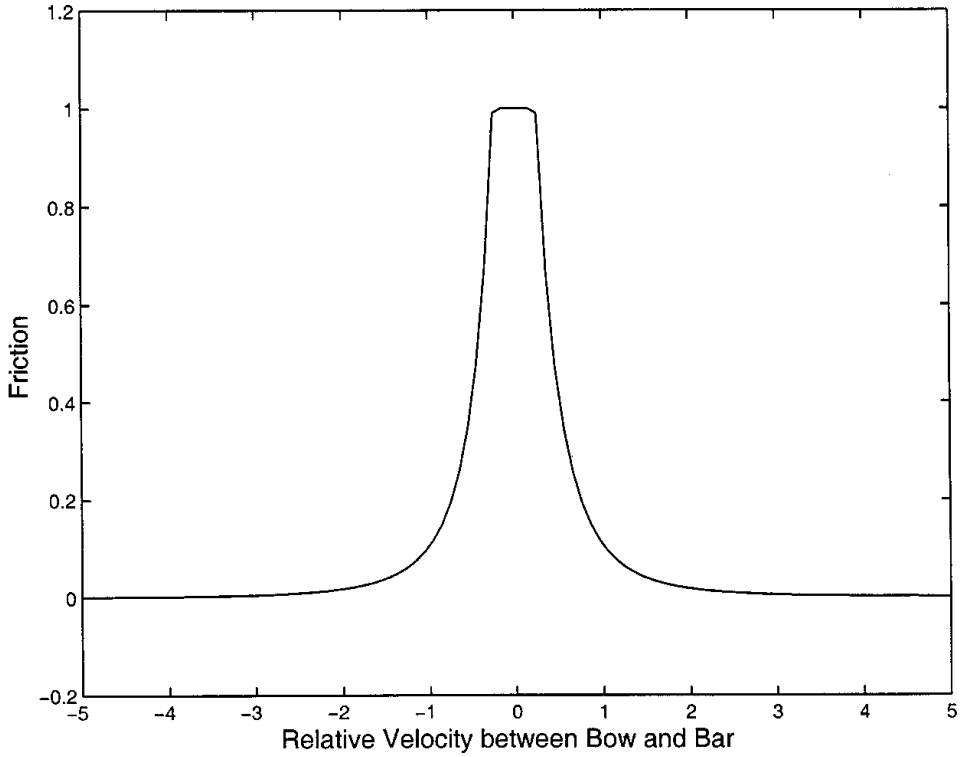

Figure 4.3: Friction characteristic used in the banded waveguide simulation. For a relative velocity around zero, the bow exerts a nearly constant strong static friction on the bow whereas when exceeding the relative break-away velocity, the characteristics drops quickly to low dynamic friction.

Simulation Results

In order to evaluate the dynamic validity of the simulation, measurements were performed and compared to simulation runs. The measurements are discussed in full detail in section 4.1.2. As input to the model and independent physical quantity for measurements, bow velocity and bow force were used. These parameters have been chosen because they are the main control parameters of bowed string dynamics, which has been extensively studied [46]. From the simulated output and the recorded dynamic response of the measurement procedure, the following response parameters are calculated: the amplitude (as a measure of loudness), onset time (the time it takes from the start the bowing action

to reach a maximum amplitude self-sustained oscillation), fundamental pitch (lowest dominant peak in measured spectrum) and spectral centroid (the center of gravity of the spectrum as measure of spectral content). All these are descriptive of the dynamic behavior.

Simulations using banded waveguides were performed in 12 steps between normalized input parameters of velocity and force yielding 144 data points. At each point, the amplitude, onset time, fundamental and spectral centroid were extracted from the data.

The simulations show qualitative similarity with the measured parameters (see section 4.1.2). The output amplitude shows a clear positive correlation with velocity and is largely independent of the force (figure 4.4) which mirrors experimental behavior (Figures 4.8 and 4.9). A separation of regions of oscillations and non-oscillation can also be seen in this figure. The onset time decreases with increasing force (Figure 4.5 is at a normalized input velocity of 0.75) which is also seen in experiment (see Figure 4.16). However the surface plot reveals a more complicated dependency of the onset time with force and velocity which goes beyond the measurements made. The fundamental frequency is independent of both force and velocity in simulation and measurement. The observed spectrum is harmonic in either case. The simulations show that the spectral centroid is independent of both force and velocity, as found in the measurements (see Figure 4.15). The details of the experiments will be discussed in the next section. In addition to the experimental comparison, the model shows additional behavior that is observed in qualitative performance and theoretically known for non-linear systems. For instance it is possible to lock to various modes depending on the input parameters, just as it is possible to lock to higher modes in performance.

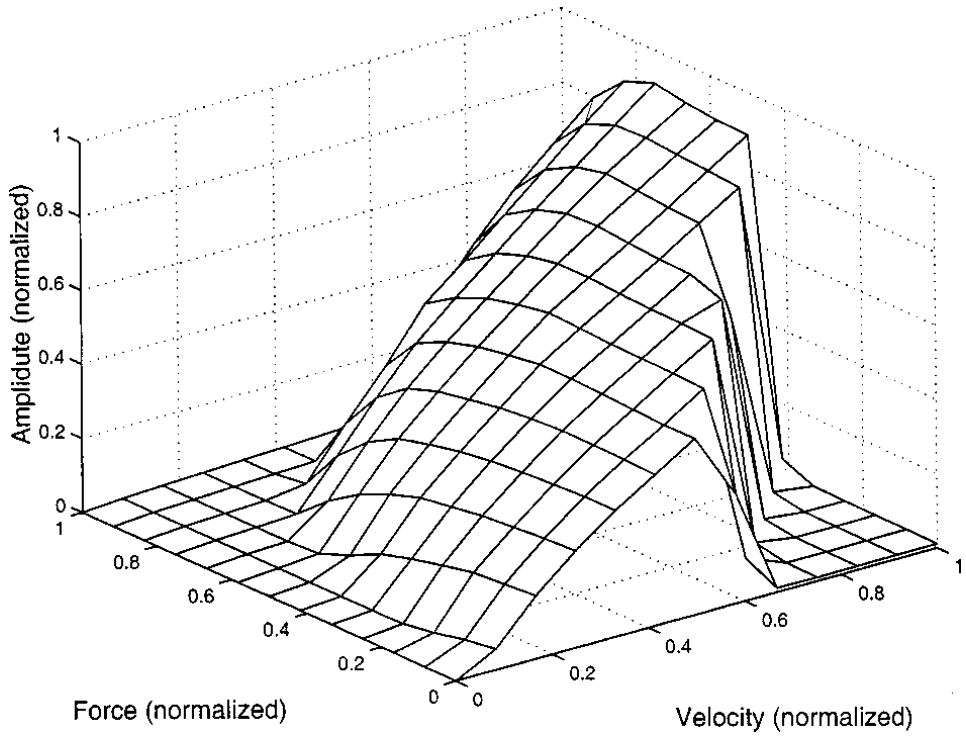

Figure 4.4: Amplitude as a function of input force and velocity in a bowed bar simulation using the banded waveguide method.

4.1.2 Experimental Measurements

Now I will discuss experiments that have been performed to study the behavior of bowing on rigid bars. This is the first time that such experiments have been performed and I describe here the complete results.

The primary goal of the experiment was the measurement of parameters which are of importance for musical performance when bowing bar percussion instruments. The parameters in control of the performer are primarily bowing velocity and bowing force. Parameters like angle, type of bow, amount of rosin were not considered in detail in these experiments. The performance parameters of interest were assumed to be loudness, temporal responsiveness, pitch, timbre and brightness. Other interesting parameters like

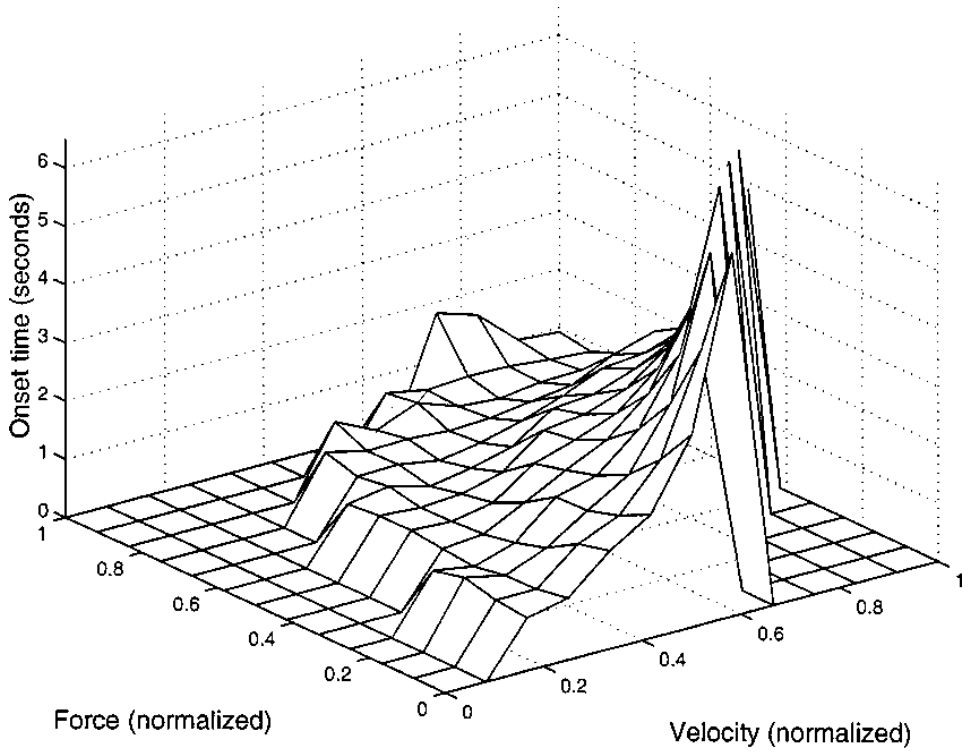

Figure 4.5: Onset time as a function of input force in a bowed bar simulation using the banded waveguide method.

ease of performance and “feel” of the bowing action were not investigated directly. From the measured parameters the region of oscillation is derived, but effects like the ease of locking to higher modes were not considered at all.

Loudness was measured by calculating the energy of the signal. Temporal responsiveness was measured as the time it took from starting the bowing action to reaching a maximum amplitude self-sustained oscillation. This time will be referred to as onset time. Pitch was measured by finding the fundamental in spectra taken from the measured signals. Timbre and brightness was measured by calculating the spectral centroid of the spectra of the measured signals.

Two distinct measurement setups were used. First, a number of bars of different size, shape and material were bowed by hand using a double bass bow. These measurements were performed to get a qualitative result of most of the described quantities.

In order to get more quantitative and reproducible measurements, a bowing machine was built and one bar was systematically studied for quantitative relationships between input (bow) velocity and force to output amplitude, energy, fundamental frequency, spectral content and onset time. These results will be described in section 4.1.2.

Measurements by Hand Bowing

Experimental Setup

For hand bowing, two different types of bars were used. One set of bars consisted of bars taken from real musical instruments. These bars are undercut to tune the upper partials to be close to harmonic. In this set, a bar representing the xylophone and marimba family and bars for vibraphones were used. Xylophone and marimba bars are made of wood (typically rosewood) whereas vibraphone bars are metal (typically aluminum).

The second set of bars consisted of wood and aluminum bars of uniform cross-section. These have inharmonic partials. The measurement of bars of uniform thickness has two purposes. For one it serves as comparison to the behavior measured for undercut bars. Secondly the Euler-Bernoulli equation for constant cross-section and homogeneous material is a linear fourth-order partial differential equation which lends itself to analytical treatment, which is otherwise not easily possible.

A sketch of the typical shape of a bar can be found in figure 4.6[5]. Table 4.1 shows the dimensions of the measured bars and table 4.2 shows the position and size of the

[5]Figure 4.6 has been corrected compared to [61]. The positions of the cord holes x_{1r}, x_{1l}, x_{2r} and x_{2l} were wrongly indicated.

	l (cm)	w (cm)	h (cm)	l_1 (cm)	l_2 (cm)	h_1 (cm)	E (GPa)	ρ (km/m^3)
Uniform wood	38.1	4.05	1.95	N/A	N/A	N/A	10	640
$C_4^\#$ wood	30.7	3.5	1.6	17.3	7.0	0.5	16	740
Uniform aluminum	17.8	3.8	0.3	N/A	N/A	N/A	70	2710
$F_4^\#$ aluminum	29.	3.9	1.3[6]	11.95	5.3	0.6	70	2710
$F_3^\#$ aluminum	36.4	5.1	1.3[6]	16.4	9.3	0.5	70	2710

Table 4.1: Dimensions and material constants of measured bars

cord holes. The material constants (Young's modulus and the mass density) were taken from a standard reference (see Table 19.1 p. 625) [70] and were not measured for the experimental bars.

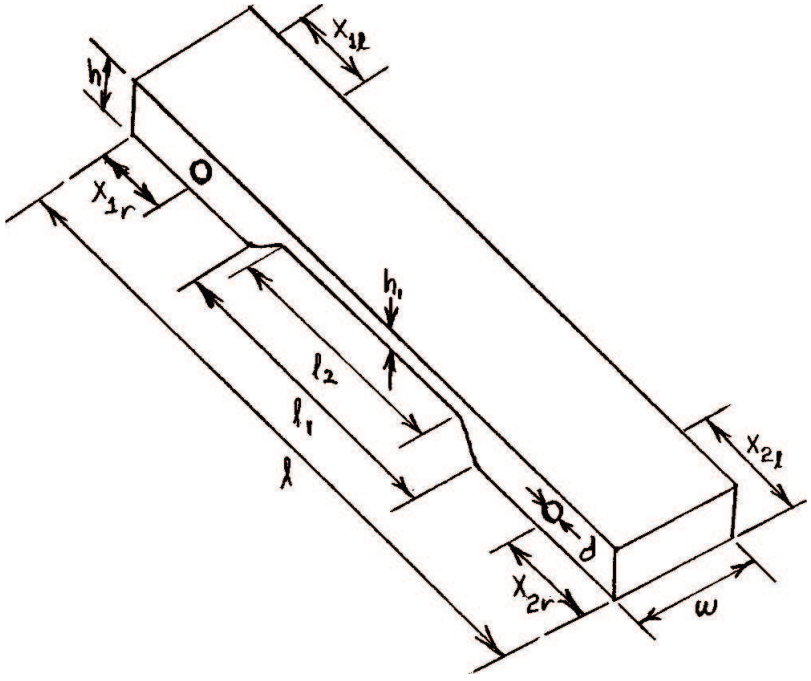

Figure 4.6: Sketch of shape and dimensions of a bar.

The bar to be measured was suspended using two stiff cords under tension between two vices. The microphone was placed underneath the middle of the bar. The typical

[6]The thickness of the vibraphone bars was misprinted as 1.8 in [61] and has been corrected.

	$x_{1r}\ (cm)$	$x_{1l}\ (cm)$	$x_{2r}\ (cm)$	$x_{2l}\ (cm)$	$d\ (cm)$
Uniform wood	3.9	3.9	3.9	3.9	0.7
$C_4^{\#}$ wood	5.8	5.8	6.	5.6	0.5
Uniform aluminum[a]	4.	4.	4.	4.	N/A
$F_4^{\#}$ aluminum	5.7	5.8	5.6	6.2	0.6
$F_3^{\#}$ aluminum	7.3	7.4	7.5	6.8	0.6

Table 4.2: Positions and diameter of cord holes in bars

[a]The aluminum bar had no cord holes. Instead if was held in place by rubber bands on thin plastic rods which were wrapped with felt at the given positions.

bowing point when bowing xylophone or vibraphone bars in a complete instrument is on the narrow end, as this is the only side which can be conveniently reached with a bow by the performer. Hence our measurements concentrate on bowing positions on the end of the bar. In some bowing strokes, especially when high bowing forces are applied, the oscillation of the mass spring system of the cords and the bar had to be damped by placing one hand on one of the cords and pulling down. The typical setup is depicted in figure 4.7. A rosined double bass bow was used for all hand bow measurements.

Measurement results

First, the response of the measured bars to impulsive excitation was measured using both a force hammer and a hard plastic glockenspiel mallet. Table 4.3 shows the frequencies of the dominant partials of each test bar along with the theoretical values for uniform bars as well as the usual tuning frequencies for undercut bars. As can be seen, the uniform aluminum bar is very close to the values predicted by the Euler-Bernoulli theory. The uniform wooden bar deviates substantially from the theoretical values, for two likely reasons. One is that the bar is not perfectly uniform due to the holes drilled 3.95 *cm* from both ends with a diameter of 0.75 *cm*. Second, the thickness is comparable to the width

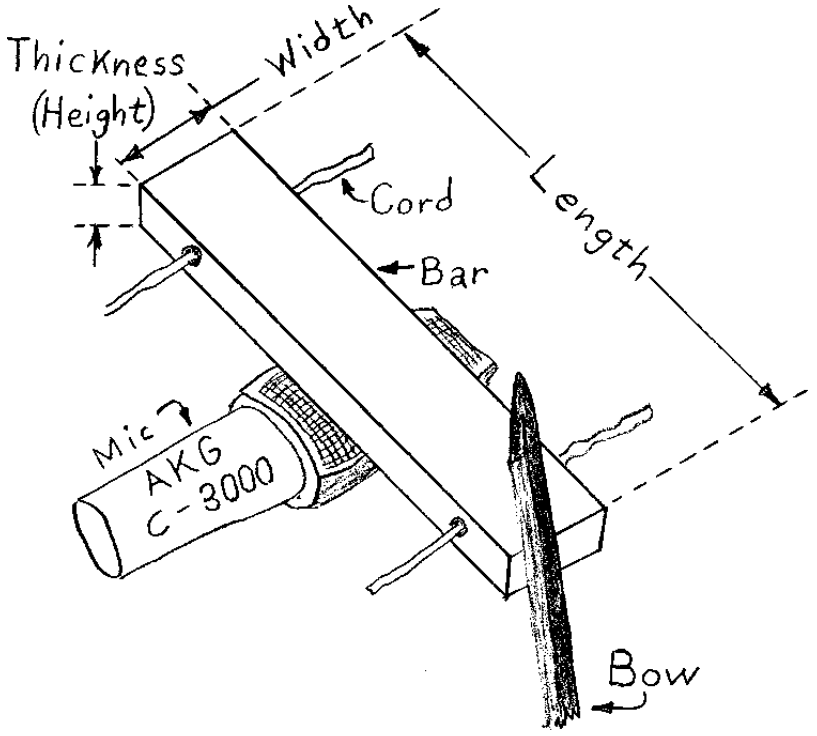

Figure 4.7: Experimental setup for hand bowing measurements of bars.

of the bar, in which case the application of the Timoshenko theory is more appropriate, which lowers the frequency of the upper partials [70].

The bowed bar exhibits a harmonic spectrum, though often weaker partials at the possibly inharmonic eigenfrequencies can be seen. This behavior can also be seen when bowing at positions other than one of the free ends. Bowing at the side is easily possible only with sufficient distance to the suspension holes. When bowing in the middle, the fundamental of the bar can also be excited. For the $F_3^{\#}$ vibraphone bar bowing in the middle will often lock to the second eigenfrequency of the bar, which lies two octaves above its fundamental eigenfrequency. This tendency to lock to the higher mode can usually only be overcome with increasing friction by tilting the bow or by other means.

n	Theory	Wooden (uniform)	Aluminum (uniform)	Usual tuning	$C_4^\#$ xylo	$F_3^\#$ vibra	$F_4^\#$ vibra
f1		693.9	487.		280.6	187.3	373.6
2	2.756	2.572	2.756	4.	3.932	3.984	3.997
3	5.404	4.644	5.423	10.	9.538	10.668	9.469
4	8.933	6.984	8.988		16.688	17.979	15.566
5	13.346	9.723	13.448		24.566	23.679	20.863
6	18.6408		18.680		31.147	33.642	29.440

Table 4.3: Spectral frequencies of dominant partials of measured bars and theoretical values given as $f_n : f_1$. The left side of the table contains the theoretical prediction for uniform bars and the actually measured ratios of the two measured bars. The right side contains the usual tuning and the measured ratio for tuned bars. The first row contains the actual fundamental frequency f_1 of the bars.

Another possible way of excitation is to contact the top surface of the bar. By bowing with little bowing force a proper regime of oscillation can be excited.

Using hand bowing, a qualitative relationship between bowing velocity and amplitude as well as between bowing force and amplitude was investigated. It should be noted that constancy of velocity and force within each measurement as well as across measurements (when applicable) were not possible as they are highly dependent on the subjective perception and the skill of the performer. As will be seen in the quantitative measurements using a bowing machine, the lack of constancy of bowing force is likely not a problem as the amplitude appears to be independent of the bowing force.

Figures 4.8 and 4.9 show the time domain envelopes of bowing strokes with increasing velocity and increasing force. From the length of the bow and the stroke time, which can be retrieved from the time-domain plot, an average input velocity can be deduced. Setting this velocity in relationship to the amplitude of the signal shows an approximately linear increase of amplitude with increasing velocity. Force was held nearly constant in the velocity measurement. The force measurement shows no clear

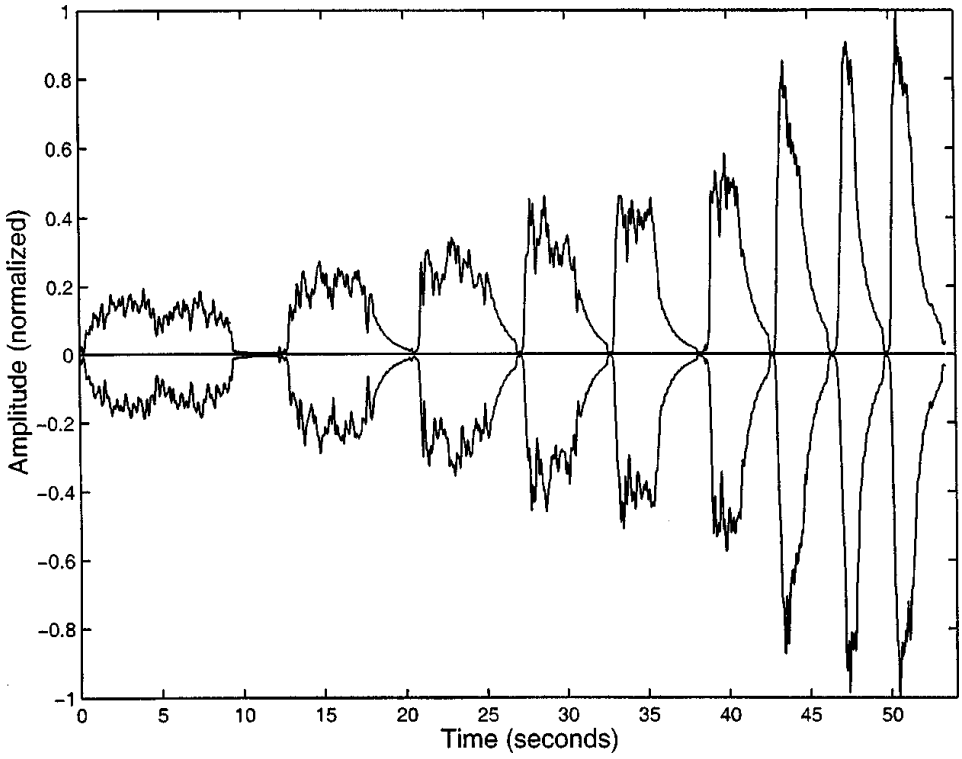

Figure 4.8: Time-domain amplitude envelope of hand strokes with increasing velocity and force held approximately constant.

influence on the amplitude. This finding was later validated by the bowing machine measurements. The time-domain shapes of the force-amplitude relation also hint at a decrease of onset time with increasing force. This result was also quantified using bowing machine measurements, as described in the next section.

Measurements using the Bowing Machine

Experimental Setup

The $F_3^{\#}$ aluminum vibraphone bar under investigation (see table 4.1) was suspended in a rigid bar holder. The holder has two effects. First it removes the cord modes or other movements which are not of interest while keeping the important degrees of freedom.

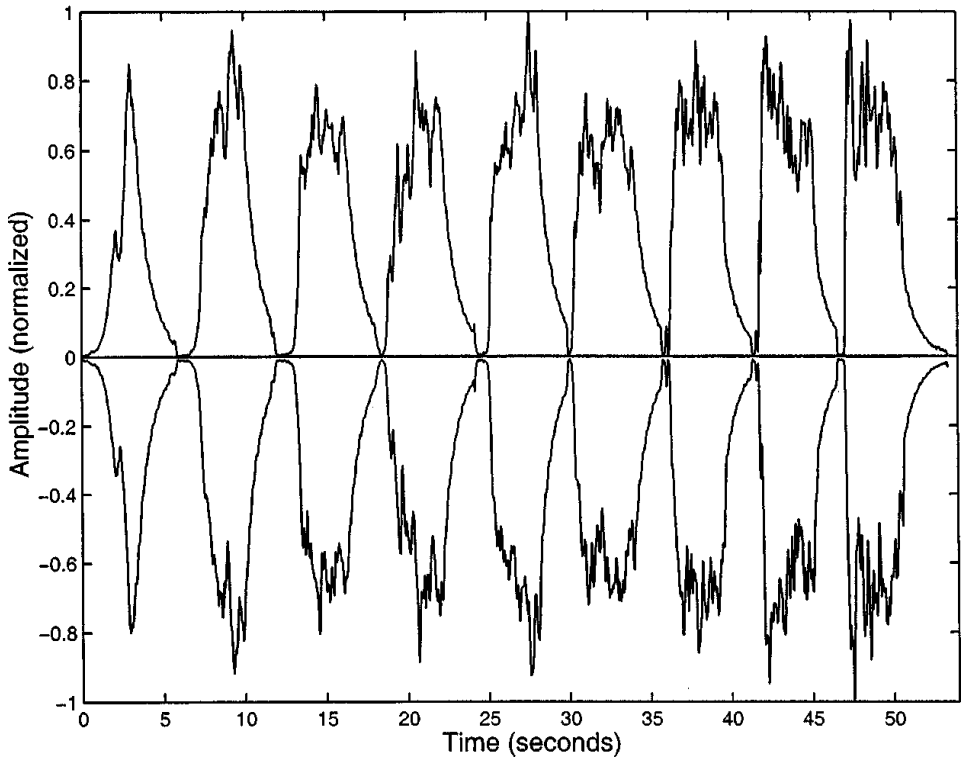

Figure 4.9: Time-domain amplitude envelope of hand strokes with increasing force and velocity held approximately constant.

Second, it allows very high bowing forces to be applied by the bowing machine. As shown in Figure 4.10 angled screws were screwed into a wooden base at the positions of the cord holes of the bar. Rubber tips were placed between the metallic holder and the bar to minimize the friction noise and keep a flexible interface. The wooden base was shaped to allow bowing at the narrow side and at the wide side at positions between the suspension holes. In the bowing machine measurement, the bar was pulled towards the bowing machine (which will be described in the next section), by means of a cord which was tied to a hook on one narrow side of the bar holder. When the applied force was measured, the cord was replaced by a spring scale with a scale range of 0 to 2000 grams.

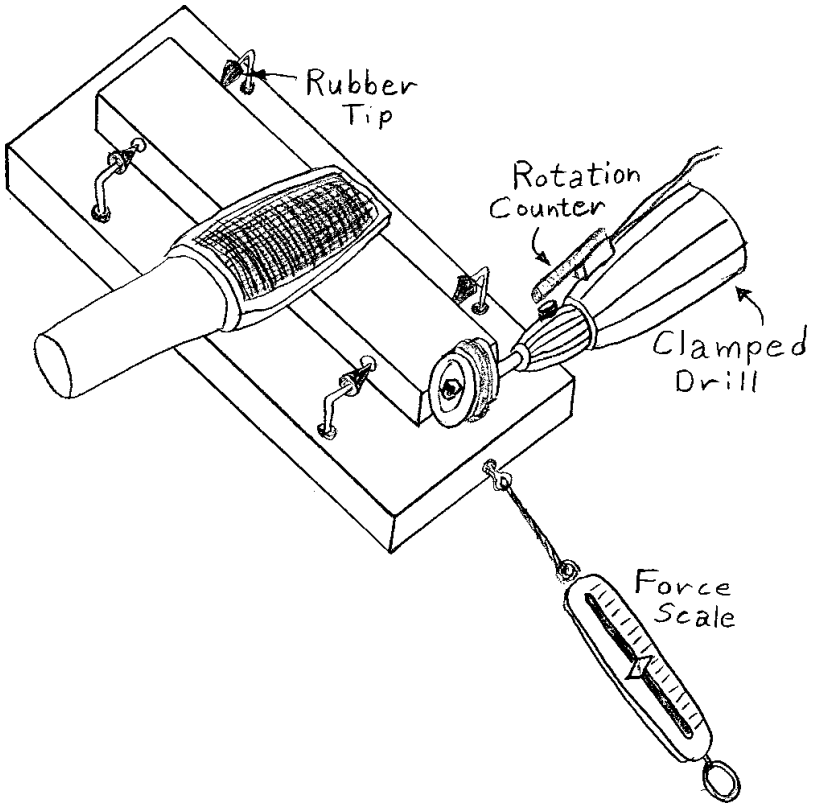

Figure 4.10: Experimental setup for bowing machine measurements of bars.

The microphone position for these measurements was above the middle of the bar as the bar holder didn't leave enough space underneath the bar.

Bowing Machine

The bowing machine consisted of a standard variable speed power drill, a cylindrical drum of hard rubber with a 2.6 *cm* radius and width of 3.75 *cm* around which a band of horse hair was wound and glued together at the open ends using super-glue to form a loop. The typical loop width and thickness was comparable to the width of the double bass bow. The horse hair was then rosined. In order to calibrate bowing speed, a bicycle speedometer was added to the drill. The magnet was placed on the rotating part and

the pickup sensor was glued to the non-rotating casing of the drill reaching over the magnet. In measurement, the bowing drill was held in place by a vice and the bar was pulled against it. The noise of the drill was damped from the recording by placing sound-absorbing foam between the drill and the microphone. Also the microphone position was generally facing away from the drill and towards the primary sound radiation direction of the bar, enhancing the signal to noise ratio. The microphone position was adjusted to maximize the signal from the bar while avoiding saturation.

Measurement procedure

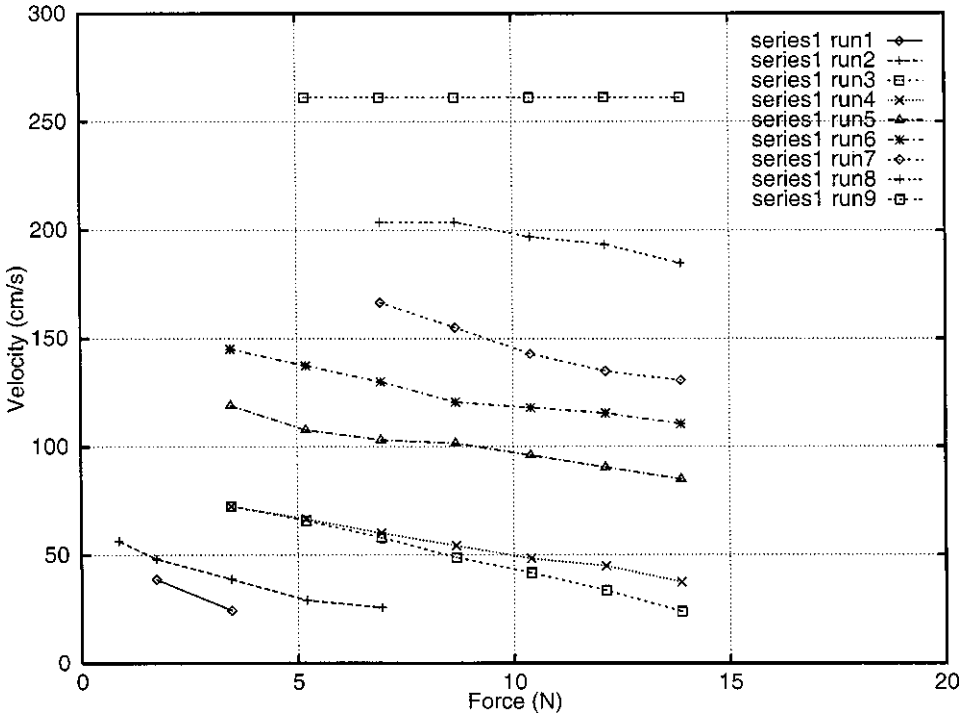

Figure 4.11: Bowing machine measurement series 1: Measured input parameters: Force and velocity.

Two series of measurements were performed using the bowing machine described in the previous section. Before each series the bowing drum had to be rehaired and

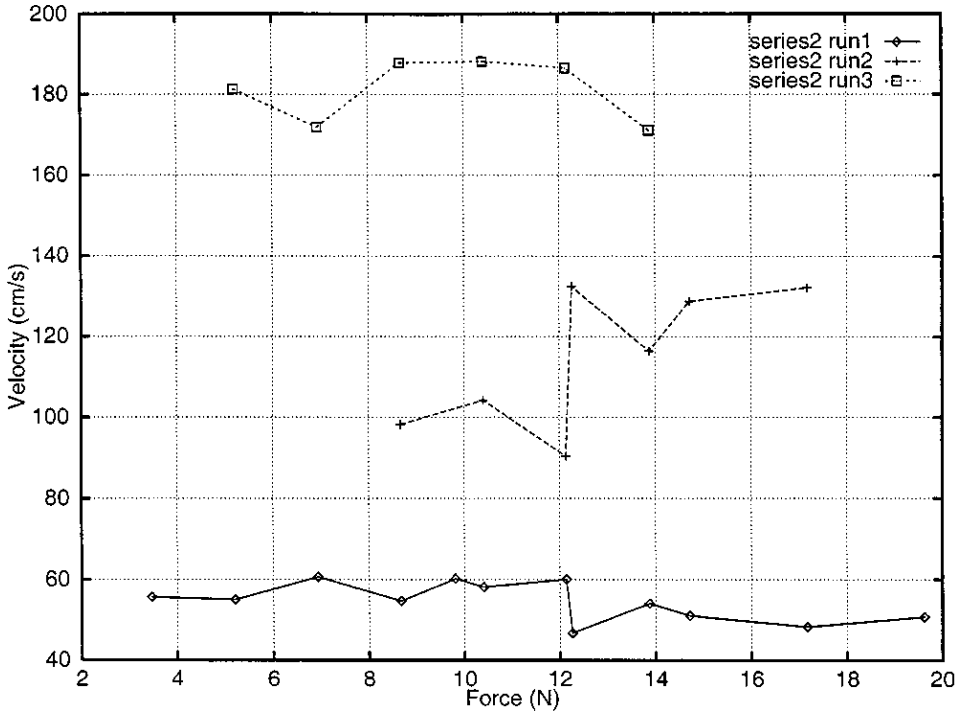

Figure 4.12: Bowing machine measurement series 2: Measured input parameters: Force and velocity.

new rosin was applied. Hence it should be noted that direct quantitative comparisons between these two series are not easily possible. The reason for the need to rehair the bowing machine stems from the fact that the high force measurements at the end of each series resulted in breaking of the hair loop and hence rendered the loop useless for more measurements. There is another reason why the measurements should not be compared between measurement series. The microphone was moved and recalibrated between the series and hence the attenuation of output levels between series should be expected to be different.

The unevenness and change of stiffness of the hair loop at the glue joint yielded an overlap of impulsive excitations over the total bowing excitation. This effect can be expected to influence some of the behavior measured. The impulses overlaying the overall

sound were used as an independent measure of velocity because of the occurrence of one impulse per revolution. Later this measurement was correlated with the independent velocity measurement using a speedometer to get an error estimate.

The first series consisted of nine runs starting at a particular bowing speed in gradually increasing forces between 0 and 14 Newtons (or 0 and 2000 grams spring scale readings with a relative force contribution of $\sqrt{2}$ due to an angle of 45 degrees). Forces were taken at the following spring scale readings if oscillations occurred: 125, 250, 500, 1000, 1250, 1500, 1750 and 2000 grams. In this measurement series, the oscillation was not damped out and restarted at each measurement point, but the force was steadily increased with the bowing machine continuously in contact. The setting of the drill speed was not adjusted, which resulted in a decrease of the actual bowing speed due to the reduced drill speed from the increased force load. All measurement points can be seen in figure 4.11. As can be seen, the velocity of each run decreases as a function of input force. The velocity was derived from the recording as described before. The last run (run 9) didn't result in oscillation and hence indicates points lying beyond the upper velocity limit.

These measurements were aimed towards finding the regions of oscillation as a function of velocity and force. In addition relative energy as a function of velocity and force was calculated from the recorded sounds and the change in spectral content was characterized using the spectral centroid, which is the center of gravity of the spectrum. The spectral centroid correlates roughly with brightness. Finally, the fundamental frequency of the recorded sounds was also measured. The results will be discussed in subsequent sections.

The second series consisted of three runs again starting at a particular bowing speed. This time the oscillation was damped out after recording for each measurement point and, using the attached speedometer, the input velocity was adjusted in the attempt to keep

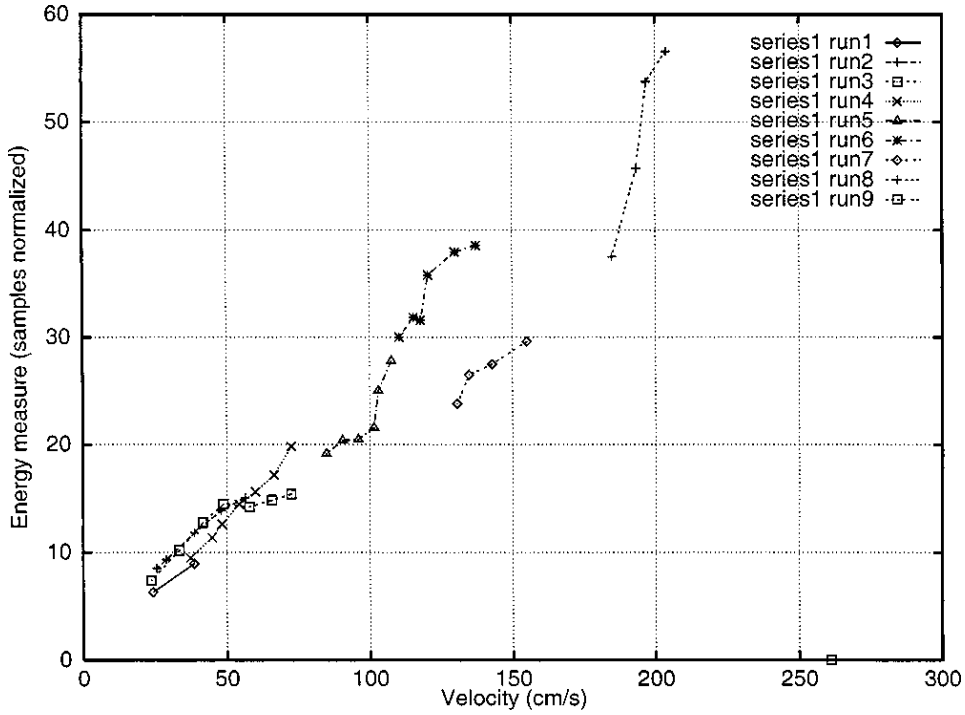

Figure 4.13: Bowing machine measurement series 1: Recorded radiation energy as a function of bowing velocity.

the actual bowing speed roughly constant. If a measurement point yielded oscillation the recording was taken long enough to measure the full oscillation build-up until the maximum and a significant part of the steady state oscillation. Hence in addition to all the measures derived from series 1, the onset transient time until maximum oscillation was reached was measured in this series. The force range was extended for the first two runs of this series to a maximum force of about 20 Newtons (or a spring scale reading of 2000 grams at 0 degrees angle).

All measurement points of this series can be found in figure 4.12. The velocities were measured both using the measure of the speedometer and from the recording. A correlation between the two independently measured velocity values shows the average error to be 2.21 cm/s (or 1.2%) with a standard deviation of 2.06 cm/s (or 1.1%). As

can be seen, the error is very low. This has to do with the high number of revolutions measured in both cases yielding a good resolution.

Results of bowing machine measurements

Region of oscillation

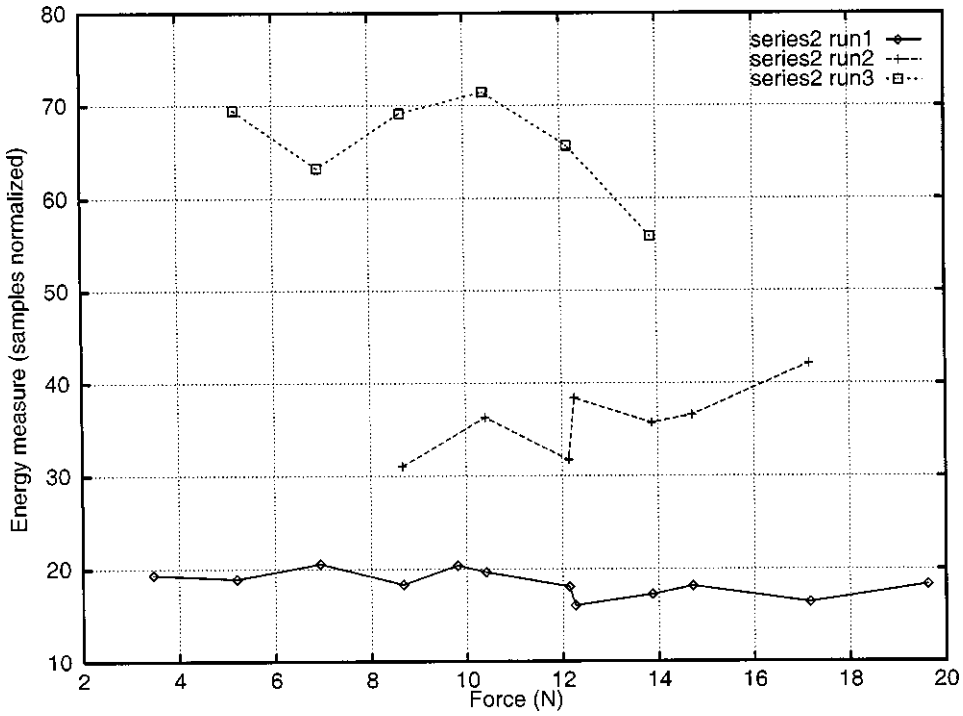

Figure 4.14: Bowing machine measurement series 2: Recorded radiation energy as a function of bowing force.

As can be clearly seen from figure 4.11 the minimum bowing force increases as a function of velocity. A maximum bowing force could only be found for the first two runs of series 1, which are at velocities below 50 cm/s. At higher bowing speeds an upper force limit could not be found within the measurement range. The minimum speed at which steady oscillation was found was 23.83 cm/s with a force of 13.87 N. It should

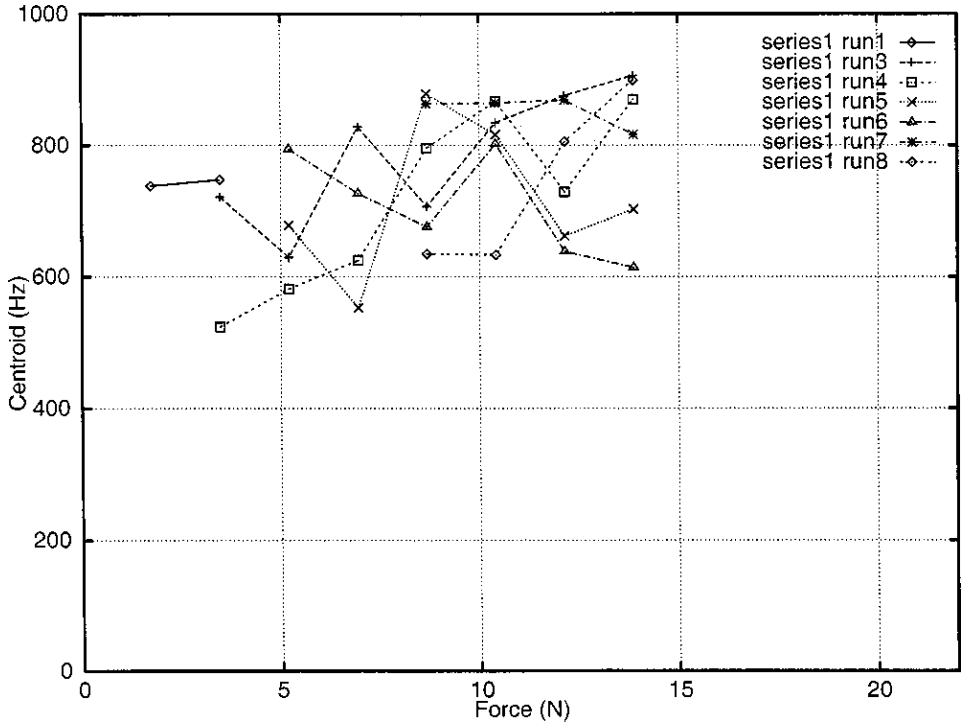

Figure 4.15: Bowing machine measurement series 1: Spectral centroid as a function of bowing force. Only measurement point with a clear steady-state oscillation are shown.

be noted that using the undamped measurement approach of series 1, very low velocities can be achieved even for high forces (as can be seen from run 3 in figure 4.11. This point is the highest measured force point in this run). The maximum bowing speed from series one is found to be above $203.72 cm/s$ and below $261.14 cm/s$.

Energy and power, spectral content, fundamental frequency and onset times

Both measurement series show that the energy of the fully developed steady state oscillation increases as a function of velocity and the relationship seems to be approximately linear (the measurements of the first series can be seen in figures 4.13). Taking this linear velocity dependency into account, the energy radiation seems to be independent of the input bowing force (this effect can be seen more clearly in series two, where the force-

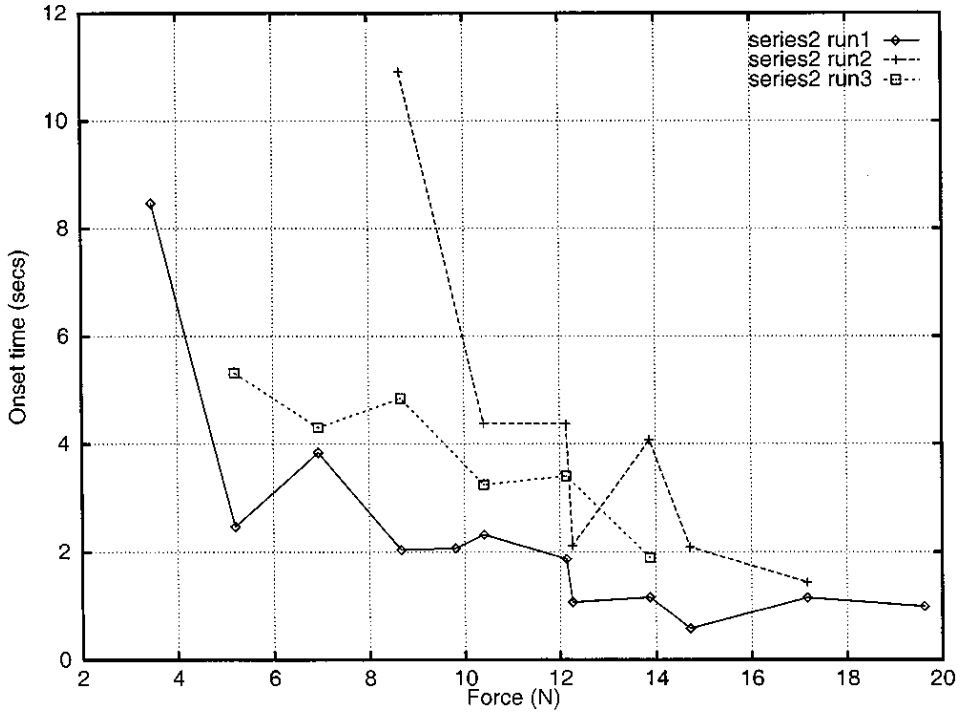

Figure 4.16: Bowing machine measurement series 2: Onset time as a function of bowing force.

energy relationship as depicted in figure 4.14 correlates closely with the force-velocity relationship as depicted in figure 4.12).

The spectral centroid of series 1 seems uncorrelated with the input force and velocity. No clear upward trend was observed with increasing force (see figure 4.15) in contrast to known behavior of the bowed string. Series 2 verifies this result.

The measurements of the fundamental frequency as a function of velocity and force result in minor fluctuations without a clear trend. In series 1, the mean frequency was 186.67 *Hz* with a standard deviation of 0.26 *Hz* (33 data points) and in series 2, the mean frequency was 186.73 *Hz* with a standard deviation of 0.27 *Hz* (25 data points). The measurements as a function of velocity seem to indicate a trend towards flattening with increasing velocity, whereas there is no trend observable in dependency of force. In any

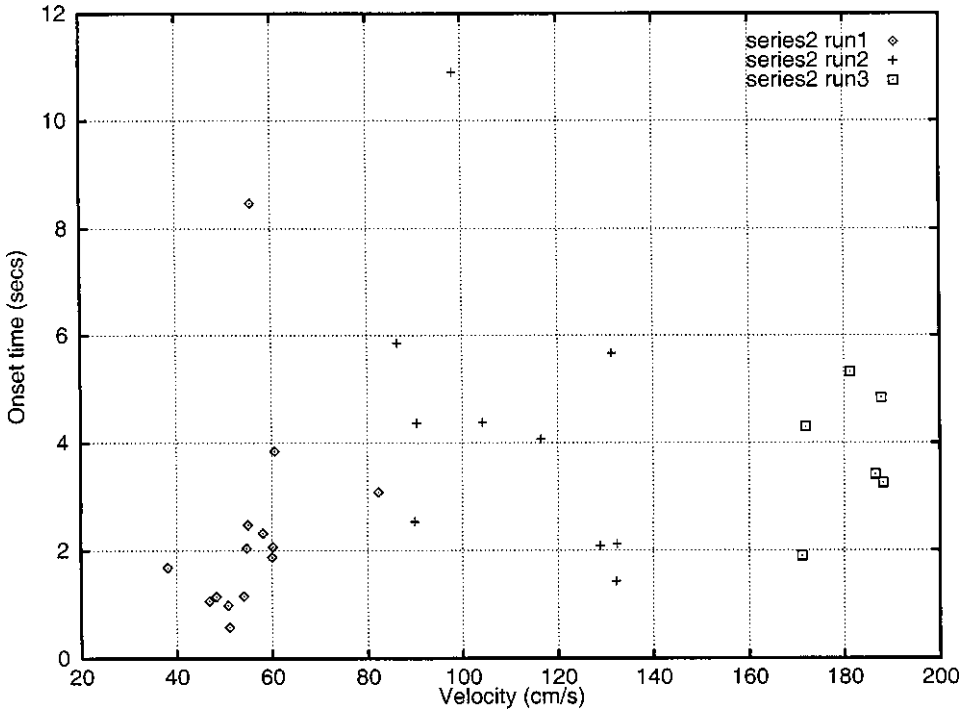

Figure 4.17: Bowing machine measurement series 2: Onset time as a function of bowing velocity.

case, the effect is very small (less than 10 cents) even over the full range. High velocities should be difficult to achieve by hand-bowing and hence within the usual bowing domain, the dependency of the fundamental on the bowing parameters is negligible.

Onset time as a function of velocity and force was measured in series 2 only. As was already noted from the time-domain shapes of hand-bowed measurements, there is a clear decrease of the onset times with increasing bowing force (see figure 4.16). The onset time appears uncorrelated with the input bowing velocity (see figure 4.17).

4.2 2-D Case: Indian Tabla Drums

Courtesy Ajay Kapur

Figure 4.18: Indian Tabla drums played by Ajay Kapur.

The Tabla is a pair of drums with a number of interesting characteristics. The modes of the first four to six partials are harmonic, unlike what one might expect from a circular membrane. To achieve this harmonic tuning, the Tabla drums are manufactured using membranes of non-uniform thickness [173]. There are a number of typical performance

strokes to Tablas. One interesting stroke is a modulating form of the “Ga” stroke, which is performed on the larger, right drum, called “bayan.” The palm of the hand resides on the drum. After the drum has been excited with a quick impact with the fingertips, the player pushes her palm down and towards the center of the drum and hence achieves a characteristic upward pitch-bending sound [173]. Figure 4.18 shows Ajay Kapur performing this stroke. The small drum is called dahina.

Using propagation modeling for this example highlights a number of issues. First, a membrane of a Tabla is essentially a two-dimensional structure, and we no longer have the simple direct interpretation of a banded waveguide as was possible for the bar. We do know, however, that the modes correspond to closed wavetrains. To remove the mentioned ambiguity, we need additional information beyond the modal frequencies. One possibility would be to try to derive this information from measured impulse responses. Alternatively one can try to derive an analytical solution for the propagation of waves. The drum head of the Tabla is non-uniform so analytical solutions of this sort are hard. Also, modal frequencies which are usually separate are tuned to be aligned with each other. This can be seen in Figure 4.19. Distinct modal patterns are tuned to be harmonic.

These modal patterns may indeed contain the information necessary to derive wavetrain closure paths. Circular modes are radially symmetric, hence the wavetrain closure path has to go from the boundary through the center and back. Diagonal modal lines, however, don’t follow that simplified one-dimensional interpretation.

In our model we chose to simply ignore the difficulties and approximate the propagation. This could be interpreted as disregarding the multiplicity of eigen-modes or as disregarding modal shapes with diagonal modal lines. However, it leaves us with a simple one-dimensional model of the Tabla.

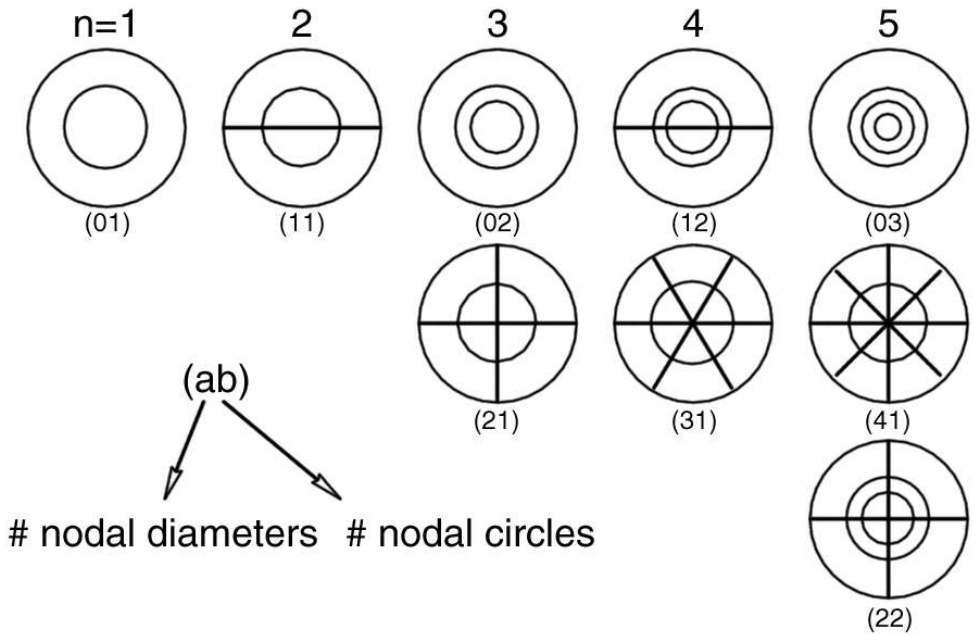

Figure 4.19: The nine nodal patterns of the Tabla tuned to harmonic modes (after Rossing [173]).

	Bayan		Dahina	
n	measured	simulated	measured	simulated
2	2.00	2.02	2.89	2.87
3	3.01	3.03	4.95	5.01
4	4.01	4.05	6.99	6.73
5	4.69	4.72	8.01	8.00
6	5.63	5.65	9.02	8.70

Table 4.4: Spectral frequencies of dominant partials of measured and simulated Tablas given as $f_n : f_1$.

In this case, the pitch-bending technique directly corresponds to shortening the physical path of waves traveling on the membrane, which can be directly implemented in a propagation style simulation.

This is not a direct geometric correspondence, but rather a resemblance which is modeled. Whether or not a precise geometric interpretation exists remains open.

The results of modal comparison between real drums and propagation simulations can be found in Table 4.4. The strokes performed are open membrane strokes in the center on both the bayan and the dahina. This was in turn modeled as impulsive excitation.

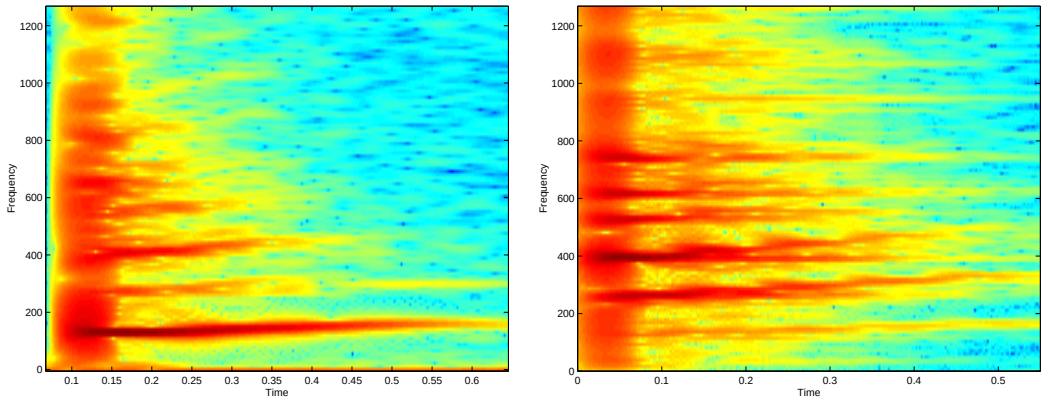

(a) Recorded (b) Simulated

Figure 4.20: Spectrogram showing the upward bending of a modulated *Ga* stroke. The fundamental bends from 136 to 162 Hz (measured) and 134 to 171 Hz (simulated).

The results for the more complicated pitch-bending strokes can be seen in Figure 4.20. The simulation shows good resemblance and sound comparable to the recorded stroke. It should be noted that the simulation method is robust to the pitch-bending manipulation. In fact, much more extreme bends than the one depicted here are possible. High pitched large-scale bends on our propagational model perceptually closely resemble water-drop sounds, suggesting a much wider range of interesting application for behaviors of this type.

Hence, despite the forced reduction in dimensionality and loss of geometric interpretation, the simulation achieves good results for complex interactions.

4.2.1 Periodic Orbit on Circular Domain

In order to recover a more full notion of spatial location, the topology of periodic orbits on the domain have to be constructed.

The circular domain is an often studied canonical example [104, 25]. It can be seen that in fact the circular domain is very similar to the rectangular domain discussed in section 3.9.2. Both examples have two independent spatial dimensions and are integrable systems[7]. Hence EBK quantization via a resonant torus applies and a canonical transform from domain variables to torus dimensions can be found.

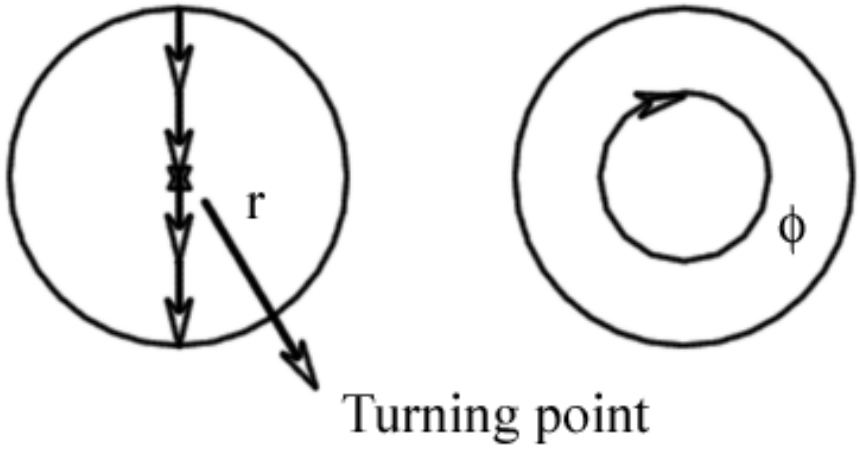

Figure 4.21: Radial and angular variables on a circular domain and their connected turning properties.

The difference between dimensions in the rectangular domain and the circular domain is the independent variables of radius r and angular position ϕ already are topologically connected (as illustrated in Figure 4.21). For the case of the radius, this can be seen

[7] A system is integrable if it admits the maximum number of integrals of motion (for a rigorous definition see [25, p. 60]).

following a diagonal trajectory through the origin of the circle. Towards the center the radial variable decreases until at $r = 0$ the radial variable "turns" and then increases until the boundary is reached. Also the angular variable repeats itself after 2π. Whereas the position of the radial turning point has a defined position on the domain (namely the center), the reference of the circular repetition is a matter of definition and the point indicated in Figure 4.21 is just a possibility. Hence looking at the circular domain the set of paths with inward and outward radial motions and connecting these two sets at the boundary yields the EBK resonant torus of Figure 3.9.

As mentioned in section 3.9.2 the class of all turning points inside the domain of a family of rays is called caustics. In this case, these are the radial turning points, which form a circle inside the domain[8] (see Figure 4.22).

In the case of the rectangular domain, the family of rays with equal winding properties on the torus were defined by the ratio $x_1 : x_2$ and now this property is defined by the ratio $r : \phi$. Hence all rays with the same reflection angle at the boundary belong to a family of rays with the same resonant properties.

Any ray with a non-zero radial propagation component (see Figure 4.22(a)) hence alternates between reflecting at the boundary and touching the caustic and hence in the quantization condition (3.24), the Maslov index μ, counting caustic turning points, and the number of boundaries reached, b, are both equal and 1 or more.

The special case of a purely angular propagation component neither reaches a boundary nor turns radial components (see Figure 4.22(b)) and hence both μ and b are zero and the path length is simply the circumference of that circular path $2\pi a_0$ (compare [104, eq. (23)]):

[8]The general theory of caustic phenomena is a rich and complex field and will not be discussed fully here. See [110] for a mathematical treatment of caustic phenomena.

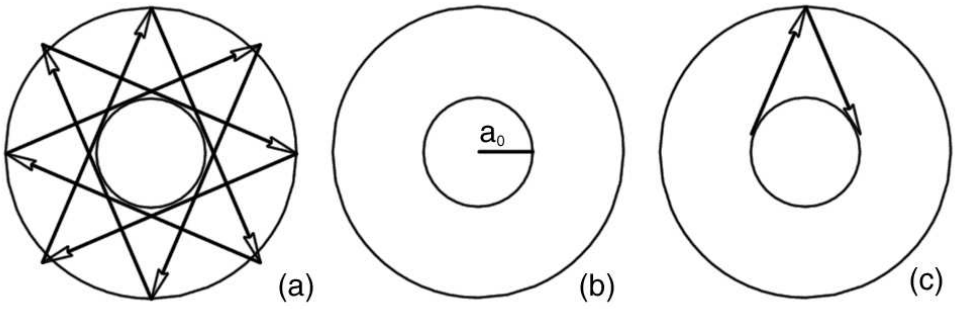

Figure 4.22: Keller-Rubinow path construction on the circular domain (compare [104, Fig. 3 and 5]). (a) Closed path touching the interior caustic. (b) Radius of the caustic circle. (c) Path containing rays traveling from caustic to boundary and back.

$$2\pi a_0 = 2\pi n_1 \quad n_1 \in \mathbb{N}_0^+ \tag{4.4}$$

The phase on the caustics is multi-valued as it both is defined by the purely angular propagation paths, and by paths which leave the caustics and return back to it. Hence there is also a phase closure condition between the arc-length traveled on the caustics and a ray leaving the caustics, reflecting at the boundary and returning to the end of the caustic arc (see Figure 4.22(c)). If a is the radius of the domain, then the arc-length can be calculated as $2a_0 \cos\frac{a_0}{a}$ and the outward and inward rays each travel $\sqrt{a^2 - a_0^2}$. With the quantization condition (3.24) this yields (compare [104, eq. (24)]):

$$2 \cdot \sqrt{a^2 - a_0^2} - 2a_0 \cos\frac{a_0}{a} = 2\pi\left(n_2 + \frac{\mu}{4} + \frac{b}{2}\right) \quad n_2 \in \mathbb{N}_0^+ \tag{4.5}$$

Then the multi-valuedness is removed by eliminating a_0 from equations (4.4) and (4.5):

$$2 \cdot \sqrt{a^2 - n_1^2} - 2n_1 \cos \frac{n_1}{a} = 2\pi \left(n_2 + \frac{\mu}{4} + \frac{b}{2} \right) \quad n_1, n_2 \in \mathbb{N}_0^+ \tag{4.6}$$

This equation corresponds to [25, p. 88, eq. (2.153)]. The quantization numbers n_1 and n_2 correspond to the nodal numbers depicted in Figure 4.19 and established the connection between ray paths and spatial modes.

In order to follow the derivation simplifying assumptions are made and hence the topological construction is an approximate one.

4.3 3-D Case I: Wine Glasses and Glass Harmonicas

Drinking glasses, in particular wine glasses, can be made to ring in many different ways. They can be excited by impact, by rubbing the top rim with a wet finger, or by radially bowing with a violin bow. While impact can easily be simulated using modal models, rubbing and bowing cannot. Geometrically, a wine glass is a three-dimensional object and disturbances travel along the object in all dimensions. The object is symmetrical, however, and the dominant modes are essentially two-dimensional [173]. One is left with bending modes along the cylindrical axis, which can be excited by rubbing, plucking or bowing, but most of the energy really goes into flexural modes of the circumference of the glass. This is a closed path — essentially a bar being bent into a circular shape, closing onto itself. Hence the path is quasi one-dimensional. The path traced along the wine glass can be seen in Figure 4.24.

Courtesy Ed Gaida

Figure 4.23: Benjamin Franklin's glass harmonica, which he called "armonica", as seen in the Franklin Institute Science Museum in Philadelphia.

From the distance to be traveled along the rim, the circumference of a circle $l = 2\pi r$, and the wave velocity from equation (4.2) we can derive the actual frequency and its connection to traveling length [173], which completely determines the wavetrain closure to be modeled:

$$\begin{aligned} \frac{1}{\omega} &= \frac{l}{v} = \frac{2\pi r}{\sqrt{a\omega}} \\ \omega &= \frac{a^*}{r^2} \end{aligned} \tag{4.7}$$

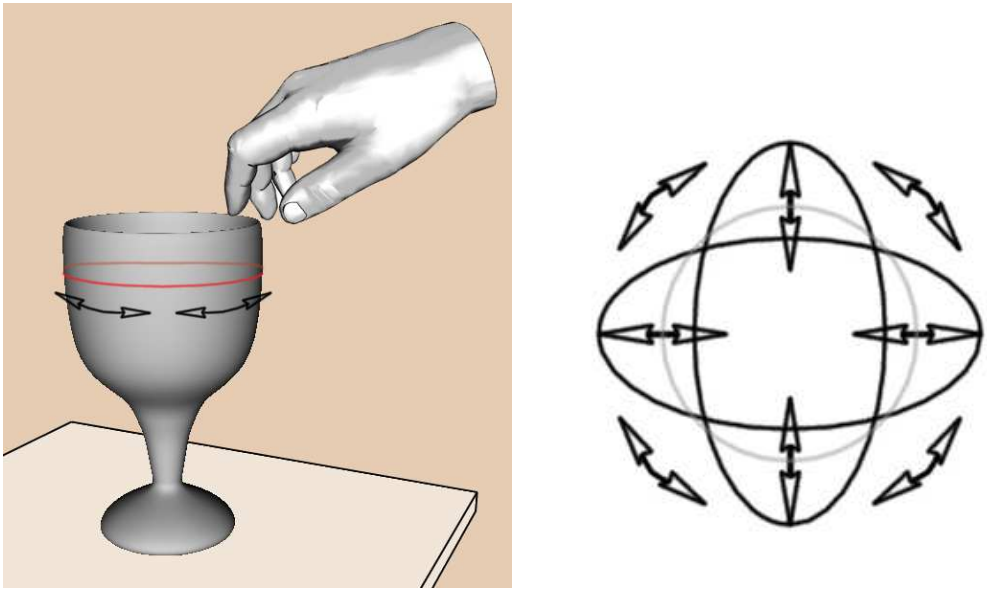

(a) 3-D model view (b) Top view

Figure 4.24: The wavetrain closure on the rim of a wine glass and corresponding flexural waves as seen from the top (after Rossing [173]).

Due to the circularity of the path, the banded waveguide system makes no reference to the actual position on the rim. In practice, however, the point of interaction provides this reference. If the glass is struck, the point of excitation is defined along the circle. The same is true for bowing, which usually happens at one point radially to the rim. Rubbing the rim is a peculiar case because the point of interaction is moving slowly along the path. In our model, we make no distinction between rubbing and bowing as the rubbing is a very slow motion compared to the wave traveling on the path, and hence treating the rubbing interaction as stationary does not significantly alter the non-linear behavior. The effect of the slowly shifting interaction point is measurable, though not audible as it is too slow [173].

	Struck		Rubbed	Bowed	
n	measured	sim.	measured	measured	sim.
2	2.32	2.31	2.00	2.00	2.00
3	4.25	4.20	3.00	2.99	3.00
4	6.63	6.69		4.00	4.00
5	9.38	8.81	5.00	5.00	5.00

Table 4.5: Spectral frequencies of dominant partials of measured and simulated struck, rubbed and bowed wine glass given as $f_n : f_1$.

Results of measurements and simulations are presented in Table 4.5. The struck excitation was a quick sharp strike with a finger nail against the glass, which was modeled using a simple impulse. Bowing on the real glass was performed using a rosined violin bow. The rubbing was performed with a wet finger. With the violin bow it is possible to excite the second harmonic as the fundamental frequency of the bowing response. The same result can also easily be achieved using the simulation model. The simulation model captures both the harmonic spectra as well as a other non-linear effects of the real interaction. We did not model a rubbed interaction separately as we assume it follows in principle the same mechanism as bowing [69][9].

4.4 3-D Case II: Tibetan Singing Bowl

The Tibetan singing bowl are geometrically close to spherical segments. A discretized mesh version of the bowl can be seen in Figure 4.25). In typical performance, the bowl is rubbed with a wooden stick wrapped in a thin sheet of leather along it's rim. Depending on the rubbing velocity and initial state of the bow (i.e. certain modes may be already

[9]After the completion of the thesis I became aware of work by Serafin and co-workers who independently implemented a Tibetan bowl using banded waveguides — the object of study of the next section — in the context of demonstrating a novel rubbing board controller. The paper [221] does not give technical details, but the sounds presented at the conference were impressive.

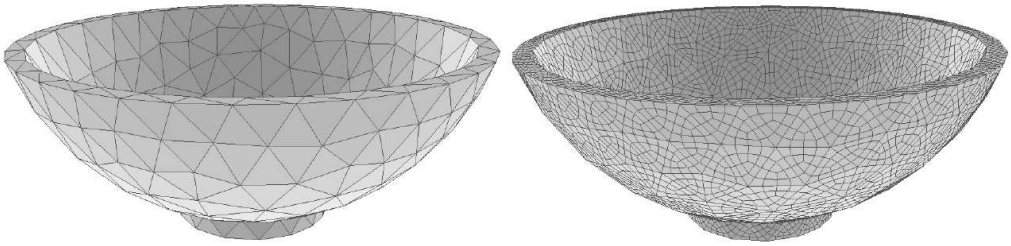

Figure 4.25: Mesh of simulated bowl.

ringing), various frequencies can be made to oscillate. Behavior is comparable to rubbing or bowing a wine glass in terms of dynamic envelope, mode locking, mode duplication and related phenomenon as a result of the non-linear interaction of the stick-slip-based rubbing.

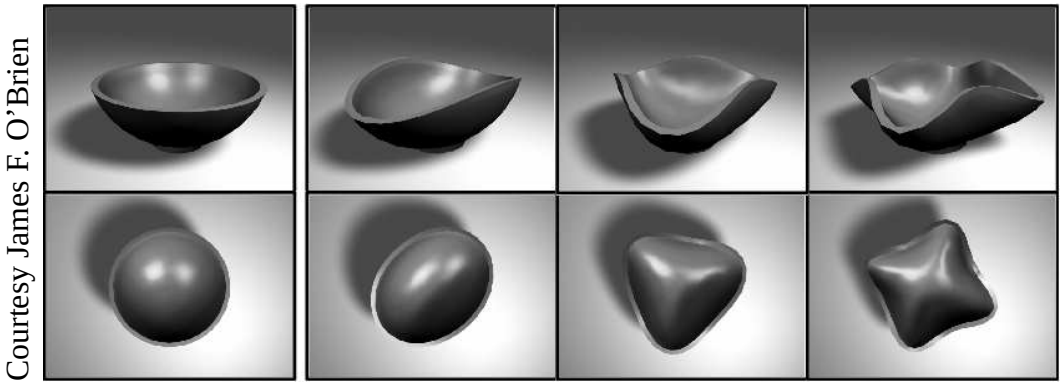

Figure 4.26: Simulated mode shapes of the bowl.

If struck, the bowl will show a modal response of circular-symmetric form. The first few modal shapes are depicted in Figure 4.26 with exaggerated amplitudes. These shapes will oscillate around the circular rest position comparable to circular flexing motion of the wine glass depicted in Figure 4.24. The circularly repeating pattern is depicted in Figure 4.27. This picture also shows non-circular modes, which tend not to be excited by the circular rubbing motion.

Figure 4.27: Path of circular mode on bowl (used with permission from (Cook 2002).)

The measured spectra of the struck bowl can be seen in Figure 4.28 for various impact positions. As can be seen, there are a number of higher modes which lie close together yielding audible beating. The beating can be seen more clearly in Figure 4.29.

4.4.1 Beating Banded Waveguides

While beating modes in physically separate structures have been studied in the case of coupled piano strings [8, 9, 6] and plucked strings with sympathetic coupling [99], the modeling of beating within the banded waveguide remains unexplored.

The beating modes combined with the very weak damping poses the main challenge for modeling the dynamics using banded waveguides (as depicted in Figure 3.3.)

For two neighboring banded wavepaths whose center frequencies get close, the respective frequency-bands start to overlap strongly. This means that energy will contribute to traveling waves in both bands simultaneously. To guarantee stability within the frequency region the sum gain of both waveguides cannot exceed unity as both are

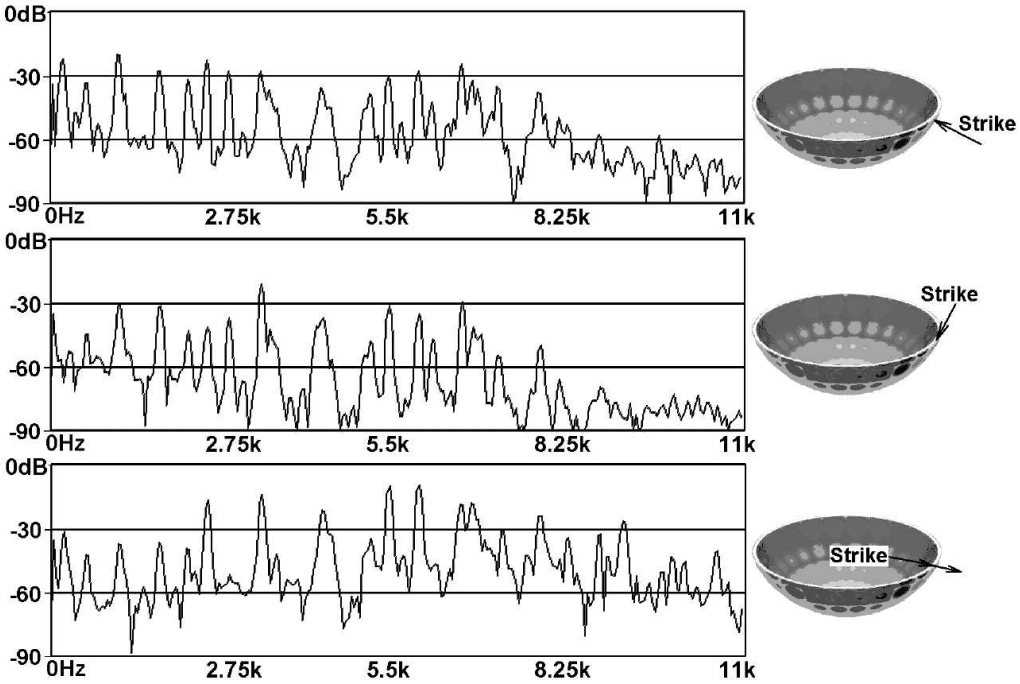

Figure 4.28: Spectra of different excitations (used with permission from (Cook 2002).)

summed together for interaction or feedback. More specifically the gain of the respective banded wavepaths can be calculated from the maximum of the overlapping bandpass filter amplitude characteristics. This maximum has to be tuned to the desired gain and the respective gain of the bandpasses is adjusted by the weight of the overlap. The resulting simulation of an isolated beating mode pair can be seen in Figure 4.30. The relative ratio between the modes is $1 : 1.05$.

The beating modes following this construct, combined with plain modes then yields the complete simulation of the Tibetan bowl, which can be achieved with 17 banded wavepaths including beating mode-pairs.

The modal data was extracted using a method proposed by van den Doel, which is based on a spectral tracking method including a linearized decay estimation [207].

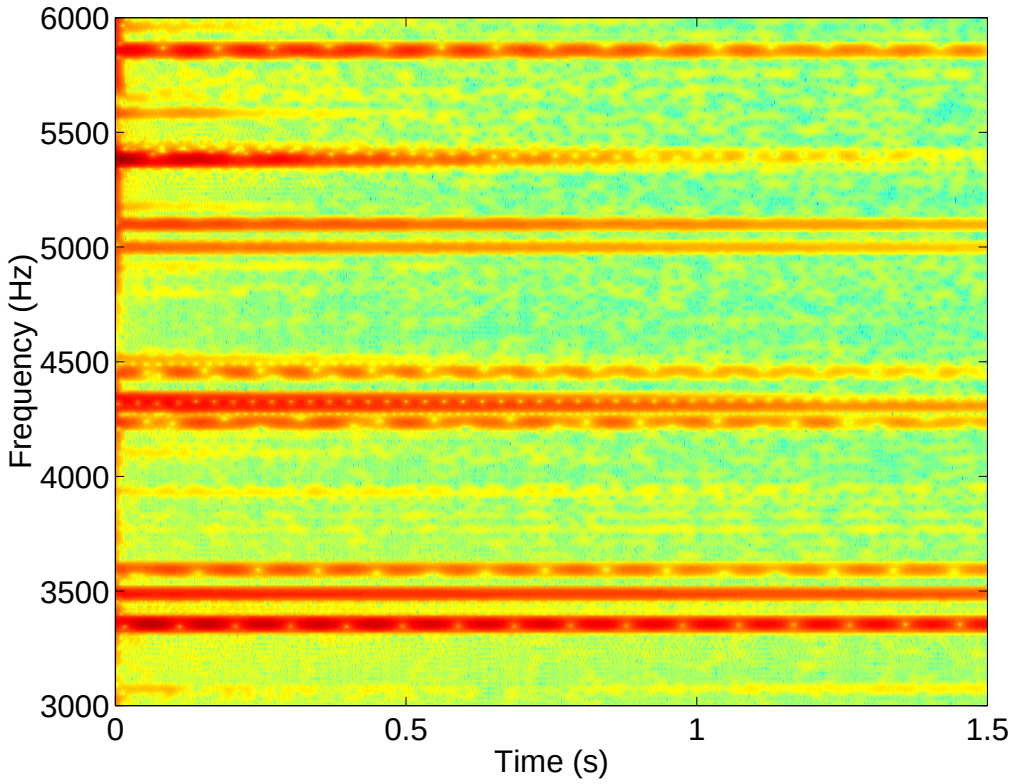

Figure 4.29: Beating upper partials in spectrogram of a recorded Tibetan bowl.

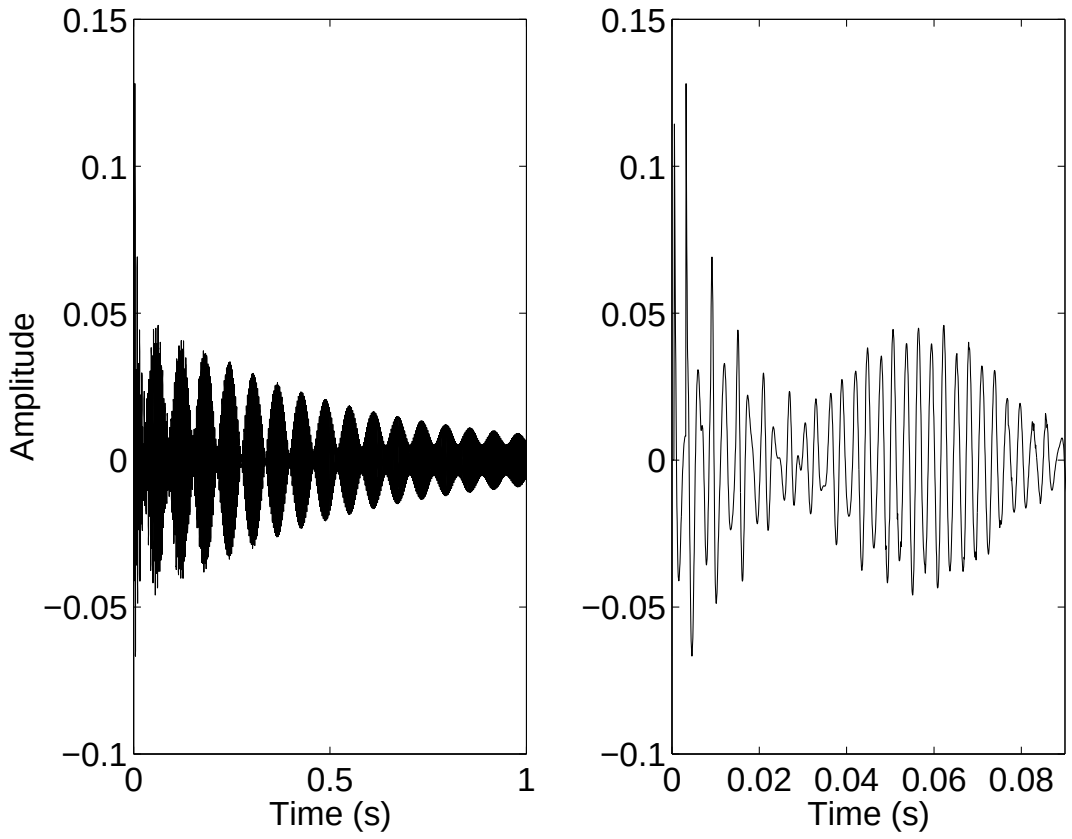

Figure 4.30: Left: Evolution of an isolated simulation of a beating mode pair. Right: Initial transient and the first beating period.

Chapter 5

Comparison with Alternative Methods

> Is it progress if a cannibal uses knife and fork? – **Stanislaw J. Lec**[1]
>
> One of the symptoms of an approaching nervous breakdown is the belief that one's work is terribly important. – **Bertrand Russell**[2]
>
> This book fills a much-needed gap. – **Moses Hadas**[3]

5.1 Modal Synthesis

Modal synthesis [208] and propagation modeling are conceptually very close. The main difference between the two is that the latter maintains the relative phase responses of the modes and approximates the phase response between modes. In terms of physical interpretation, modal synthesis is blind to the mechanism that gives rise to the resonance, whereas propagation synthesis is not. Modal synthesis is inflexible with regards to interaction and observation points, whereas propagation modeling allows for constructions

[1] In "Unkempt Thoughts," Funk & Wagnalls, p. 78 (1962)

[2] In "The Conquest of Happiness," chap 5. according to [147, p. 551, q. 10]

[3] Attributed by J. E H. Shaw, "Some Quotable Quotes for Statistics," 2001, available at `http://www.warwick.ac.uk/statsdept/Staff/JEHS/data/jehsquot.pdf`

which give a physically meaningful interpretation to interaction points and observation points, at least in the one-dimensional case. In higher-dimensional cases, the spatial interpretation is difficult and symmetries have to be exploited. Computationally, both methods share the same complexity. Banded waveguides model the same number of modes but with the addition of one inexpensive delay-line per mode.

5.2 Waveguide Synthesis

Waveguide synthesis [187] can be seen as a special case of propagation modeling in which the group delay of all frequencies is constant and hence band-limiting and separation of modes become unnecessary. Both methods share an obvious physical interpretation and justification. For both, results of linear transmission line and digital filter theory can be utilized. Two and three-dimensional waveguide meshes differ from propagation modeling, as waveguide meshes maintain the physical space, whereas propagation models reduce dimensionality to wavetrain path analogues. It should be noted, however, that waveguide meshes are not computationally efficient as the commutability is lost. Propagation modeling maintains efficiency even for higher-dimensional simulations. Another way of comparing traditional waveguide models and propagation models is by the way they handle dispersion. In waveguide models dispersion effects are lumped together and modeled in one all-pass filter [187] whereas in propagation models the dispersion is distributed. Propagation models hence more closely model the physical qualities at local points with regards to dispersion. This difference is relevant as waveguide models become inefficient with increasing dispersion as the filter order to implement appropriate lumped all-pass filters becomes high.

5.3 All-pass Chains and Frequency Warping

An alternative approach to the banded waveguide structure to model non-constant wave-propagation is to replace the unit delay with all-pass filters that model the non-constant propagation characteristics. In [60] we called this structure "generalized waveguide" although in this thesis I referred to banded waveguides as "generalized digital waveguides" (see section 3.6). Here I will rather call the first "all-pass waveguides" to note the distinction.

The all-pass waveguide is the spatial discretization of the propagation equation (see 3.14). As can be seen, the phase velocity depends on the frequency. Starting from the picture of the usual waveguide, the unit delays are replaced by frequency dependent delays as symbolically depicted in figure 5.1. *R* is the appropriate reflection-function at the boundary.

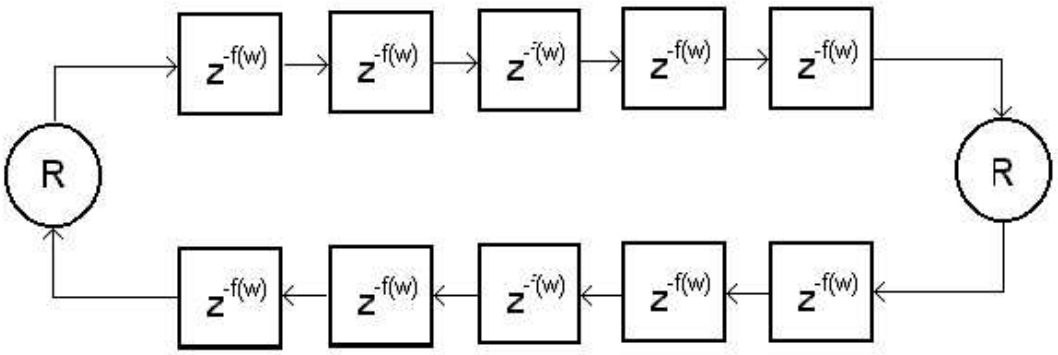

Figure 5.1: All-pass-chain or warped frequency waveguide.

If losses are modeled separately, the frequency dependent delays are all-pass filters with an appropriately modeled phase delay response. This has strong connections to and is strongly motivated by work on modeling the stiffness of strings starting from a mixed bar/string-equation using all-passes [94, 145, 213, 169].

The effect of all-passes replacing unit delays has long been studied and is classically known as frequency warping [192, 141, 140] and has been theoretically extended until today [216, 138]. To the same extent, the design of all-passes has been extensively studied [116]. An example design can be seen in Figure 5.2.

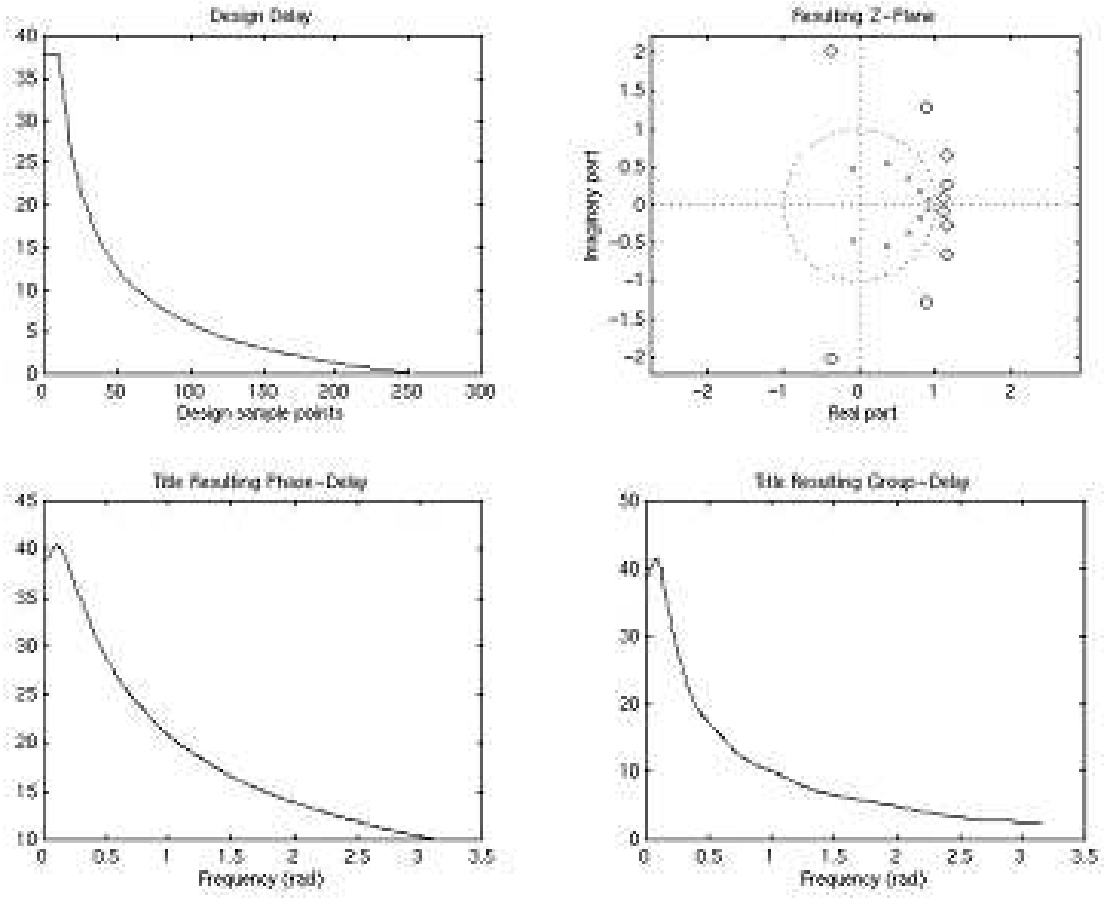

Figure 5.2: All-pass filter design for a given delay characteristic (following Lang [116]).

In fact, the early work regards a special case of second-order all-passes which relate to the Laguerre transform [141] and later also the Kautz transform [79]. The stretching effect on partials of this kind of structure has been repeatedly observed and suggested for synthesis [81, for an example]. In different form musical application of this approach has been used for warped linear prediction [117, 80], instrument body modeling [148],

reduction of dispersion errors in waveguide meshes [176], audio effects [66, 65] and warping to perceptual scales [189]. Otherwise it's been studied in modeling room impulse responses [107], the approximation of delay systems [119, 118] and system identification [7, 67], filter design [120], and image compression [41]. Cascaded all-passes, possibly mixed with delays have long been used in reverberation algorithms [49, for example].

In the case of all-pass waveguides, depending on the order of the all-passes used, good approximation to the propagation characteristics can be achieved, this approach shows poor performance. The number of all-passes needed depends on the fundamental frequency of the instrument. It was found that for the same spatial and temporal sampling, 10th order all-pass chains require more computation than an implicit finite difference method implementation (after [35]). This performance comparison matches the counted number of floating-point multiplications and additions as found in the all-passes and the band-diagonal solver used in the finite difference implementation. While this model preserves spatial sampling and hence would allow for non-linear spatially localized interactions, it is neither useful for musical performance nor advisable for acoustical modeling purposes, because finite differencing also model local coupling terms at the same complexity.

In fact, it should be noted that an interesting conceptual difference between all-pass waveguides and banded waveguides is the spatial sampling. All-pass waveguides use uniform spatial sampling with each all-pass unit corresponding to a spatial unit. As was discussed in section 3.7 banded waveguide have multi-scale spatial sampling. This difference provides the crucial performance improvement.

5.4 Modal Decomposition & Green's Function

Propagation modeling is a simplification and possibly an approximation to full modal decomposition or Green's function modeling. By full modal decomposition modeling, we mean the modal description of the system which keeps both the modal frequencies (as modal synthesis does) and modal shapes (corresponding to eigenvectors of the system) [134]. In a propagation perspective, eigenvectors can intuitively be interpreted as capturing the details of the wave-path which gives rise to the closed wavetrain. Propagation modeling keeps only the total roundtrip time and drops the local variations. This corresponds to a tradeoff between detail and computational speed. Eigenvectors contain values for all data points in the mesh-discretization, whereas the propagation models only preserve a highly reduced set of data. Whether or not piecewise propagation modeling in higher dimensions has an obvious physical interpretation remains an open question. Full decomposition is obviously more desirable if the oscillation of an object should be visible and hence the motion of all geometric points has to be modeled. Both methods require explicit prior knowledge of the means that give rise to the modal response, though both could be automatically derived before the simulation starts from the general system describing the objects.

5.5 Finite Element Methods

Finite element methods (see chapter 6 and [135]) solve for the modal response implicitly, whereas propagation modeling carries the modal response explicitly. Solving for the modal response is only necessary, however, if it can change during the simulation and the mechanisms of the modal response change are not known. A good example where the modal change is very hard to predict is brittle fracture. An example of modal change that

is explicitly understood is the Tabla pitch-bending described earlier. Also, finite element methods can be used to solve some distributed non-linear systems, for which any linear propagation assumption is in general invalid.

The difference between general finite element methods, and methods which use delay-lines as modeling structures or substructures can be seen by bringing the function of a delay-line into matrix notation. Assume a numbering of the delay-line cells as depicted in figure 5.3.

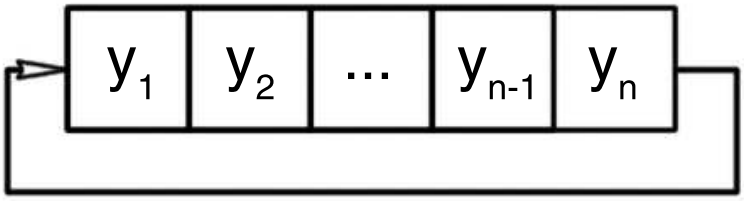

Figure 5.3: Labeling of delay-line cells for matrix notation.

Then at each time step the content of each element gets copied into the neighboring cell, which leads to a matrix of the form:

$$Z_n = \begin{bmatrix} 0 & 0 & 0 & \cdots & 0 & 0 \\ 1 & 0 & 0 & \cdots & 0 & 0 \\ 0 & 1 & 0 & 0 & \ddots & 0 \\ \vdots & \ddots & \ddots & \ddots & \ddots & \vdots \\ 0 & \cdots & 0 & 1 & 0 & 0 \\ 0 & \cdots & 0 & 0 & 1 & 0 \end{bmatrix} \tag{5.1}$$

This is a matrix with 1's in the first subdiagonal and zeros elsewhere. This matrix type is called *lower shift matrix* in [37]. If the delay-line forms a closed loop then there is an additional one in the upper-right corner (corresponding to the copy operation of the last

delay-cell into the first one. The resulting matrix is called is called *downshift permutation matrix* [77, p. 202]:

$$S_n = \begin{bmatrix} 0 & 0 & 0 & \cdots & 0 & 1 \\ 1 & 0 & 0 & \cdots & 0 & 0 \\ 0 & 1 & 0 & 0 & \ddots & 0 \\ \vdots & \ddots & \ddots & \ddots & \ddots & \vdots \\ 0 & \cdots & 0 & 1 & 0 & 0 \\ 0 & \cdots & 0 & 0 & 1 & 0 \end{bmatrix} \tag{5.2}$$

Then the speed-enhancing realization of waveguide methods is that vector multiplication unit-subdiagonals[4] of a matrix can be computed in $O(1)$ if sub-diagonal elements are arranged in a queue structure.

$$y_t = Z_n \cdot y_{t-1} \tag{5.3}$$

with $y = [y_1, y_2, \cdots, y_{n-1}, y_n]$ according to Figure 5.3.

The key condition for the running time $O(1)$ to hold is that there be no individual access to more than a constant number of elements out of y. For instance, an exhaustive radiation sum following Huygen's principle as used in the finite element calculations of section 6.1.3 would not be possible as it accesses all n elements of y. In other words waveguide style methods have high performance only if *a constant number of elements are observed at every timestep*. This is obviously a necessary condition and it should be noted that it does not restrict what the observation points at every time step are[5].

[4] More generally this is also true of any row-permutation of matrices Z_n and S_n, for instance an "upshifting" matrix can be constructed by rotating S_n upward two rows.

[5] Implications for future work are mentioned in section 7.6.2.

Chapter 6

Geometric Simulation Using Finite Elements

> When ideas fail, words come in very handy. – **Johann Wolfgang von Goethe**[1]

> Sometimes when reading Goethe I have the paralyzing suspicion that he is trying to be funny. – **Guy Davenport**[2]

In this chapter the limitations of the proposed method will be outlined more clearly by showing simulations using more general finite element techniques. It is based on joint work with James F. O'Brien and Perry R. Cook [135] that investigated the simultaneous finite element simulation of motion dynamics and sound generation. In addition, perfor-

[1] A commonly used loose translation of a passage in "Faust", pt 1. The original is "*Denn eben, wo Begriffe fehlen, Da stellt ein Wort zur rechten Zeit sich ein.*," (in "Faust" Benno Schwabe Verlag, Basel, line 1995 (1949)). Note that "Begriff" doesn't translate easily. The translation of Anna Swanwick is "For there precisely where ideas fail, A word comes opportunely into play," Faust, part 1, lines 1673-1674, Harvard Classic, Barertleby.com `http://www.bartleby.com/19/1/4.htm`. Bayard Taylor, Boston (1871) translates it as "comprehension" whereas George Madison Priest, Covici-Friede Publishers, New York (1932) translates it as "concept".

[2] Often cited on the world-wide web, though I failed to find a believable attribution. Hence it should be considered hearsay.

mance numbers will be presented that illustrate the performance deficit of finite element methods compared to banded waveguides, as already mentioned earlier (see section 5.5).

The starting point of a finite element simulation is a mesh discretization and a dynamic discription. The technique does not make use of specialized heuristics, assumptions about the shape of the objects, or prerecorded sounds. The audio is generated automatically as the simulation runs and does not require any additional implementation work. This in fact is a significant difference from banded waveguide methods. As has been seen in previous chapters, banded waveguides require additional path constructions, which in addition are not known for arbitrary geometries.

The remaining sections of this chapter provide a detailed description of the finite element technique that was developed, several examples of the results we have obtained, and a comparisons to banded waveguide and other methods.

6.1 Sound Modeling

6.1.1 Motions of Solid Objects

The first step in the technique used requires computing the motions of the animated objects that will be generating sounds.

The method models the motions of solid objects using a nonlinear finite element method similar to the one developed by O'Brien and Hodgins [136, 137]. This method makes use of tetrahedral elements with linear basis functions to compute the movement and deformation of three-dimensional, solid objects. (See figure 2.5.) Green's nonlinear finite strain metric is used so that the method can accurately handle large magnitude deformations. Both these conditions already show the difference from banded waveguides. For one, arbitrary meshes are used. Also, the finite element method has been refined to

allow simulation outside the linear realm of small displacement. Banded waveguides as presented here require this linearity and hence don't allow for large deformations.

This particular method was selected because it is reasonably fast, reasonably accurate, easy to implement, and treats objects as solids rather than shells. However, the sound generation process is largely independent of the method used to generate the object motion. So long as it fulfills a few basic criteria, another method for simulating deformable objects could be selected instead. These criteria are

- *Temporal Resolution* — Vibrations at frequencies as high as about $20,000\ Hz$ generate audible sounds. If the simulation uses an integration time-step larger than approximately $10^{-}5\ s$, then it will not be able to adequately model high frequency vibrations.

- *Dynamic Deformation Modeling* — Most of the sounds that an object generates as it moves arise from vibrations driven by elastic deformation. These vibrations will not be present with techniques that do not model deformation (e.g. rigid body simulators). Similarly, these vibrations will not be present with inertia-less techniques.

- *Surface Representation* — Because the surfaces of the objects are where vibrations are transmitted from the objects to the surrounding medium, the simulation technique must contain some explicit representation of the object surfaces.

The tetrahedral finite element method we are using meets all of these criteria, but so do many other methods that are commonly used for physically based animation. For example, a mass and spring system [31] would be suitable, provided the exterior faces of the system were defined.

6.1.2 Surface Vibrations

After computing the motion of the objects, the next step in the process requires analyzing the surface's motions to determine how it will affect the pressure in the surrounding fluid. Let Ω be the surface of the moving object(s), and let ds be a differential surface element in Ω with unit normal $\hat{\boldsymbol{n}}$ and velocity $\boldsymbol{v}$. If we neglect viscous shear forces then the acoustic pressure, p, of the fluid adjacent to ds is given by

$$p = z\boldsymbol{v} \cdot \hat{\boldsymbol{n}} \tag{6.1}$$

where $z = \rho c$ is the fluid's specific acoustic impedance. From [106], the density of air at $20°C$ under one atmosphere of pressure is $\rho = 1.21 kg/m^3$, and the acoustic wave speed is $c = 343 m/s$, giving $z = 415 Pa \cdot s/m$.

Representing the pressure field over Ω requires some form of discretization. We will assume that a triangulated approximation of Ω exists (denoted Ω^-) and we will approximate the pressure field as being constant over each of the triangles in Ω^-.

Each triangle is defined by three nodes. The position, $\boldsymbol{x}$, and velocity, $\dot{\boldsymbol{x}}$, of each node are computed by a physical simulation method as discussed in the previous section. We will refer to the nodes of a given triangle by indexing the position $\boldsymbol{x}_n$ with $n \in 1,2,3$. The surface area of each triangle is given by

$$a = \|(\boldsymbol{x}_{[2]} - \boldsymbol{x}_{[1]}) \times (\boldsymbol{x}_{[3]} - \boldsymbol{x}_{[1]})\|/2 \tag{6.2}$$

and its unit normal by

$$\hat{\boldsymbol{n}} = \frac{(\boldsymbol{x}_{[2]} - \boldsymbol{x}_{[1]}) \times (\boldsymbol{x}_{[3]} - \boldsymbol{x}_{[1]})}{2a} \tag{6.3}$$

The average pressure over the triangle is computed by substituting the triangle s normal and average velocity, $\bar{\boldsymbol{v}}$, into Equation (6.1) so that

$$\bar{p} = z\bar{\boldsymbol{v}}\hat{\boldsymbol{n}} = z\left(\frac{1}{3}\sum_{i=1}^{3}\dot{\boldsymbol{x}}_{[i]}\right)\cdot\hat{\boldsymbol{n}} \tag{6.4}$$

The variable $\bar{p}$ tells us how the pressure over a given triangle fluctuates, but we are only interested in fluctuations that correspond to frequencies in the audible range.

6.1.3 Wave Radiation and Propagation

Once the pressure distribution is known over the surface of the objects it is computed how the resulting wave propagates outward towards the listener.

Huygen's principle states that the behavior of a wavefront may be modeled by treating every point on the wavefront as the origin of a spherical wave, which is equivalent to stating that the behavior of a complex wavefront can be separated into the behavior of a set of simpler ones. Using this principle, we can approximate the result of propagating a single pressure wave outward from Ω by summing the results of many simpler waves, each propagating from one of the triangles in Ω^{-}:

$$s = \frac{\tilde{p}a\delta_{\bar{x}-r}}{\|\bar{\boldsymbol{x}}-\boldsymbol{r}\|}\cos(\theta) \tag{6.5}$$

where r is the location of the receiver, $\bar{\boldsymbol{x}}$ is the center of the triangle, θ is the angle between the triangle s surface normal and the vector $\boldsymbol{r}-\bar{\boldsymbol{x}}$, and $\delta_{\bar{x}-r}$ is a visibility term that is one if an unobstructed ray can be traced from $\bar{\boldsymbol{x}}$ to $\boldsymbol{r}$ and zero otherwise.

To account for propagation delay we make use of a delay line. All entries in the buffer are initially set to zero. When we compute s for each of the triangles in Ω^{-} at a given time, we also compute a corresponding time delay

$$d = \frac{\|\bar{\boldsymbol{x}} - \boldsymbol{r}\|}{c} \tag{6.6}$$

with c being the acoustic wave speed (speed of sound) in the fluid. The s values are then added to the entries of the buffer that correspond to the current simulation time plus the appropriate delay.

As the simulation advances forward in time, values are read from the entry in the accumulation buffer that corresponds to the current time. This value is treated as an audio sample that is sent to the output. This radiation method would not be possible for banded waveguides without pushing the computational complexity of the method up to calculations per sample point and hence would eliminate the performance advantage.

6.2 Results

Using the described technique for generating audio, several examples were tested. For all of the examples, two listener locations were used to produce stereo audio. The locations are centered around the virtual viewpoint and separated by 20 cm — roughly the separation of human ears — along a horizontal axis that is perpendicular to the viewing direction. The sound spectra shown in the following figures follow the convention of plotting frequency amplitude using decibels, so that the vertical axes are scaled logarithmically.

Figure 6.1 shows an image taken from an animation of a bowl falling onto a hard surface and a spectrogram of the resulting audio. In this example, only the surface of the bowl is used to generate the audio, and the floor is modeled as rigid constraint. Variations in the degree to which each of the modes are excited occur because different parts of the bowl hit the surface on each bounce.

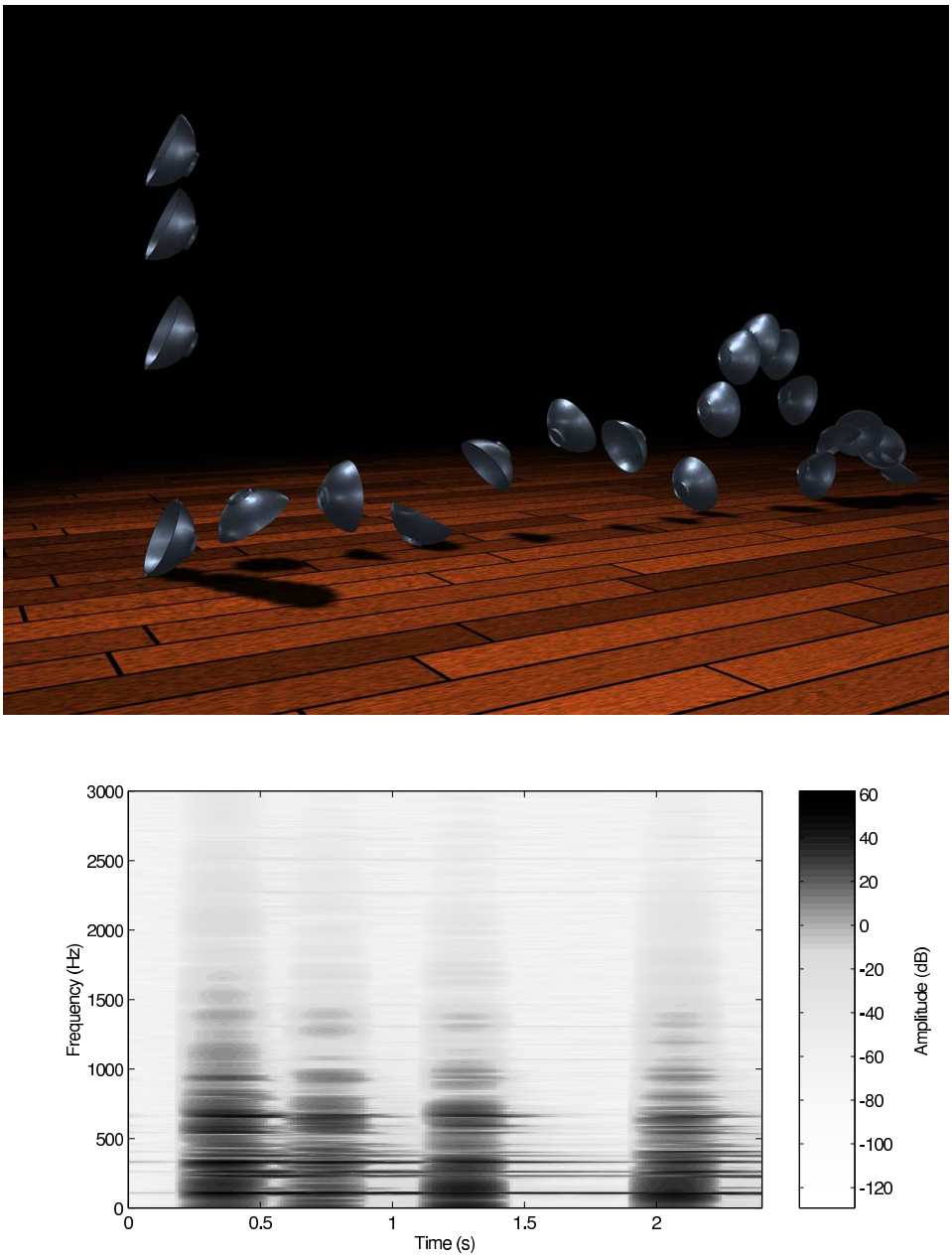

Figure 6.1: The top image shows a multi-exposure image from an animation of a metal bowl falling onto a hard surface. The lower image shows a spectrogram of the resulting audio for the first five impacts.

The bowl's shape is arbitrary and there is no known analytical solution for its vibrational modes. The bowl could also be replaced with an arbitrary shape without additional work. This generality is a clear advantage over banded waveguides.

However this generality entails cost beyond increased computation time. In addition, the conditions of stability (of error accumulation), convergence (approaching a stable solution in the limit of infinitesimal elements) and consistency (converges to the correct differential equation) have to be satisfied, which can be non-trivial or laborious to check [5]. In case of banded waveguides, the stability condition is checked easily by calculating the loop gains. The response converges and is consistent in the sense that modal parameters have been chosen to that end. By the asymptotic and lumped properties the banded waveguide does not necessarily converge to the detailed dynamics though it does converge to a continuous wave-propagation solution of the WKB type (as has been shown in section 3.8.3).

A verification of the finite element method used has been performed and is described in detail in [135].

Of particular interest is the simulation of a vibraphone bar that has been tuned by undercutting. A mesh has been constructed (see Figure 2.5) based on the bar also used in the measurements presented in section 4.1.2.

The undercutting results in a change in transverse impedance between the thin and thick portions of the bar, which prevents an analytical solution. Two simulations of the bar have been computed with mesh resolutions of 1 *cm* and 2 *cm*, and compared them to a recording of a real bar being struck. (The 1 *cm* mesh is shown in Figure 3.) To facilitate the comparison, the simulated audio was warped linearly in frequency to align the first partials to that of the real bar at 187 *Hz* ($F^{\sharp}3$), which is equivalent to adjusting the simulated bar's density so that it matches the real bar. The results of this comparison

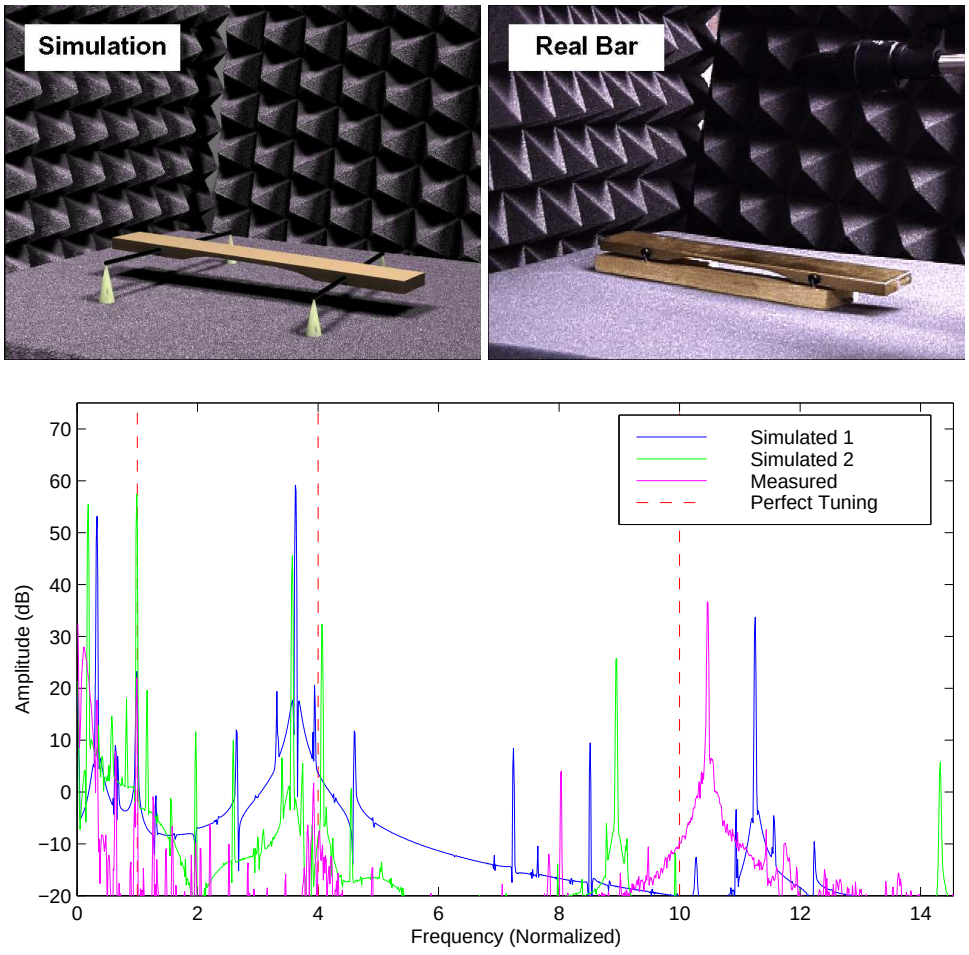

Figure 6.2: The top image plots a comparison between the spectra of a real vibraphone bar (Measured), and simulated results for a low-resolution (Simulated 1) and high-resolution mesh (Simulated 2). The vertical lines located at 1, 4, and 10 show the tuning ratios reported in [70].

are shown in figure 6.2. Although both the simulated and real bars differ slightly from the ideal tuning, they are quite similar to each other. All three sounds also contain a low frequency component below the bar's first mode that is created by the interaction with the real or simulated supports. The discrepancy here is of interest mostly because it highlights the fact that the results of finite element methods depend on the detail of the model description and the accuracy of the mesh. Scatterings at impedance changes are

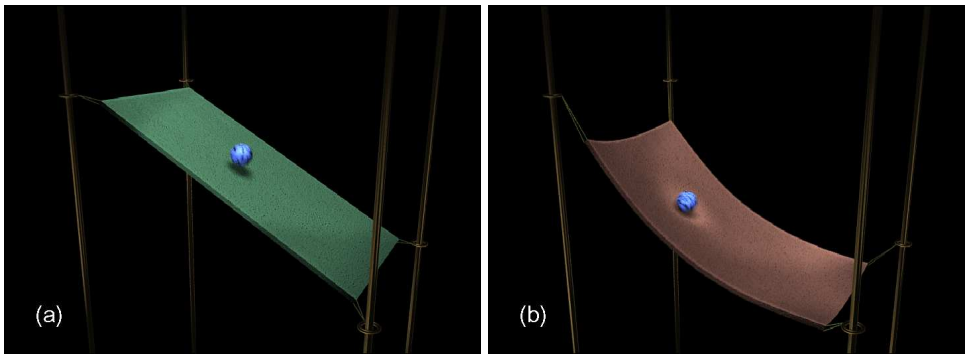

Figure 6.3: These figures show a round weight being dropped onto two different surfaces. The surface shown in (a) is rigid while the one shown in (b) is more compliant.

Figure 6.4: A slightly bowed sheet being bent back and forth.

implicitly solved for and carried through, whereas in banded waveguide simulation these scatterings would either have to be explicitly added or neglected.

Finally I would like to mention examples which are not directly possible using banded waveguides but can be achieved directly using the finite element method discussed here.

Because the finite element method does not make additional assumptions about how waves travel in the solid objects, it can be used with nonlinear simulation methods to generate sounds for objects whose internal vibrations are not modeled by the linear wave

Example	Figure	Time-step (10^{-7}s)	Nodes	Elements	Surface Elements	Total Time (min)	Audio Time (min)	
Bowl	6.1	10	387	1081	742	91.3	4.01	4.4%
Clampled Bar	[135, 5]	1	125	265	246	240.4	1.26	0.5%
Square Plate (on center)	[135, 6.a]	10	688	1864	1372	245.0	8.14	3.3%
Square Plate (off center)	[135, 6.b]	10	688	1864	1372	195.7	7.23	3.7%
Vibraphone Bar	6.2	1	539	1484	994	1309.7	5.31	0.4%
Swinging Bar	[135, 8]	3	130	281	254	88.4	1.42	1.6%
Rigid Sheet	6.3.a	6	727	1954	1438	1041.8	7.80	0.7%
Compliant Sheet	6.3.b	20	727	1954	1438	313.1	7.71	2.5%
Bent Sheet	6.4	1	678	1838	1350	1574.2	6.45	0.4%

Table 6.1: Computation times for the finite element simulations. The total times indicate the total number of minutes required to compute one second of simulated data, including graphics and file I/O. The audio times listed indicate the amount of the total time that was spent generating audio, including related file I/O. The percentages listed indicate the time spent generating audio as a percentage of the total simulation time. Timing data were measured on an SGI Origin using one 350 MHz MIPS R12K processor while unrelated processes were running on the machine's other processors.

equation. The finite element method we are using employs a nonlinear strain metric that is suitable for modeling large deformations. Figure 6.3 shows frames from two animation of a ball dropping onto a sheet. In the first one, the sheet is nearly rigid and the ball rolls off. In the second animation, the sheet is highly compliant and it undergoes large deformations as it interacts with the ball. Another example demonstrating large deformations is shown in figure 6.4 where a slightly bowed sheet is being bent back and forth to create a crinkling sound. Animations containing the audio for these, and other, examples have been included on the proceedings video tape and DVD of [135].

All simulations times, including the examples discussed here and those discussed in [135], are listed in table 6.1. As can be seen, none of the rendered examples is close to real-time performance. This is true even for simple examples as a clamped uniform bar. This has to do with the small time-steps required for stability (which in some examples is smaller than perceptually necessary) in this method but largely because of the mesh discretization and the required solution of linear systems equations of related size.

Chapter 7

Conclusions, Future Directions and Applications

> [..] the other is a conclusion.
>
> shewing from various causes why the execution has not been equal to what the author promised to himself and the publick (*sic*).[1] – **Samuel Johnson**[2]

> I hate quotations. Tell me what you know. – **Ralph Waldo Emerson**[3]

> Don't let it end like this. Tell them I said something. – **(maybe not the) last words of Pancho Villa**[4]

[1] First half of the quote to be found in the introduction chapter.

[2] James Boswell, "Life of Samuel Johnson," (1755) available at `http://newark.rutgers.edu/~jlynch/Texts/BLJ/blj55.html` or according to [147, p. 371, q. 17] in vol. 1, p. 292 (1755)

[3] In "Journals of Ralph Waldo Emerson", Houghton Mifflin Company, Boston, vol. 8, May 3, (1849), last entry.

[4] Though this quote is usually attributed to Villa on many web-pages, online information by the Tucson-Pima public library claims no. See `http://www.lib.ci.tucson.az.us/government/infoline/archivesq15.htm`. K. S. Guthke (in "Last Words," Princeton University Press, p. 10, (1992)) is undecided and writes: "Whether authentic or not, this often-cited remark pointedly plays up the collective fascination with last words."

7.1 Conclusions

The principle of closed wavetrains, also known as the principle of equal phase closure has been one of the main guiding principles for the work in this thesis.

By using closed wavetrains as a starting point, the resulting simulations and the descriptive dynamics give insights into the dynamics of musical instruments, the connection between modal synthesis [1], digtal waveguide filter synthesis [187] and simulation based on finite difference or finite elements. In this concluding notes, I would like to again highlight the connections that have been made through that guiding principle.

7.2 Separation of Wavetrains and Geometry

Digital waveguide filters assume that the propagation speed of traveling waves is roughly the same for all frequencies. Small deviations can be implemented using all-pass filters but large deviations require high-order filters and the extension becomes computationally expensive. This is equivalent to having one equal phase condition for all frequencies. The effect is that all modes come about from the same closed wavetrain. As part of this thesis, I showed that modeling one closed wavetrain per associated mode allows modeling stiff systems, like bars, which don't have a constant propagation speed (section 4.1 and [60]). This separation of wavetrains has a second effect. It also allows for modes to arise from different, independent paths. This is crucial to allow the idea to be used on dynamic systems of higher dimensions like membranes, cymbals, or wine glasses (sections 4.2-4.4 and [62, 179]).

A square membrane can serve as illustration of this concept. The first mode corresponds to the family of rays which bounce at the boundary at a 45 degree angle (or a total of 90 degrees between incoming and outgoing ray). As can easily be seen in Figure 7.1

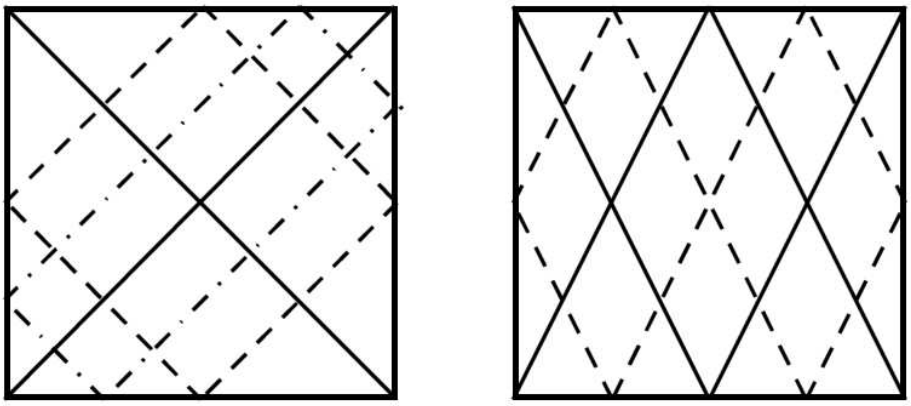

Figure 7.1: Left: Closed paths with one reflection at each side. Right: Closed paths with two reflection at the top and bottom and one at the sides.

all of the rays have the same length (the length of twice the diagonal), the same number of boundary reflections (one on each side). The second mode is the result of rays bouncing twice at the top and bottom and once on the sides. Again, the family of rays has the same length and number of reflections. These are two distinct closed paths on the domain leading to two distinct closed wavetrains and two contributions to the modal response. The modes are not necessarily unique, however. If accurate modeling is the goal, these degenerate modes have to be taken into account. If the propagation speed on the medium is the same on both paths, a condition which is necessarily true in a homogeneous medium, the two paths may in fact also dynamically be indistinguishable. In this case the necessary care corresponds to noting, that even though the traveling paths have the same length and speed, the interaction points may be distinct, as the paths are geometrically different. If this is being taken care of this mode can in fact be modeled as a “fused” banded wavepath. If the paths are distinguishable, this does not necessarily require separating the wavepaths, though that is a possibility. It still requires only that the interaction points are appropriately adjusted according to the separate wavepath geometries. This is of

course the case only if there are no local scatterings, they are weak and can be ignored or not significant for a dynamic response of interest. The efficiency of waveguide style simulation is directly connected to the amount of modeled local scatterings. This can be seen from Bilbao's work on the connection of finite differencing and digital waveguide networks [16, 17, 18]. This suggests that considering the perceptual and dynamical relevance of scatterings is important when trying to achieve efficient models.

7.3 The Link Between Lumped Modal Synthesis and Digital Waveguide Synthesis

Adrien proposed an interpretive link between additive sinusoidal modeling and physical modeling by giving additive sinusoids the physical interpretation of damped harmonic oscillators (mass-spring-damper system) which correspond to the eigensolutions of the actual physical system and the finite differencing scheme [1]. However, the point then was, that physical modeling was understood as finite differencing and that modes corresponded to decaying sinusoids.

Banded waveguides provide a similar interpretive link between modal synthesis and digital waveguide filters. The key here is again the equivalence between the principle of closed wavetrains and modal response. In essence, the principle explains how modes come about dynamically, whereas in Adrien's picture modes are solutions of the governing equations without a clear dynamic connection.

While previously we have discussed banded waveguides as a generalization of digital waveguide filters for arbitrary linearly propagating media, banded waveguides can also be viewed as generalized modal models. The bandpass filters correspond to the resonant filters of a lumped modal model and the delays correspond to a "phase-delay correction"

for the mode. That is in the lumped modal model, the spatial information has been discarded and aspects of this spatial information is restored using banded waveguides. Dynamically this can be seen as the time for a wave to travel one cycle to finally close onto itself. This delay has been discarded in the lumped model and hence transients are expected to be less accurate in lumped models.

7.4 The Link Between Geometry and Modes

As mentioned before, the connection between closed wavetrain paths and modes leads to an immediate consideration of geometry. If the underlying dynamics is fixed, then indeed the resulting modes directly depend on the geometry of the object. This direct connection was highlighted by Kac's famous question "Can we hear the shape of a drum?" [97]. While this question has been answered with "no" for specific nonsmooth constructions [57], the question remains open for most and very general classes of shapes (like all smooth boundaries). Of course, one can reinterpret Kac's question as referring to perceptual equivalence between shapes rather than mathematical equivalence. This question has started to get attention in the Computer Music community recently [168].

7.4.1 Geometry, Modes and Efficiency

The reason why the link between modes and geometry is relevant for physical models of musical instruments has to do with the efficiency gap between modal, waveguide and banded waveguide models, and mesh-based models like waveguide networks or finite element methods. The first class of methods is independent of the spatial resolution of the simulation [62]. The efficiency of the second is dependent on the number of mesh points. The first class is however dependent on the number of perceptually relevant

modes. If this number gets too high, the method becomes inefficient. Hence there is a trade-off between these two dimensions, which was first observed by Serafin and co-workers, who proposed a hybrid method to accommodate high densities of modes by modeling those regions with meshes of low spatial cost and low density regions in the spectrum using the banded waveguide method [179]. But even in the case of low mode density, the connection between modes and geometry remains an important one. One could imagine using a banded waveguide approach blindly, that is, just as a form of phase-corrected modal model, where the tuning parameters of the banded waveguides, band-center frequency and delay-length are derived from measurements or precomputation. Then the interpretation of spatial interaction away from the measurement point would disappear, an aspect that is very important in the dynamic simulation of many musical instruments (for the complex interaction with the Indian Tabla drums see [62]).

7.5 Summary

The summary of all these connections can be seen in figure 7.2. By generalizing both waveguides and modal synthesis, banded waveguides overcome the respective limitations of media/material type and interaction type. While finite element methods are slow, they are the solution of choice for complex and highly non-linear media as well as for arbitrarily complex geometries.

Method	Speed	Media	Interaction	Shape
Modal	O(1)	Linear	Linear	No
Waveguides	O(1)	Restricted	All	1-D
Banded Waveguides	O(1)	Linear	All	Some
Finite Elements	O(n)	General	All	All

Figure 7.2: Comparison of modal synthesis, waveguides, banded waveguides and finite element methods.

7.6 Future Work

7.6.1 Perceptual Measures for Synthesis Methods

An interesting and important question has not been thoroughly addressed in this thesis: the question of a quantitative measure of perceptual quality of a sound simulation. Perceptual models have a history of research behind them [26, 130], though only recently in the context of digital speech coding for wireless telephony [4, 11, 164] led attempts at using them to arrive at quantitative measures. Another field where perceptual models have found an application is music coding for compression (for a review see [144]). This work has let to a wealth of experimental data which can be used as reference for recorded music quality and in fact has been used to validate computational model measures by Thiede and Kabot [196]. While this line of research definitely shows promise for the use with synthesis methods, it does not directly address a number of specific problems. In particular the focus of the mentioned work is that differences are imperceptible. In simulation other determinants of quality may be more desirable. For instance, a simulation may sound different from an actual instrument from which its model parameters

have been derived as long as it is "believable" to the listener as being such an instrument (assuming ignorance of the listener of the original instrument). In fact, Bonebright and co-workers realized the multiplicity of perceptual qualities when proposing methods for evaluating such qualities [19].

The perceptual dimension indeed has received some attention in very recent history in the physical modeling community [95, 168].

I would like to propose taking the perceptual quality coding of Thiede and Kabot as starting point but extending such a model to a "believability" measure by adding a judgment of closeness in timbre space [43, chap. 7]. If a quantitative measure along this lines or in other forms is possible, it still remains to be explored.

7.6.2 Waveguide Preconditioning for Matrix Methods

As seen in section 5.5, delay operations can be seen as a special type of matrix multiplication. A subdiagonal unitary matrix can be implemented using queues and the multiplication (rather the shift operation that corresponds to the multiplication) can be performed in $O(1)$ and maintains this performance if no more than constant of the resulting vector elements are observed at any time-step. Hence if the latter condition holds one might assume that, given the original matrix or subspaces thereof can be brought into subdiagonal form, that solution beyond $O(N)$ are possible. This field remains to be explored, and I just want to mention a number of guiding intuitions.

If indeed subspaces of this type can be found, then they should correspond to a scatter-free dynamics. In such cases performance enhancing preconditioning is possible without approximation. Another approach would be to identify scatterings, define a measure of the strength of the scattering and discard "weak scatterings" to achieve sparsing heuristics. Finally, an approach that is widely used in waveguide modeling is commutation. If

The observation points can be fixed, then the behavior between those points in a linear dynamics can be commuted and can also be commuted into the observation or interaction operations. Also the effect of "limited observation" that is imposed by the condition of efficiency is worthy of exploration.

7.6.3 Multirate Banded Waveguides, Perturbations and Extensions in the Banded Case

Also largely unexplored is the study of perturbations to ideal banded waveguide paths. In particular there exist literature which study specific modifications to standard waveguides which should be applicable to the banded waveguide case. For instance in this thesis rate decimation (multirate modeling, critical sampling in time) was not discussed. Such approaches have been proposed and implemented in the context of waveguides [206, 180]. Though it should be noted that time-decimation may or may not yield performance gain [9]. All these questions remain to be explored.

Appendix A

Glossary for Terms in Asymptotic and Traveling Wave Methods

The purpose of this glossary is mostly to facilitate the reading of related literature for readers who are not familiar with the nomenclature as it is not part of conventional textbooks in the computer music and signal processing community.

As introductory books introducing the topic I recommend mostly Brack and Bhaduri's recent textbook [25] which guides the mathematics with physical intuition and Dahlen and Tromp [50] who despite treating seismological problems explain the method in a way that is appealing to engineers in general. Bouche, Molinet and Mittra [23] provide a gentle applied mathematics perspective with emphasis on optics and electromagnetism. Classical texts include Olver [139], Bender and Orszag [13]. Cvitanović *et al* [48] provide a comprehensive treatment, though with emphasis on chaos. More advanced mathematical texts include Fedoryuk [68], Mishchenko *et al* [129], Kravtsov and Orlov [110] and Kozlov and Treshchëv [109]. A related text in pure mathematics treating the scattering problem is Melrose [128].

Asymptotics an Ansatz that approaches the exact solution in the limit of some variable. More precisely the generalized Poincaré definition of asymptotics is: $f(z) = \sum_{s=0}^{n-1} a_s \phi_s(z) + O(\phi_n(z))$ with $(z \to c \text{ in } \mathbb{R})$ for all non-negative n with c being a finite limit point, $f(z)$ being the exact function, $\phi(z)$ being the asymptotic sequence and a_s being asymptotic amplitudes (from [139, p. 25, eq. (10.03)], which in the case of a ray asymptotics (here I write the Keller-asymptotics [104, eq. (3)] has the form $u = \sum_{j=1}^{N} e^{ikS_j}[A_j + O(1/k)]$ with k being the wave-number and S_j and A_j being phase and amplitude. Obviously the expansion is a good one as $k \to \infty$, that is for short wave-lengths. See also WKB.

Caustics usually higher dimensional turning points [103, p. 492].

Conjugate points see turning points [25, p. 79].

EBK short for Einstein-Brillouin-Keller [103, p. 493] [25, pp. 78-82], corresponds to the derivation of the Maslov index by finding closed windings around an N-torus, where N is the number of dimensions of the dynamic space. For membranes and other two-dimensional structures the 2-torus looks like a doughnut. See also resonant torus.

JWKB short for Jeffreys-Wenzel-Kramers-Brillouin [121, p. 27], same as WKB.

Lagrangian manifold a topological structure in phase-space that relates the dynamics of the system to the occurance of caustics in physical space [58] also [129, P. 28], [110, p. 15].

LG approximation short for Liouville-Green approximation [139, p. 190 and 228] alternative term for WKB or JWKB. Refers to the exponential Ansatz in the absence of turning point treatment which is attributed to Liouville (1837) and Green (1837)

though earlier work is traced to Carlini in 1817. JWKB and also Gans (1915) and Rayleigh [160] treated approximate connection formulas across turning points.

Maslov index counts the number of turning points [25, p. 77] and other phase corrections along a periodic orbit [25, p. 218].

Mode-ray duality also eigenvalue-periodic orbits duality [48, pp. 131ff] the correspondence of modes to closed ray-paths [50, chap. 12].

Periodic orbit a dynamic trajectory that closes onto itself [109, p. 53] or [48]. The periodic orbit condition [48, p. 259] corresponds to the principle of equal phase closure.

Principle of equal phase closure refers to the condition that a taveling wave, following a closed trajectory, has to return to it's initial phase at the starting point for resonance to occur [25, p. 79] or [47, 126].

Principle of wavetrain closure same as the principle of equal phase closure.

Quasi-periodic orbits is an orbit on an integrable domain (and hence on the EBK resonant torus) which does not close onto itself in finite length [25, p. 92].

Resonant torus is the topological structure which can be constructed using canonical transforms for integrable dynamical systems and which lead to EBK quantization conditions [25, p. 78ff] and are used in the study of chaos [25, p. 98].

Stationary points see turning points [205, p. 11].

Turning points points at which WKB becomes invalid due to singularity [13, p. 497], similar to caustics, though it also refers to boundaries that induce phase-shifts [25,

p.434]. Caustic turning points inside the domain are also referred to as “smooth” turning points and fixed boundaries are referred to as “hard” turning points [25, p. 88].

Winding number number of windings along a topological dimension of the EBK N-torus [25, p. 81].

WKB short for Wenzel-Kramers-Brillouin [13, p. 486] [121, p. 27] but going back to Rayleigh [160] (see [13, p. 486]) and Jeffreys (see [13, p. 486][121, p. 27]). Wigner-Kramers-Brillouin [25, p. 63]. Refers to the traveling wave Ansatz to solve differential equations. Specifically, Olver [139] defines WKB to refer to this Ansatz in the presence of treatement across turning points. See also LG approximation.

Appendix B

Implementation

All application examples have been implemented within the framework of the synthesis toolkit (STK) developed by Perry R. Cook and Gary Scavone and is available with Perry Cook's recent book [45] and online at `http://www-ccrma.stanford.edu/software/stk/`.

STK uses C++ for implementation of the synthesis algorihms. Graphical user interfaces are provided using Tcl/tk. In addition, STK provides an input interface for MIDI.

The core routine to be performed at every time step is exactly the banded waveguide structure of Figure 1.1.

The primitives used in this filter diagram are implemented using already existing classes in STK. Each banded wave-path is constructed from a second-order resonant filter (`BiQuad.cpp`) and a delay-line (`Delay.cpp`). The free parameters are the length of the delay-line and the three filter coefficients of the second-order infinite impulse response filter [193]:

$$y_t = A_0 x_t + (2R\cos\theta) y_{t-1} - R^2 y_{t-2} \tag{B.1}$$

These then can be recalculated to gain, resonant frequency and bandwidth [194, p. 92]:

$$R \approx 1 - B/2 \tag{B.2}$$

$$\cos\theta = \frac{2R}{1+R^2}\cos\omega \tag{B.3}$$

$$A_0 = (1-R^2)\sin\theta \tag{B.4}$$

The the overall delay d in feedback (forming a comb filter structure[194]) shows a harmonic resonant response and fundamental frequency f_0 and harmonics f_m correspond to the delay length d:

$$f_m = \frac{m \cdot N_r}{d} \quad m \in \mathbb{N}_0^+ \tag{B.5}$$

where N_r is the sampling rate. The resonant frequency and one resonant peak of the of the comb filter must coincide as they both follow from the same closure condition. Usually the resonant filter frequency is tuned using modal esimation and the multi-valuedness of B.5 by knowing the quotient of propagation speed c_n to path length l. This can be derived from equations 3.11 and 3.12 as the delay length d_n^* is calculated from this quotient plus the sampling rate:

$$d_n^* = \frac{l \cdot N_r}{c_n} \tag{B.6}$$

The bandwidth of the resonant filter is a non-physical parameter and defines the spectral neighborhood of a mode. In general a fairly wide bandwidth is used as the actual frequency response is achieved throught the closure condition of the wave-path (compare section 4.1).

The sum of all wave-paths defines both the output as well as the interaction point. This point can be used for impulsive excitations or can be fed into an interaction algoritm. In our implementation the bow excitation algorithm (`BowTabl`) provided by STK is used.

The collection of all these parameters then can be controlled either via MIDI or through a graphical user interface as depicted in Figure B.1. This example shows the graphical user interface written in Tcl/TK for the one-dimensional and quasi-one-dimensional instruments discussed in this thesis.

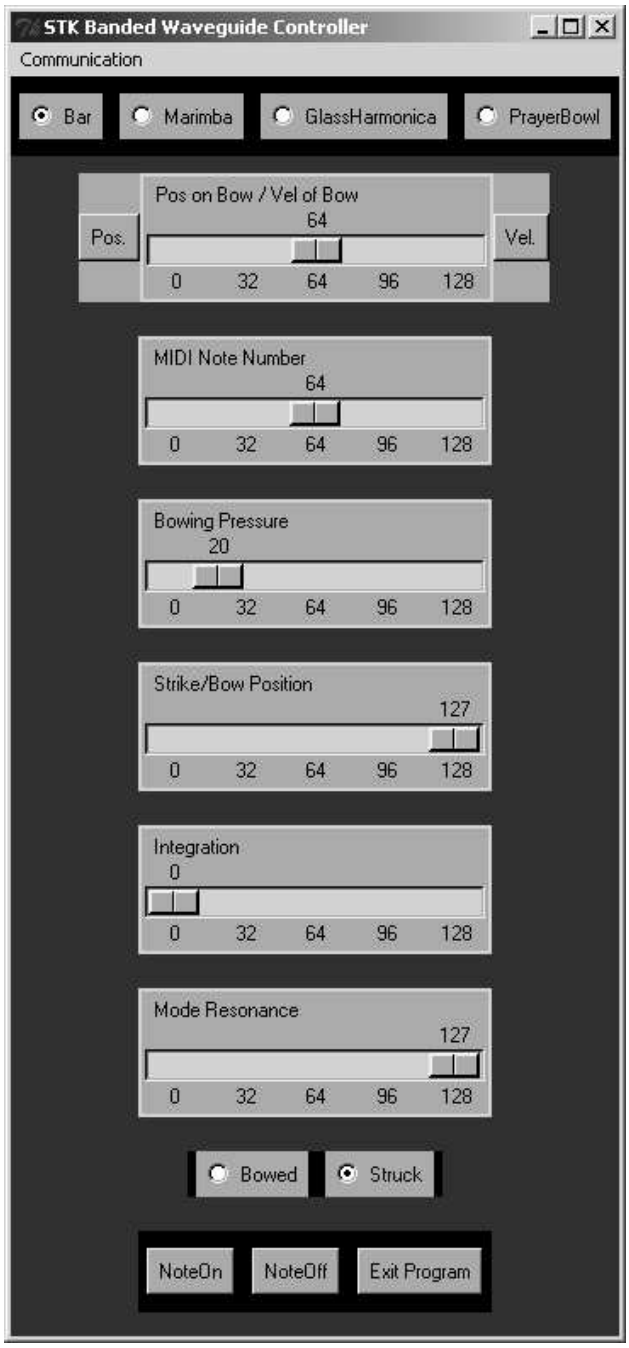

Figure B.1: STK graphical user interface for bars and bowls using banded waveguides.

To none more grateful than to me; escaped

From the vast city, where I long had pined

A discontented sojourner; now free,

Free as a bird to settle where I will. – **William Wordsworth**[1]

[1]In “The Prelude,” bk. 1, l. 1, (1850) according to [147, p. 746, q. 17]

Index of Authors

Bibliography

[1] J.-M. Adrien. The missing link: Modal synthesis. In G. De Poli, A. Piccialli, and C. Roads, editors, *Representations of Musical Signals*, chapter 8, pages 269–297. MIT Press, Cambridge, 1991.

[2] M. Aird and J. Laird. Extending Digital Waveguides to Include Material Modelling. In *Proceedings of the COST G-6 Conference on Digital Audio Effects (DAFX-01)*, Limerick, Ireland, December 6-8 2001.

[3] A. Akay. Acoustics of friction. *Journal of the Acoustical Society of America*, 111(4):1525–1548, April 2002.

[4] A. Alwan, S. Narayanan, B. Strope, and A. Shen. Speech Production and Perception Models and Their Applications to Synthesis, Recognition, and Coding. In *Proceedings of the International Symposiun of Signals, Systems, and Electronics (ISSSE-95)*, pages 367–372, October 1995.

[5] W. F. Ames. *Numerical Methods for Partial Differential Equations*. Academic Press, San Diego, 3 edition, 1992.

[6] F. Avanzini, B. Bank, G. Borin, G. De Poli, F. Fontana, and D. Rocchesso. Musical instrument modeling: the case of the piano. In *Proceedings of the Workshop on Current Research Directions in Computer Music*, Barcelona, November 15-17 2001. Available online: `http://www.iua.upf.es/mtg/mosart/paper/p18.pdf`.

[7] A. D. Back and A. C. Tsoi. Nonlinear System Identification Using Discrete Laguerre Functions. *Journal of Systems Engineering*, 6(3):194–207, August 1996.

[8] B. Bank. Physics-Based Sound Synthesis of the Piano. Master's thesis, Budapest University of Technology and Economics, 2000. Also available at Helsinki University of Technology, Laboratory of Acoustics and Audio Signal Processing, Report 54.

[9] B. Bank. Accurate and efficient modeling of beating and two-stage decay for string instrument synthesis. In *Proceedings of the MOSART Workshop on Current Research Directions in Computer Music*, pages 134–137, Barcelona, Spain, 2001.

[10] R. W. Batterman. *The Devil in the Details*. Oxford University Press, 2002.

[11] J. G. Beerends, A. P. Hekstra, A. W. Rix, and M. P. Hollier. Perceptual Evaluation of Speech Quality (PESQ), the new ITU standard for end-to-end speech quality assessment. Part II — Psychoacoustic Model. Unpublished manuscript. Psytechnics reference number 2001-P03b. Available at: `http://www.psytechnics.com/papers/2001-P03b.pdf`, July 2001.

[12] D. R. Begault. *3-D Sound for Virtual Reality and Multimedia*. Academic Press, 1994.

[13] C. M. Bender and S. A. Orszag. *Advanced Mathematical Methods for Scientists and Engineers*. McGraw-Hill, 1978.

[14] M. Berry. Why are special functions special? *Physics Today*, 54(4):11–12, April 2001.

[15] M. Berry. Singular Limits. *Physics Today*, 55(5):10–11, May 2002.

[16] S. D. Bilbao. Digital Waveguide Networks as Multidimensional Wave Digital Filters. In *Proceedings of the COST G-6 Conference on Digital Audio Effects (DAFX-00)*, pages 49–54, Verona, Italy, December 7-9 2000.

[17] S. D. Bilbao. Digital Waveguide Networks for Inhomogeneous Media. In *Proceedings of the COST G-6 Conference on Digital Audio Effects (DAFX-00)*, pages 249–252, Verona, Italy, December 7-9 2000.

[18] S. D. Bilbao. *Wave and Scattering Methods for the Numerical Integration of Partial Differential Equations*. PhD thesis, Stanford University, May 2001.

[19] T. L. Bonebright, N. E. Miner, T. E. Goldsmith, and T. P. Caudell. Data Collection and Analysis Techniques for Evaluating the Perceptual Qualities of Auditory Stimuli. In *Proceedings of the International Conference of Auditory Display (ICAD'98)*, `http://www.ewic.org.uk/ewic/workshop/view.cfm/ICAD-98`, 1998.

[20] I. Bork. Practical Tuning of Xylophone Bars and Resonators. *Applied Acoustics*, 46:103–127, 1995.

[21] I. Bork, A. Chaigne, L.-C. Trebuchet, M. Kosfelder, and D. Pillot. Comparison between Modal Analysis and Finite Element Modelling of a Marimba Bar. *Acustica united with acta acustica*, 85(2):258–266, 1999.

[22] F. A. Bornemann and R. Krause. Classical and Cascadic Multigrid — A Methodological Comparison. In P. E. Bjørstad, M. S. Espedal, and D. E. Keyes, editors, *Proceedings of the 9th International Conference on Domain Decomposition Methods 1996, Ullensvang, Norway*, chapter 7, pages 64–71. Domain Decomposition Press, 1998.

[23] D. Bouche, F. Molinet, and R. Mittra. *Asymptotic Methods in Electromagnetics*. Springer Verlag, 1997.

[24] J. P. Boyd. The Devil's Invention: Asymptotic, Superasymptotic and Hyperasymptotic Series. *Acta Applicandae*, 56:1–98, 1999.

[25] M. Brack and R. K. Bhaduri. *Semiclassical Physics*, volume 96 of *Frontiers in Physics*. Addison-Wesley Publishing, 1997.

[26] A. S. Bregman. *Auditory Scene Analysis*. MIT Press, Cambridge, Massachusetts, 1990.

[27] J. Bretos, C. Santamaría, and J. A. Moral. Finite element analysis and experimental measurements of natural eigenmodes and random responses of wooden bars used in musical instruments. *Applied Acoustics*, 56:141–156, 1999.

[28] S. Browne. Hybrid Reverberation Algorithm using Truncated Impulse Response Convolution and Recursive Filtering. Master's thesis, University of Miami, Coral Gables, Florida, June 2001.

[29] V. Bucur. *Acoustics of Wood*. CRC Press, Boca Raton, 1995.

[30] C. Cadoz, A. Luciani, and J.-L. Florens. Responsive Input Devices and Sound Synthesis by Simulation of Instrumental Mechanisms: The Cordis System. *Computer Music Journal*, 8(3):60–73, 1984.

[31] C. Cadoz, A. Luciani, and J.-L. Florens. CORDIS-ANIMA: A Modeling and Simulation System for Sound and Image Synthesis - The General Formalism. *Computer Music Journal*, 17(1):19–29, Spring 1993.

[32] M. Cavagnero. Addendum to JWKB. Unpublished lecture notes available online at `http://www.pa.uky.edu/~mike/courses/phy614/html/pdf/addend.pdf`, April 29 2002.

[33] A. Chaigne and A. Askenfelt. Numerical simulations of piano strings. I. A physical model for a struck string using finite difference methods. *Journal of the Acoustical Society of America*, 95(2):1112–1118, 1994.

[34] A. Chaigne and A. Askenfelt. Numerical simulations of piano strings. II. Comparisons with measurements and systematic exploration of some hammer-string parameters. *Journal of the Acoustical Society of America*, 95(3):1631–1640, 1994.

[35] A. Chaigne and V. Doutaut. Numerical simulations of xylophones. I. Time-domain modeling of the vibrating bars. *Journal of the Acoustical Society of America*, 101(1):539–557, 1997.

[36] A. Chaigne and C. Lambourg. Time-domain simulation of damped impacted plates. I. Theory and experiments. *Journal of the Acoustical Society of America*, 109(4):1422–1432, April 2001.

[37] R. H. Chan and M. K. Ng. Iterative Methods for Linear Systems with Matrix Structure. In T. Kailath and A. Sayed, editors, *Fast Reliable Algorithms for Matrices with Structure*, pages 117–152. SIAM, 1999.

[38] S. J. Chapman, J. M. H. Lawry, J. R. Ockendon, and R. H. Tew. On the Theory of Complex Rays. *SIAM Review*, 41(3):417–509, 1999.

[39] G. Chen, M. P. Coleman, and J. Zhou. Analysis of Vibration Eigenfrequencies of a Thin Plate by the Keller-Rubinow Wave Method I: Clamped Boundary Conditions With Rectangular or Circular Geometry. *SIAM Journal on Applied Mathematics*, 51(4):967–983, August 1991.

[40] E. F. F. Chladni. *Die Akustik*. Breitkopf & Härtel, Leipzig, Germany, 1830.

[41] M. I. Cho and S. K. Mitra. Warped Discrete Cosine Transform and Its Application in Image Compression. *IEEE Transactions on Circuits and Systems for Video Technology*, 10(8):1364–1373, December 2000.

[42] P. R. Cook. Physically Informed Sonic Modeling (PhISM): Synthesis of Percussive Sounds. *Computer Music Journal*, 21(3):38–49, 1997.

[43] P. R. Cook, editor. *Music Cognition, and Computerized Sound*. MIT Press, Cambridge, Massachusetts, 1999.

[44] P. R. Cook. Toward Physically-Informed Parametric Synthesis of Sound Effects. In *Proceedings of the 1999 IEEE Workshop on Applications of Signal Processing to Audio and Acoustics (WASPAA-99)*, pages 1–5, New Paltz, NY, October 17-20 1999.

[45] P. R. Cook. *Real Sound Synthesis for Interactive Applications*. A K Peters, Ltd., July 2002.

[46] L. Cremer. *The Physics of the Violin*. MIT Press, Cambridge, 1984.

[47] L. Cremer, M. Heckl, and E. Ungar. *Structure-Borne Sound*. Springer Verlag, 2nd edition, 1988.

[48] P. Cvitanović, R. Artuso, P. Dahlqvist, R. Mainieri, G. Tanner, G. Vattay, N. Whelan, and A. Wirzba. *Classical and Quantum Chaos*. Webbook, January 30 2002. version 9.1.1 available online at `http://www.nbi.dk/ChaosBook/`.

[49] L. Dahl and J.-M. Jot. A Reverberator Based on Absorbent All-Pass Filters. In *Proceedings of the COST G-6 Conference on Digital Audio Effects (DAFX-00)*, pages 67–72, Verona, Italy, December 7-9 2000.

[50] F. A. Dahlen and J. Tromp. *Theoretical Global Seismology*. Princeton University Press, 1998.

[51] I. Daubechies. Where do wavelets come from? — A personal point of view. *Proceedings of the IEEE — Special Issue on Wavelets*, 84(4):510–513, April 1996.

[52] P. Denissenko and D. Y. Hsieh. Surface water waves interaction in a circular vessel with oscillating walls. In *Division for Fluid Dynamics (DFD98) Meeting of The American Physical Society (abstract only)*, Philadelphia, PA., November 22-24 1998.

[53] P. Denissenko and D. Y. Hsieh. Water Waves in a Circular Elastic Vessel: The Experiiment. Online document to abstract only conference contribution [52], November 1998.

[54] D. K. DiFilippo, D. Pai. Contact Interaction with Integrated Audio and Haptics. In *Proceedings of the International Conference on Auditory Display (ICAD)*, 2000.

[55] C. Dodge and T. A. Jerse. *Computer Music: Synthesis, Composition, and Performance*. Schirmer Books, 1985.

[56] V. Doutaut, D. Matignon, and A. Chaigne. Numerical simulations of xylophones. II. Time-domain modeling of the resonator and of the radiated sound pressure. *Journal of the Acoustical Society of America*, 104(3):1633–1647, 1998.

[57] T. A. Driscoll. Eigenmodes of Isospectral Drums. *SIAM Review*, 39(1):1–17, March 1997.

[58] J. J. Duistermaat. Book Review - Lagrangian Manifolds and the Maslov operator. *Bulletin of the American Mathematical Society*, 27(1):174–179, July 1992.

[59] M. Eichler. On Finding One's Way in the Uncharted Swamps of Interdisciplinarity. In *Outside the Lines: Issues in Interdisciplinary Research*, pages 58–62. McGill-Queen's University Press, 1996.

[60] G. Essl and P. R. Cook. Banded Waveguides: Towards Physical Modeling of Bowed Bar Percussion Instruments. In *Proceedings of the International Computer Music Conference (ICMC)*, pages 321–324, Beijing, China, 1999. International Computer Music Association (ICMA).

[61] G. Essl and P. R. Cook. Measurements and efficient simulations of bowed bars. *Journal of the Acoustical Society of America*, 108(1):379–388, 2000.

[62] G. Essl and P. R. Cook. Sound Propagation Modeling in Objects: Rubbing, Sliding and Scratching the Surface. Unpublised manuscript, available by request from the first author., November 2001.

[63] G. Essl and P. R. Cook. Banded Waveguides on Circular Topologies and of Beating Modes: Tibetan Singing Bowls and Glass Harmonicas. Submitted to the International Computer Music Conference (ICMC-02), Göteborg, Sweden., 2002.

[64] G. Essl and P. R. Cook. The Principle of Closed Wavetrains, Resonance and Efficiency: The Missing Link Revisited. Submitted to the International Computer Music Conference (ICMC-02), Göteborg, Sweden., 2002.

[65] G. Evangelista. Real-Time Time-Varying Frequency Warping via Short-Time Laguerre Transform. In *Proceedings of COST G-6 Conference on Digital Audio Effects (DAFX-00)*, pages 7–12, Verona, Italy, December 2000.

[66] G. Evangelista and S. Cavaliere. Representation and Modification of Time-Varying Sound Signals. In *Proceedings of the 13th Colloquium on Musical Informatics*, pages 25–28, L'Aquila, Italy, September 2000.

[67] G. Evangelista and S. Cavaliere. Signal Transforms for the Detection and Identification of Signals. In *Proceedings of EUSIPCO 2000*, pages 1069–1072, Tampere, Finland, September 2000.

[68] M. V. Fedoryuk, editor. *Partial Differential Equations V: Asymptotic Methods for Partial Differential Equations*, volume 34 of *Encyclopaedia of Mathematical Sciences*. Springer Verlag, 1999.

[69] B. Fenny, A. Guran, N. Hinrichs, and K. Popp. A historical review on dry friction and stick-slip phenomena. *Applied Mechanics Review*, 51(5):321–341, May 1998.

[70] N. H. Fletcher and T. D. Rossing. *The Physics of Musical Instruments*. Springer Verlag, New York, 2 edition, 1998.

[71] J.-L. Florens and C. Cadoz. The Physical Model: Modeling and Simulating the Instrumental Universe. In G. De Poli, A. Piccialli, and C. Roads, editors, *Representations of Musical Signals*, chapter 7, pages 227–268. MIT Press, Cambridge, 1991.

[72] F. G. Friedlander. On the Oscillations of a Bowed String. *Proceedings of the Cambridge Philosophical Society*, 49(3):516–530, 1952.

[73] S. A. Fulling. Reflections on the Role of Asymptotic Analysis in Physics. In A. Semikhatov, M. Vasiliev, and V. Zaikin, editors, *Proceedings of the International Conference on Quantization, Gauge Theory and Strings*, pages 307–315, Moscow, 2001. Scientific World.

[74] T. Funkhouser, I. Carlbom, G. Elko, G. Pingali, M. M. Sondhi, and J. West. A beam tracing approach to acoustic modeling for interactive virtual environments. In *Proceedings of SIGGRAPH 98*, Computer Graphics Proceedings, Annual Conference Series, pages 21–32, July 1998.

[75] W. G. Gardner. A Realtime Multichannel Room Simulator. In *Proceedings of the 124th meeting of the Acoustical Society of America*, New Orleans, November 1992.

[76] W. G. Gardner. The Virtual Acoustic Room. Master's thesis, Massachusetts Institute of Technology, Cambridge, MA, September 1992.

[77] G. H. Golub and C. F. Van Loan. *Matrix Computations*. Johns Hopkins University Press, Baltimore, Maryland, third edition, 1996.

[78] F. B. Hanson. Singular Point and Exponential Asymptotics. In R. Wong, editor, *Asymptotics and Computational Analysis*, volume 124 of *Lecture Notes in Pure and Applied Mathematics*, pages 211–240. Marcel Dekker, Inc., 1990.

[79] A. Härmä. *Frequency-Warped Autoregressive Modeling and Filtering*. PhD thesis, Helsinki University of Technology, Espoo, Finland, May 2001. Also available as Technical Report 61 from the same institution.

[80] A. Härmä and U. K. Laine. A Comparison of Warped and Conventional Linear Predictive Coding. *IEEE Transactions on Speech and Audio Processing*, 9(5):579–588, July 2001.

[81] A. Härmä and T. Paatero. Discrete Representation of Signals on a Logarithmic Frequency Scale. In *Proceedings of the IEEE Workshop on Applications of Signal Processing to Audio and Acoustics (WASPAA-01)*, pages 39–42, New Paltz, New York, October 21-14 2001. IEEE Signal Processing Society.

[82] M. A. Heckl. Curve Squeal of Train Wheels, Part 2: Which Wheel Modes are Prone to Squeal? *Journal of Sound and Vibration*, 229(3):695–707, 2000.

[83] M. A. Heckl and I. D. Abrahams. Active Control of Friction-Driven Oscillations. *Journal of Sound and Vibration*, 193(1):417–426, 1996.

[84] M. A. Heckl and I. D. Abrahams. Curve Squeal of Train Wheels, Part 1: Mathematical Model for its Generation. *Journal of Sound and Vibration*, 229(3):669–693, 2000.

[85] M. A. Heckl and X. Y. Huang. Curve Squeal of Train Wheels, Part 3: Active Control. *Journal of Sound and Vibration*, 229(3):709–735, 2000.

[86] H. L. F. Helmholtz. *On the Sensations of Tone*. Dover, 1885/1954.

[87] N. Hinrichs, M. Oestreich, and K. Popp. On the Modelling of Friction Oscillators. *Journal of Sound and Vibration*, 216(3):435–459, 1998.

[88] D. Holz. Acoustically important properties of xylophone-bar materials: Can tropical woods be replaced by European species? *Acustica united with acta acustica*, 82(6):878–884, 1996.

[89] C. J. Howls. Development of Exponential and Hyper-asymptotics. In C. J. Howls, T. Kawai, and Y. Takei, editors, *Toward the Exact WKB Analysis of Differential Equations, Linear or Non-Linear*. Kyoto University Press, 2000.

[90] J. Huopaniemi. *Virtual Acoustics and 3-D Sound in Multimedia Signal Processing*. PhD thesis, Helsinki University of Technology, Espoo, Finland, November 1999. Also available at Helsinki University of Technology, Laboratory of Acoustics and Audio Signal Processing, Report 53.

[91] C. Hutchins and V. Benade, editors. *Research Papers in Violin Acoustics 1975-1993*. Acoustical Society of America, Woodbury, 1997.

[92] R. A. Ibrahim. Friction-induced vibration, chatter, squeal, and chaos Part I: Mechanics of contact and friction. *Applied Mechanics Review*, 47(7):209–226, July 1994.

[93] R. A. Ibrahim. Friction-induced vibration, chatter, squeal, and chaos Part II: Dynamics and modeling. *Applied Mechanics Review*, 47(7):227–253, July 1994.

[94] D. Jaffe and J. O. Smith. Extensions of the Karplus-Strong plucked string algorithm. *Computer Music Journal*, 7(2):56–69, 1983.

[95] H. Järveläinen. Applying perceptual knowledge to string instrument synthesis. In *Proceedings of the Workshop on Current Research Directions in Computer Music*, Barcelona, November 15-17 2001. Available online: `http://www.iua.upf.es/mtg/mosart/paper/p09.pdf`.

[96] H. Järveläinen, V. Välimäki, and M. Karjalainen. Audibility of the timbral effects of inharmonicity in stringed instrument tones. *Acoustics Research Letters Online*, 2(3):79–84, April 2001.

[97] M. Kac. Can One Hear the Shape of a Drum? *American Mathematical Monthly*, 73(4):1–23, April 1966.

[98] A. Kapur, G. Essl, P. Davidson, and P. R. Cook. The Electronic Tabla Controller. In *Proceedings of the 2002 Conference on New Instruments for Musical Expression (NIME-02)*, pages 77–81, Dublin, Ireland, May 24-26 2002.

[99] M. Karjalainen, V. Välimäki, and T. Tolonen. Plucked-String Models: From the Karplus-Strong Algorithm to Digital Waveguides and Beyond. *Computer Music Journal*, 22(3):17–32, 1998.

[100] K. Karplus and A. Strong. Digital synthesis of plucked string and drum timbres. *Computer Music Journal*, 7(2):43–55, 1983.

[101] J. B. Keller. Bowing of Violin Strings. *Communications on Pure and Applied Mathematics*, 6:483–495, 1953.

[102] J. B. Keller. A Geometrical Theory of Diffraction. In L. M. Graves, editor, *Proceedings of Symposia in Applied Mathematics*, volume 8, pages 27–52. American Mathematical Society, 1958.

[103] J. B. Keller. Semiclassical Mechanics. *SIAM Review*, 27(4):485–504, December 1985.

[104] J. B. Keller and S. I. Rubinow. Asymtotic Solution of Eigenvalue Problems. *Annals of Physics*, 9:24–75, 1960.

[105] G. S. Kendall, W. L. Martens, and S. L. Decker. Spatial Reverberation: Discussion and Demonstration. In M. V. Mathews and J. R. Pierce, editors, *Current Directions in Computer Music*, chapter 7, pages 65–87. MIT Press, 1991.

[106] L. E. Kinsler, A. R. Frey, A. B. Coppens, and J. V. Sanders. *Fundamentals of Acoustics*. John Wiley and Sons, Inc., New York, fourth edition edition, 2000.

[107] P. Kovintavewat. Modeling the Impulse Response of an Office Room. Master's thesis, Chalmers University of Technology, 1998.

[108] V. V. Kozlov. *Symmetries, Topology, and Resonances in Hamiltonian Mechanics*, volume 31 of *A Series of Modern Surveys in Mathematics, Series 3*. Springer Verlag, 1996.

[109] V. V. Kozlov and D. V. Treshchëv. *Billiards - A Genetic Introduction to the Dynamics of Systems with Impacts*, volume 89 of *Translations of Mathematical Monographs*. American Mathematical Society, 1991.

[110] Y. A. Kravtsov and Y. I. Orlov. *Caustics, Catastrophes and Wave Fields*, volume 15 of *Series on Wave Propagation*. Springer Verlag, 1993.

[111] E. Kreyszig. *Advanced Engineering Mathematics*. John Wiley & Sons, Inc., seventh edition, 1993.

[112] M. Kurz. Klangsynthese mittels physikalisher Modellierung einer schwingenden Saite durch numerische Integration der Differentialgleichung. Master's thesis, Technical University Berlin, September 1995. In german. See [113] for a concise English summary.

[113] M. Kurz and B. Feiten. Physical modelling of a striff string by numerical integration. In *Proceedings of the International Computer Music Conference (ICMC-96)*, pages 361–364, Hong Kong, August 19-24 1996.

[114] T. I. Laakso, V. Välimäki, M. Karjalainen, and U. K. Laine. Splitting the Unit Delay: Tools for fractional delay filter design. *IEEE Signal Processing Magazine*, 13(1):30–60, January 1996.

[115] C. Lambourg, A. Chaigne, and D. Matignon. Time-domain simulation of damped impacted plates. II. Numerical model and results. *Journal of the Acoustical Society of America*, 109(4):1433–1447, April 2001.

[116] M. Lang. Allpass Filter Design and Applications. *IEEE Transactions on Signal Processing*, 46(9):2505–2514, September 1998.

[117] P. Lansky and K. Steiglitz. Synthesis of Timbral Families by Warped Linear Prediction. *Computer Music Journal*, 5(3):45–49, Fall 1981.

[118] P. M. Mäkilä and J. R. Partington. Laguerre and Kautz shift approximations of delay systems. *International Journal of Control*, 72(10):932–946, 1999.

[119] P. M. Mäkilä and J. R. Partington. Shift Operator Induced Approximations of Delay Systems. *SIAM Journal on Control and Optimization*, 37(6):1897–1912, 1999.

[120] A. Makur and S. K. Mitra. Warped Discrete-Fourier Transform: Theory and Applications. *IEEE Transactions on Circuits and Systems - I: Fundamental Theory and Applications*, 48(9):1086–1093, September 2001.

[121] J. Mathews and R. L. Walker. *Mathematical Methods of Physics*. W. A. Benjamin, Inc., second edition, 1970.

[122] M. E. McIntyre, R. T. Schumacher, and J. Woodhouse. On the oscillation of musical instruments. *Journal of the Acoustical Society of America*, 74(5):1325–1344, 1983.

[123] A. J. McMillan. A Non-Linear Friction Model for Self-Excited Vibrations. *Journal of Sound and Vibration*, 205(3):323–335, 1997.

[124] D. J. Mead. Wave Propagation and Natural Modes in Periodic Systems: I. Mono-Coupled Systems. *Journal of Sound and Vibration*, 40(1):1–18, 1975.

[125] D. J. Mead. Wave Propagation and Natural Modes in Periodic Systems: II. Multi-Coupled Systems, With and Without Damping. *Journal of Sound and Vibration*, 40(1):19–39, 1975.

[126] D. J. Mead. Waves and Modes in Finite Beams: Application of the Phase-Closure Principle. *Journal of Sound and Vibration*, 171(5):695–702, 1994.

[127] D. J. Mead. Wave Propagation in Continuous Periodic Structures: Research Contributions from Southampton 1964-1995. *Journal of Sound and Vibration*, 190(3):495–524, 1996.

[128] R. B. Melrose. *Geometric Scattering Theory*. Cambridge University Press, 1995.

[129] A. S. Mishchenko, V. E. Shatalov, and B. Y. Sternin. *Lagrangian Manifolds and the Maslov Operator*. Springer Verlag, 1990.

[130] B. C. J. Moore. *An Introduction to the Psychology of Hearing*. Academic Press, 4th edition, 1997.

[131] J. L. Moore. *Acoustics of Bar Percussion Instruments*. PhD thesis, Ohio State University, Columbus, 1970.

[132] P. M. Morse and K. U. Ingard. *Theoretical Acoustics*. Princeton University Press, Princeton, NJ, 1968.

[133] G. Müller and W. Lauterborn. The Bowed String as a Nonlinear Dynamical System. *Acustica*, 82(4):657–664, 1996.

[134] J. F. O'Brien. private communication, 2001.

[135] J. F. O'Brien, P. R. Cook, and G. Essl. Synthesizing Sounds from Physically Based Motion. In *Proceedings of SIGGRAPH 2001*, Computer Graphics Proceedings, Annual Conference Series, pages 529–536, August 2001.

[136] J. F. O'Brien and J. K. Hodgins. Graphical modeling and animation of brittle fracture. In *Proceedings of SIGGRAPH 99*, Computer Graphics Proceedings, Annual Conference Series, pages 137–146, August 1999.

[137] J. F. O'Brien and J. K. Hodgins. Animating fracture. *Communications of the ACM*, 43(7):68–75, July 2000.

[138] T. Olivera e Silva. On the Design of Linear-in-the-Parameters Adaptive Filters. In *Proceedings of the 5th International Conference on Electronics, Circuits and Systems*, volume 1, pages 385–388. IEEE, 1998.

[139] F. W. J. Olver. *Asymptotics and Spectial Functions*. Academic Press, 1974.

[140] A. V. Oppenheim and D. H. Johnson. Discrete Representation of Signals. *Proceedings of the IEEE*, June 1972.

[141] A. V. Oppenheim, D. H. Johnson, and K. Steiglitz. Computation of Spectra with Unequal Resolution Using the Fast Fourier Transform. *Proceedings of the IEEE*, 59(2):299–301, February 1971.

[142] A. V. Oppenheim and R. W. Schafer. *Discrete-Time Signal Processing*. Prentice Hall, 1989.

[143] F. Orduña Bustamante. Nonuniform beams with harmonically related overtones for use in percussion instruments. *Journal of the Acoustical Society of America*, 90(6):2935–2941, 1991. Erratum: Journal of the Acoustical Society of America 91(6), 3582–3583 (1992).

[144] T. Painter and A. Spanias. Perceptual Coding of Digital Audio. *Proceedings of the IEEE*, 88(4):451–513, April 2000.

[145] A. Paladin and D. Rocchesso. A Dispersive Resonator in Real Time on MARS Workstation. In *Proceedings of the International Computer Music Conference (ICMC-92)*, pages 146–149, 1992.

[146] M. Palumbi and L. Seno. Physical modeling by directly solving wave PDE. In *Proceedings of the International Computer Music Conference (ICMC)*, pages 325–328, Beijing, China, 1999. International Computer Music Association (ICMA).

[147] A. Partington, editor. *The Oxford Dictionary of Quotations*. Oxford University Press, revised 4th edition, 1996.

[148] H. Penttinen, M. Karjalainen, T. Paatero, and H. Järveläinen. New techniques to model reverberant instrument body responses. In *Proceedings of the International Computer Music Conference (ICMC-2001)*, Havana, Cuba, September 17-23 2001.

[149] J. Petrolito and K. A. Legge. Optimal undercuts for the tuning of percussion beams. *Journal of the Acoustical Society of America*, 102(4):2432–2437, 1997.

[150] R. Pitteroff. *Contact mechanics of the bowed string*. PhD thesis, University of Cambridge, Cambridge, UK., 1995. Also published in a series of papers in an archival journals [151, 152, 153].

[151] R. Pitteroff and J. Woodhouse. Mechanics of the Contact Area Between a Violin Bow and a String. Part I: Reflection and Transmission Behaviour. *Acustica united with acta acustica*, 84(3):543–562, 1998.

[152] R. Pitteroff and J. Woodhouse. Mechanics of the Contact Area Between a Violin Bow and a String. Part II: Simulating the Bowed String. *Acustica united with acta acustica*, 84(4):744–757, 1998.

[153] R. Pitteroff and J. Woodhouse. Mechanics of the Contact Area Between a Violin Bow and a String. Part III: Parameter Dependence. *Acustica united with acta acustica*, 84(5):929–946, 1998.

[154] D. P. Pivin. Semiclassical Periodic Orbit Theory and Possible Application to Open Quantum Ballistic Cavities. Unpublished manuscript available online at `http://www.eas.asu.edu/~pivin/Comps/pot.pdf`, November 1997.

[155] K. C. Pohlmann. *Principles of Digital Audio*. McGraw-Hill, third edition, 1995.

[156] W. H. Press, S. A. Teukolsky, W. T. Vetterling, and B. P. Flannery. *Numerical Recipes in C*. Cabridge University Press, second edition, 1992.

[157] R. Rabenstein and L. Trautmann. Digital Sound Synthesis by Physical Modelling. In *Proceedings of the Symposion on Image and Signal processing and Analysis (ISPA'01)*, Pula, Croatia, June 2001.

[158] C. V. Raman. *Scientific Papers of C. V. Raman*, volume 2 – Acoustics. Indian Academy of Sciences, Bangalore, India, 1988.

[159] J. W. S. Rayleigh. *The Theory of Sound*, volume 1&2. Dover, 1894/1945.

[160] J. W. S. Rayleigh. On the Propagation of Waves through a Stratified Medium, with Special Reference to the Question of Reflection. *Proceedings of the Royal Society of London. Series A, Containing Papers of a Mathematical and Physical Character*, 86(586):207–226, Februrary 1912.

[161] S. Ree and L. E. Reichl. Classical and quantum chaos in a circular billiard with a straight cut. *Physical Review E*, 60(2):1607–1615, August 1999.

[162] L. Rhaouti, A. Chaigne, and P. Joly. Time-domain modeling and numerical simulation of a kettledrum. *Journal of the Acoustical Society of America*, 105(6):3545–3562, June 1999.

[163] J. L. Richmond and D. K. Pai. Robotic measurement and modeling of contact sounds. In *Proceedings of the International Conference on Auditory Display (ICAD)*, 2000.

[164] A. W. Rix and M. P. Hollier. The Perceptual Analysis Measurement System for Robust End-to-End Speech Quality Assessment. In *Proceedings of the International Conference on Acoustics, Speech and Signal Processing (ICASSP-00)*, June 5-9 2000.

[165] C. Roads. *The Computer Music Tutorial*. MIT Press, 1996.

[166] D. Rocchesso. The Ball within the Box: a sound-processing metaphor. *Computer Music Journal*, 19(4):47–57, Winter 1995.

[167] D. Rocchesso and P. Dutilleux. Generalization of a 3-D Acoustic Resonator Model for the Simulation of Spherical Enclosures. *Applied Signal Processing*, 1:15–26, 2001.

[168] D. Rocchesso and L. Ottaviani. Can One Hear the Volume of a Shape? In *Proceedings of the 2001 IEEE Workshop on Applications of Signal Processing to Audio and Acoustics*, pages 115–118, New Paltz, NY, October 21-24 2001. IEEE Signal Processing Society.

[169] D. Rocchesso and F. Scalcon. Accurate Dispersion Simulation for Piano Strings. In *Proceedings of the Nordic Acoustical Meeting (NAM-96)*, pages 407–414, Helsinki, Finland, June 12-14 1996.

[170] D. Rocchesso and J. O. Smith. Circulant and Elliptic Feedback Delay Networks for Artificial Reverberation. *IEEE Transaction on Speech and Audio*, 5(1):51–60, January 1996.

[171] T. D. Rossing. Acoustics of percussion instruments – Part I. *The Physics Teacher*, 14:546–556, 1976.

[172] T. D. Rossing. Acoustics of the glass harmonica. *Journal of the Acoustical Society of America*, 95(2):1106–1111, 1994.

[173] T. D. Rossing. *Science of Percussion Instruments*, volume 3 of *Series In Popular Science*. World Scientific Publishing, 2000.

[174] P. M. Ruiz. A Technique for Simulating the Vibrations of Strings with a Digital Computer. Master's thesis, University of Illinois, 1969.

[175] L. Savioja, J. Huopaniemi, T. Lokki, and Väänänen. Virtual environment simulation - advances in the DIVA project. In *Proceedings of the International Conference on Auditory Display (ICAD)*, pages 43–46, 1997.

[176] L. Savioja and V. Välimäki. Reducing the Dispersion Error in the Digital Waveguide Mesh Using Interpolation and Frequency-Warping Techniques. *IEEE Transaction on Speech and Audio Processing*, 8(2):184–194, March 2000.

[177] A. Schiela and F. A. Bornemann. Sparsing in Real Time Simulation. Unpublised manuscript available at `http://www-m3.ma.tum.de/m3/ftp/Bornemann/pdf/sparsing.pdf`, May 2002.

[178] L. I. Schiff. *Quantum Mechanics*. McGraw-Hill, New York, second edition, 1955.

[179] S. Serafin, P. Huang, and J. O. Smith. The Banded Digital Waveguide Mesh. In *Proceedings of the Workshop on Current Research Directions in Computer Music*, Barcelona, November 15-17 2001. Available online: `http://www.iua.upf.es/mtg/mosart/paper/p38.pdf`.

[180] S. Serafin and J. O. Smith. A Multirate, Finite-Width, Bow-String Interaction Model. In *Proceedings of the COST G-6 Conference on Digital Audio Effects (DAFX-00)*, pages 207–210, Verona, Italy, December 7-9 2000.

[181] S. Serafin, C. Vergez, and X. Rodet. Friction and Application to Real-time Physical Modeling of a Violin. In *Proceedings of the International Computer Music Conference (ICMC)*, pages 216–219, Beijing, China, 1999. International Computer Music Association (ICMA).

[182] X. Serra. A Computer Model for Bar Percussion Instruments. In *Proc. International Computer Music Conference (ICMC)*, pages 257–262, The Hague, 1986. International Computer Music Association (ICMA).

[183] J. H. Smith. *Stick-Slip Vibration and its Constitutive Laws*. PhD thesis, University of Cambridge, March 1990.

[184] J. H. Smith and J. Woodhouse. The tribology of rosin. *Journal of the Mechanics and Physics of Solids*, 48(8):1633–1681, August 2000.

[185] J. O. Smith. *Techniques for Digital Filter Design and System Identification with Application to the Violin*. PhD thesis, Stanford University, Stanford, California, 1983. Also available as technical report from Stanford Center for Computer Research in Music and Acoustics (CCRMA) Department of Music Report No. STAN-M-14.

[186] J. O. Smith. Efficient Simulation of the Reed-Bore and Bow-String Mechanisms. In *Proceedings of the International Computer Music Conference (ICMC)*, pages 275–280, The Hague, 1986. International Computer Music Association (ICMA).

[187] J. O. Smith. Physical Modeling Synthesis Update. *Computer Music Journal*, 20(2):44–56, 1996.

[188] J. O. Smith. Digital Waveguide Modeling of Musical Instruments. draft of unpublished online manuscript, available at `http://ccrma-www.stanford.edu/~jos/waveguide/`, 2002.

[189] J. O. Smith and J. S. Abel. Bark and ERB Bilinear Transforms. *IEEE Transactions on Speech and Audio Processing*, 7(6):697–708, November 1999.

[190] J. Stam. *Multi-Scale Stochastic Modelling of Complex Natural Phenomena*. PhD thesis, University of Toronto, 1995.

[191] J. Stautner and M. Puckette. Designing Multi-Channel Reverberators. *Computer Music Journal*, 6(1):52–65, Spring 1982.

[192] K. Steiglitz. Derivation of frequency warping by contour integrals. Unpublished manuscript. Alternate derivation to [141], 1970.

[193] K. Steiglitz. A Note on Constant-Gain Digital Resonators. *Computer Music Journal*, 18(4):8–10, 1994.

[194] K. Steiglitz. *A Digital Signal Processing Primer*. Addison-Wesley, 1996.

[195] C. R. Sullivan. Extending the Karplus-Strong Algorithm to Synthesize Electric Guitar Timbres with Distortion and Feedback. *Computer Music Journal*, 14(3):26–37, 1990.

[196] T. Thiede and E. Kabot. A New Perceptual Quality Measure for Bit Rate Reduced Audio. In *Proceedings of the 100th AES Convention*, Copenhagen, Denmark, May 11-14 1996. Preprint 4280.

[197] J. J. Thomsen. Using Fast Vibration to Quench Friction-Induced Oscillations. *Journal of Sound and Vibration*, 228(5):1079–1102, 1999.

[198] T. Tolonen, V. Välimäki, and M. Karjalainen. Evaluation of Modern Sound Synthesis Methods. Technical Report Laboratory of Acoustics and Audio Signal Processing, Report 48, Helsinki University of Technology, Epsoo, Finland, March 1998.

[199] T. Tolonen, V. Välimäki, and M. Karjalainen. Modeling of Tension Modulation Nonlinearity in Plucked Strings. *IEEE Transactions on Speech and Audio Processing*, 8(3):300–310, May 2000.

[200] L. Trautmann and R. Rabenstein. Digital Sound Synthesis Based on Transfer Function Models. In *Proceedings of the 1999 IEEE Workshop on Applications of Signal Processing to Audio and Acoustics (WASPAA-99)*, pages 83–86, New Paltz, New York, October 17-20 1999.

[201] L. N. Trefethen. Finite Difference and Spectral Methods for Ordinary and Partial Differential Equations. Available online at `http://web.comlab.ox.ac.uk/oucl/work/nick.trefethen/pdetext.html`, 1996.

[202] B. Truax. Computer Music and Acoustic Communication: Two Emerging Interdisciplines. In A. Salter, L. Hearn, editor, *Outside the Lines: Issues in Interdisciplinary Research*, pages 64–73. McGill-Queen's University Press, 1996.

[203] W. W. Tworzydlo, E. E. Becker, and J. T. Oden. Numerical modeling of friction-induced vibrations and dynamic instabilities. *Applied Mechanics Review*, 47(7):255–274, July 1994.

[204] P. P. Vaidyanathan. *Multirate Systems and Filter Banks*. Signal Processing Series. Prentice Hall, 1993.

[205] R. Vaillancourt and A. L. Smirnov, editors. *Asymptotic Methods in Mechanics*, volume 3 of *CRM Proceedings & Lecture Notes*. American Mathematical Society, 1993.

[206] V. Välimäki and T. Tolonen. Multirate Extensions for Model-Based Synthesis of Plucked String Instruments. In *Proceedings of the International Computer Music Conference (ICMC-97)*, pages 244–247, Thessaloniki, Greece, September 25-30 1997.

[207] K. van den Doel. *Sound Synthesis for Virtual Reality and Computer Games*. PhD thesis, University of British Columbia, Vancouver, Canada, November 1998.

[208] K. van den Doel, P. G. Kry, and D. K. Pai. FoleyAutomatic: Physically-Based Sound Effects for Interactive Simulation and Animation. In *Proceedings of SIGGRAPH 2001*, Computer Graphics Proceedings, Annual Conference Series, pages 537–544, August 2001.

[209] K. van den Doel and D. K. Pai. Synthesis of shape dependent sounds with physical modeling. In *Proceedings of the International Conference on Auditory Display (ICAD)*, 1996.

[210] K. van den Doel and D. K. Pai. The Sound of Physical Shapes. Technical report, Dept. of Computer Science, University of British Columbia, Canada, Vancouver, 1996.

[211] K. van den Doel and D. K. Pai. The Sound of Physical Shapes. *Presence*, 7(4):382–395, August 1998.

[212] K. van den Doel and D. K. Pai. Modal Synthesis for Resonating Objects. Unpublished manuscript available at: urlhttp://www.cs.ubc.ca/ kvdoel/publications/modalpaper.pdf, 2002.

[213] S. van Duyne and J. Smith. A Simplified Approach to Modeling Dispersion Caused by Stiffness in Strings and Plates. In *Proceedings of the International Computer Music Conference (ICMC-94)*, pages 407–410, 1994.

[214] S. van Duyne and J. O. Smith. Physical Modeling With the 2D Waveguide Mesh. In *Proceedings of the International Computer Music Conference (ICMC)*, pages 40–47, The Hague, 1993. International Computer Music Association (ICMA).

[215] A. I. Volpert, V. A. Volpert, and V. A. Volpert. *Traveling Wave Solutions of Parabolic Systems*, volume 140 of *Translations of Mathematical Monographs*. American Mathematical Society, 1994.

[216] T. Von Schroeter. Frequency Warping with Arbitrary Allpass Maps. *IEEE Signal Processing Letters*, 6(5):116–118, May 1999.

[217] C. Wagner. Introduction to Algebraic Multigrid. Course Notes of an Algebraic Multigrid Course at the University of Heidelberg in Fall of 1998/99: `http://www.iwr.uni-heidelberg.de/groups/techsim/chris/amg.pdf`, 1998.

[218] M. D. Waller. *Chladni Figures — A Study in Symmetry*. G. Bell and Sons, London, 1961.

[219] J. Wawrzynek. VLSI Models for Sound Synthesis. In M. Mathews and J. Pierce, editors, *Current Directions in Computer Music Research*, chapter 10, pages 113–148. MIT Press, Cambridge, 1989.

[220] P. Wesseling. *An Introduction to Multigrid Methods*. John Wiley & Sons, 1991. Also available online at: `http://www.mgnet.org/mgnet-books-wesseling.html`.

[221] C. Wilkerson, C. Ng, and S. Serafin. The Mutha Rubboard Controller: Interactive Heritage. In *Proceedings of the 2002 Conference on New Instruments for Musical Expression (NIME-02)*, pages 82–85, Dublin, Ireland, May 24-26 2002.

[222] O. C. Zienkiewicz and R. L. Taylor. *The Finite Element Method*, volume 1: The Basis. Butterworth-Heinemann, fifth edition, 2000.

[223] O. C. Zienkiewicz and R. L. Taylor. *The Finite Element Method*, volume 2: Solid Mechanics. Butterworth-Heinemann, fifth edition, 2000.

[224] O. C. Zienkiewicz and R. L. Taylor. *The Finite Element Method*, volume 3: Fluid Dynamics. Butterworth-Heinemann, fifth edition, 2000.